

EFFECT OF CYCLIC SWELL-SHRINK ON SWELL PERCENTAGE OF
AN EXPANSIVE CLAY STABILIZED BY CLASS C FLY ASH

A THESIS SUBMITTED TO
THE GRADUATE SCHOOL OF NATURAL AND APPLIED SCIENCES
OF
MIDDLE EAST TECHNICAL UNIVERSITY

BY

MEHMET AS

IN PARTIAL FULFILLMENT OF THE REQUIREMENTS
FOR
THE DEGREE OF MASTER OF SCIENCE
IN
CIVIL ENGINEERING

JANUARY 2012

Approval of the thesis:

**EFFECT OF CYCLIC SWELL-SHRINK ON SWELL PERCENTAGE OF AN
EXPANSIVE CLAY STABILIZED BY CLASS C FLY ASH**

submitted by **MEHMET AS** in partial fulfillment of the requirements for the degree of **Master of Science in Civil Engineering Department, Middle East Technical University** by,

Prof. Dr. Canan Özgen
Dean, Graduate School of **Natural and Applied Sciences** _____

Prof. Dr. Güney Özcebe
Head of Department, **Civil Engineering** _____

Prof. Dr. Erdal Çokça
Supervisor, **Civil Engineering Dept., METU** _____

Examining Committee Members:

Prof. Dr. M. Yener Özkan
Civil Engineering Dept., METU _____

Prof. Dr. Erdal Çokça
Civil Engineering Dept., METU _____

Assist. Prof. Dr. Nejan Huvaj Sarihan
Civil Engineering Dept., METU _____

Dr. Onur Pekcan
Civil Engineering Dept., METU _____

Mustafa Toker, M.Sc.
Toker Drilling and Cons. Co. _____

Date: 27.01.2012

I hereby declare that all information in this document has been obtained and presented in accordance with academic rules and ethical conduct. I also declare that, as required by these rules and conduct, I have fully cited and referenced all material and results that are not original to this work.

Name, Last Name : MEHMET AS

Signature :

ABSTRACT

EFFECT OF CYCLIC SWELL – SHRINK ON SWELL PERCENTAGE OF AN EXPANSIVE CLAY STABILIZED BY CLASS C FLY ASH

As, Mehmet

M.Sc., Department of Civil Engineering

Supervisor: Prof. Dr. Erdal Çokça

January 2012, 115 pages

Expansive soils are a worldwide problem especially in the regions where climate is arid or semi arid. These soils swell when they are exposed to water and shrink when they dry. Cyclic swelling and shrinkage of clays and associated movements of foundations may result in cracking of structures. Several methods are used to decrease or prevent the swelling potential of such soils like prewetting, surcharge loading, chemical stabilization etc. Among these, one of the most widely used method is using chemical admixtures (chemical stabilization). Cyclic wetting and drying affects the swell – shrink behaviour of expansive soils. In this research, the effect of cyclic swell – shrink on swell percentage of a chemically stabilized expansive soil is investigated. Class C Fly Ash is used as an additive for stabilization of an expansive soil that is prepared in the laboratory environment by mixing kaolinite and bentonite. Fly ash was added to expansive soil with a predetermined percentage changing between 0 to 20 percent. Hydrated lime with percentages changing between 0 to 5 percent and sand with 5 percent were also used instead of fly ash for comparison. Firstly, consistency limits, grain size distributions and swell percentages of mixtures were determined. Then to see the effect of cyclic swell – shrink on the swelling behavior of the mixtures, swell – shrink cycles applied to samples and swell percentages were

determined. Swell percentage decreased as the proportion of the fly ash increased. Cyclic swell-shrink affected the swell percentage of fly ash stabilized samples positively.

Keywords: Cyclic Swell-Shrink, Expansive Soil, Class C Fly Ash, Swell Percentage, Drying- Wetting

ÖZ

DÖNGÜSEL ŞİŞME VE BÜZÜŞMENİN C SINIFI UÇUCU KÜL İLE STABİLİZE EDİLEN ŞİŞEN ZEMİNİN, ŞİŞME YÜZDESİ ÜZERİNDEKİ ETKİSİ

As, Mehmet

Yüksek Lisans, İnşaat Mühendisliği Bölümü

Tez Yöneticisi: Prof. Dr. Erdal Çokça

Ocak 2012, 115 sayfa

Şişen zeminler, özellikle iklimin kurak veya yarı kurak olduğu bölgelerde olmak üzere bütün dünyada problem oluşturmaktadır. Bu zeminler suya maruz bırakıldıklarında şişmekte, kuruduklarında ise büzüşmektedirler. Döngüsel şişme ve büzüşme ve yapı temellerinde meydana getirdikleri hareketler yapılarda çatlaklara neden olmaktadır. Bu tarz zeminlerin şişme potansiyelini düşürmek veya ortadan kaldırmak için ön ıslatma, ilave yükleme ve kimyasal stabilizasyon gibi bir çok metot kullanılmaktadır. Bu metotlar arasında en yaygın olanlardan biri kimyasal katkı kullanmaktır (kimyasal stabilizasyon). Döngüsel ıslanma ve kuruma şişen zeminlerin şişme - büzüşme davranışlarını etkilemektedir. Bu araştırmada döngüsel şişme - büzüşmenin kimyasal katkı yardımıyla stabilizasyonu sağlanan şişen zeminlerin şişme yüzdeleri üzerindeki etkisi incelenmiştir. Laboratuvar ortamında kaolin ve bentonit karıştırılarak elde edilen şişen zeminin stabilizasyonu için katkı maddesi olarak C Sınıfı Uçucu Kül kullanılmıştır. Uçucu kül şişen zemine önceden belirlenen, %0 ile %20 arasında değişen, oranlarda eklenmiştir. Ayrıca deneylerde karşılaştırma amacıyla, uçucu kül yerine %1 ile %5 oranında değişen sönmüş kireç ve %5 oranında kum kullanılmıştır. Öncelikle karışımların kıvam limitleri, dane boyu dağılımları ve şişme yüzdeleri belirlenmiştir. Daha sonra döngüsel

şişme - b z şmenin numunelere etkisini g rmek i in numuneler şişme – b z şmeye maruz bırakılmış ve şişme y zdeleri belirlenmiştir. Numunelerin şişme y zdeleri u ucu k l oranı arttık a azalma g stermiştir. D ng sel şişme- b z şmenin ise u ucu k l ile stabilize edilen numunelerin şişme y zdelerini pozitif olarak etkilediđi g zlenmiştir.

Anahtar Kelimeler: D ng sel Şişme - B z şme, Şişen Zeminler, C Sınıfı U ucu K l, Şişme Y zdesi, Kuruma - İslanma

To My Dad

ACKNOWLEDGEMENTS

I would like to express sincere appreciation to my supervisor, Prof. Dr. Erdal Çokça for his guidance, continuous understanding, invaluable patience and support throughout this research.

I also wish to express my special thanks to Dr. Kartal Toker for his valuable advices throughout the laboratory works.

Special thanks go to the staff of Toker Drilling and Construction Co., especially to Mustafa Toker for their great encouragements during my studies.

My thankfulness goes to geology engineer Mr. Ulaş Nacar and technician Mr. Kamber Bilgen for their support and friendly approach throughout the laboratory works.

I would like to acknowledge my friends Melih Bozkurt, Nilsu Kıstak, Güliz Ünlü, Ertaç Tuç, Mustafa Bilal and Erdem İspir for their helpful suggestions and encouragements during this study.

Finally, I express my sincere thanks to my aunt Sibel Ören, to my sister Merve As and to my mother Ayşe As for their endless supports throughout my life.

TABLE OF CONTENTS

ABSTRACT	iv
ÖZ	vi
ACKNOWLEDGEMENTS.....	ix
TABLE OF CONTENTS.....	x
LIST OF TABLES	xii
LIST OF FIGURES	xiv
LIST OF ABBREVIATIONS	xiv
CHAPTERS	
1. INTRODUCTION	1
1.1 General	1
1.2 Aim of the Study	2
1.3 Scope of the Study	2
2. LITERATURE REVIEW	4
2.1 Expansive Soils	4
2.1.1 Clay Mineralogy.....	4
2.1.2 Factors Influencing Swelling	11
2.2 Soil Stabilization	15
2.2.1 Chemical Stabilization	15
2.2.2 Lime Stabilization	15
2.2.3 Fly Ash Stabilization	17
3. FLY ASH	18
3.1 General	18
3.2 Factors that influence Fly Ash Properties	20
3.2.1 Coal Source	20
3.2.2 Boiler and Emission Control Design	20
3.3 Classification of Fly Ashes.....	21
3.4 Soma Thermal Power Plant.....	21
3.5 Utilization of Fly Ash	23

4. PREVIOUS STUDIES ON CYCLIC SWELL-SHRINK BEHAVIOUR OF SOILS.....	26
4.1 General	26
4.2 Studies on Nonstabilized Soils	26
4.3 Studies on Stabilized Soils	31
5. EXPERIMENTAL WORKS	40
5.1 Purpose.....	40
5.2 Materials.....	40
5.3 Preparation and Properties of Test Samples	43
5.4 Properties of Samples	46
5.5 Procedures for Cyclic Swell and Shrink Tests	54
5.5.1 Compaction of Specimens.....	54
5.5.2 Cyclic Swell – Shrink Tests	55
5.5.3 Test Results	59
5.6 SEM – EDX Analysis	72
6. DISCUSSION ON TEST RESULTS	79
6.1 Effect of Additives on Grain Size Distribution.....	79
6.2 Effect of Additives on Specific Gravity	80
6.3 Effect of Additives on Liquid Limit.....	81
6.4 Effect of Additives on Plastic Limit	82
6.5 Effect of Additives on Plasticity Index	82
6.6 Effect of Additives on Shrinkage Limit	82
6.7 Effect of Additives on Linear Shrinkage	83
6.8 Effect of Additives on Shrinkage Index	83
6.9 Effect of Additives on Activity.....	84
6.10 Effect of Additives on Swell Percentage	84
6.11 Effect of Curing on Swell Percentage	85
6.12 Effect of Cyclic Swell-Shrink on Swell Percentages of Samples	86
6.13 Discussions on SEM-EDX Analysis	91
7. CONCLUSIONS	93
REFERENCES.....	97
APPENDICES	
A- CHEMICAL ANALYSIS REPORT OF SOMA FLY ASH	103
B- SWELL VERSUS TIME GRAPHS.....	104

LIST OF TABLES

TABLES

Table 2.1 Soil Properties that influence shrink-swell potential (Nelson and Miller, 1992).....	12
Table 2.2 Environmental Conditions that influence shrink-swell potential (Nelson and Miller, 1992).....	13
Table 2.3 Stress Conditions that influence shrink-swell potential (Nelson and Miller, 1992).....	14
Table 3.1 Utilization of Fly Ash by 2009 in USA (ACAA, 2011).....	25
Table 4.1 Swell-Shrink Procedures applied on nonstabilized expansive soils in previous studies by different researchers	30
Table 4.1 Swell-Shrink Procedures applied on nonstabilized expansive soils in previous studies by different researchers (continued).....	31
Table 4.2 Properties of the materials used in Güney et al, (2007) studies.	33
Table 4.3 Swell-Shrink Procedures applied on stabilized expansive soils in previous studies by different researchers	38
Table 5.1 Chemical Composition of Fly Ash and Lime.....	41
Table 5.2 Composition of Prepared Specimens.....	44
Table 5.3 Properties of Samples.....	53
Table 5.4 Samples chosen for SEM Analysis	72
Table 6.1 Specific gravity values obtained in Çetiner, (2004) study	80
Table 6.2 Percent Changes in Specific Gravity (G_s), Liquid Limit (LL), Plastic Limit (PL), Plasticity Index (PI), Shrinkage Limit (SL), Linear Shrinkage (L_s), Shrinkage Index (SI) and Activity (A_c).....	81
Table 6.3 Swell Percentages and Percent Change in Swell Percentage with the addition of stabilizers	85

Table 6.4. Axial swell percentages ($\Delta H_i/H_{id}$) of samples	86
Table 6.5. Volumetric swell percentages ($\Delta V_i/V_{id}$) of samples at the end of each cycle	87
Table 6.6. Volumetric swell percentages ($\Delta V/V_0$) of samples with respect to initial volume.....	88
Table 6.7. Swell percentages for 5% fly ash samples with no cure, 7 days cured and 28 days cured	90
Table 6.8. Curing conditions and unconfined compressive strength (q_u) values in Beeghly, (2003) study.....	91

LIST OF FIGURES

FIGURES

Figure 2.1 Basic Unit of Clay Minerals (Craig, 1997)	5
Figure 2.2 Synthesis pattern of Clay Minerals (modified from Mitchell, 2005) ..	6
Figure 2.3 Structure of Kaolinite (USGS, 2001)	7
Figure 2.4 Scanning Electron Micrograph of Kaolinite (Murray, 2007)	7
Figure 2.5 Structure of Illite (USGS, 2001)	8
Figure 2.6 Scanning Electron Micrograph of Illite (source: http://webmineral.com/specimens/picshow.php?id=1284&target=Illite)	9
Figure 2.7 Structure of Montmorillonite (USGS, 2001).....	10
Figure 2.8 Scanning Electron Micrograph of Sodium Montmorillonite (Murray, 2007)	10
Figure 3.1 Coal Ash Pollution Chain (Greenpeace, 2010).....	19
Figure 3.2 Ash Disposal Site of Soma Thermal Power Plant (Baba and Kaya, 2004).....	22
Figure 3.3 Scanning Electron Micrograph of Soma Fly Ash (Çelik, 2004).....	23
Figure 3.4 Fly Ash production and utilization statistics for USA (adapted from American Coal Ash Association, 2011).....	24
Figure 3.5 Fly Ash production and utilization comparison for USA (adapted from American Coal Ash Association, 2011).....	24
Figure 4.1 Total pressure cells data for the Power House linings of Masjed-Soleiman Hydroelectric Power Plant Project (Doostmohammadi, 2009)	28
Figure 4.2 Effect of full swell-full shrink and full swell-partial shrink on swell potential of an expansive soil (Tawfiq & Nalbantoğlu, 2009)	29

Figure 4.3 Effect of wetting-drying cycles on clay content of lime treated soils (Rao, 2011)	32
Figure 4.4 Effect of wetting-drying cycles on plastic limit of lime treated soils (Rao, 2011)	32
Figure 4.5 Change of Swell Percent for Soil A and lime treated Soil A (Güney et al, 2007).....	34
Figure 4.6 Change of Swell Percent for Soil C and lime treated Soil C (Güney et al, 2007)	34
Figure 4.7 Experimental set up used in Rao A.& Rao M.,(2008) studies.....	35
Figure 4.8 Cyclic swell-shrink behavior of samples containg 20% bentonite treated with lime (Akcanca & Aytekin, 2011).....	36
Figure 4.9 Cyclic swell-shrink behavior of expansive soil stabilized with silica fume (Kalkan, 2011)	37
Figure 5.1. Views from Materials (1-kaolinite, 2-bentonite, 3-fly ash, 4-lime)	41
Figure 5.2.View from mixtures before titration.....	42
Figure 5.3. Preparation of Samples	45
Figure 5.4. Crystals formed in fly ash during the hydrometer test	46
Figure 5.5 Effect of Addition of Fly Ash, Lime and Sand on Specific Gravity (G_s) of the Samples	47
Figure 5.6 Effect of Addition of Fly Ash, Lime and Sand on Liquid Limit (LL) of the Samples.....	48
Figure 5.7 Effect of Addition of Fly Ash, Lime and Sand on Plastic Limit (PL) of the Samples	48
Figure 5.8 Effect of Addition of Fly Ash, Lime and Sand on Plasticity Index (PI) of the Samples	49
Figure 5.9 Effect of Addition of Fly Ash, Lime and Sand on Shrinkage Limit (SL) of the Samples.....	49
Figure 5.10 Effect of Addition of Fly Ash, Lime and Sand on Linear Shrinkage (L_s) of the Samples	50

Figure 5.11 Effect of Addition of Fly Ash, Lime and Sand on Shrinkage Index (SI) of the Samples.....	50
Figure 5.12 Grain Size Distribution Curves for Sample A and Fly Ash Treated Samples	51
Figure 5.13 Grain Size Distribution Curves for Sample A and Lime Treated Samples	51
Figure 5.14 Plasticity Chart.....	52
Figure 5.15 Swelling Potential Classification Chart (after Seed et al.,1962)...	52
Figure 5.16 View from Static Compaction	54
Figure 5.17 Free Swell Test Setup Drawing (İpek, 1998).....	55
Figure 5.18 View from Oedometers during testing	56
Figure 5.19 Measuring height with digital caliper	57
Figure 5.20 Measuring volume with mercury	57
Figure 5.21 Effect of Addition of Fly Ash, Lime and Sand on Free Swell of the Samples	58
Figure 5.22 Axial Swell Potential of Sample A and Fly Ash Treated Samples	60
Figure 5.23 Volumetric Swell Potential of Sample A and Fly Ash Treated Samples with respect to dry volume at the beginning of each cycle.....	61
Figure 5.24 Volumetric Swell Potential of Sample A and Fly Ash Treated Samples with respect to initial volume	62
Figure 5.25 Axial Swell Potential of Sample A and Lime Treated Samples	63
Figure 5.26 Volumetric Swell Potential of Sample A and Lime Treated Samples with respect to dry volume at the beginning of each cycle.....	64
Figure 5.27 Volumetric Swell Potential of Sample A and Lime Treated Samples with respect to initial volume	65
Figure 5.28 Axial Swell Potential of Sample A and Samples containing 5% Additives.....	66

Figure 5.29 Volumetric Swell Potential of Sample A and Samples containing 5% Additives with respect to dry volume at the beginning of each cycle	67
Figure 5.30 Volumetric Swell Potential of Sample A and Samples containing 5% Additives with respect to initial volume	68
Figure 5.31 Axial Swell Potential of 5% fly ash added Samples with and without curing	69
Figure 5.32 Volumetric Swell Potential of of 5% fly ash added Samples with and without curing with respect to dry volume at the beginning of each cycle	70
Figure 5.33 Volumetric Swell Potential of 5% fly ash added Samples with and without curing with respect to initial volume	71
Figure 5.34 SEM image of Sample A after compaction (magnification factor=10000)	73
Figure 5.35 SEM images of Sample A after compaction and cycles (magnification factor=20000)	71
Figure 5.36 SEM images of 5%FA treated sample after compaction and cycles (magnification factor=10000)	73
Figure 5.37 SEM images of 20%FA treated sample after compaction and cycles (magnification factor=10000)	74
Figure 5.38 SEM images of 20%FA treated sample after cycles (magnification factor=3000)	75
Figure 5.39 SEM images of Calcium Silicate Hydrate crystals (CSH) and Ettringite formed within 20%FA treated sample after cycles (magnification factor=10000)	75
Figure 5.40 SEM images of 3%L treated sample after compaction and first condition (at dry state of first cycle) (magnification factor=20000)	76
Figure 5.41 SEM images of 5%L treated sample after compaction and cycles (magnification factor=10000)	76
Figure 5.42 EDX Diagram of fly ash within the 5%FA treated sample	77

Figure 5.43 EDX Diagram of fly ash within the 20%FA treated sample (after cycles)	78
Figure 6.1 Views From 3% lime treated sample after drying ((a)-before first cycle, (b) – before second cycle)	89
Figure 6.2 View from fungi-shaped heaves occurred in the upper portion of 5% lime treated sample	89
Figure 6.3 SEM views obtained in Ismaiel, (2006) study.....	92
Figure A.1 Chemical Analysis Report of Soma Fly Ash	103
Figure B.1 Swell Amount versus Time Graph for Sample A.....	105
Figure B.2 Swell Amount versus Time Graph for 5%FA treated sample with no curing	106
Figure B.3 Swell Amount versus Time Graph for 5%FA treated sample with 7 days curing.....	107
Figure B.4 Swell Amount versus Time Graph for 5%FA treated sample with 28 days curing.....	108
Figure B.5 Swell Amount versus Time Graph for 10%FA treated sample	109
Figure B.6 Swell Amount versus Time Graph for 15%FA treated sample	110
Figure B.7 Swell Amount versus Time Graph for 20%FA treated sample	111
Figure B.8 Swell Amount versus Time Graph for 1%L treated sample.....	112
Figure B.9 Swell Amount versus Time Graph for 3%L treated sample.....	113
Figure B.10 Swell Amount versus Time Graph for 5%L treated sample.....	114
Figure B.11 Swell Amount versus Time Graph for 5%S treated sample	115

LIST OF ABBREVIATIONS

ACAA: American Coal Ash Association

ASTM: American Society for Testing and Materials

CH: Clay with high plasticity

EDX: Energy Dispersive X-Ray

F: Fly Ash

FSw-FSh: Full Swell-Full Shrink

FSw-PSh: Full Swell- Partial Shrink

G_s : Specific gravity

H_{id} = Height at dry state

L: Lime

LL: Liquid limit

L_s : Linear Shrinkage

METU: Middle East Technical University

PI: Plasticity index

PL: Plastic limit

S: Sand

SI: Shrinkage Index

SEM: Scanning Electron Microscope

SL: Shrinkage limit

V_{id} = Volume at dry state

V_0 = Initial volume of the sample

ΔH_i = Height difference between dry and wet state in a cycle

ΔV : Change in volume (with respect to initial volume, V_0)

ΔV_i = Volume difference between dry and wet state in a cycle

CHAPTER 1

INTRODUCTION

1.1 General

In arid and semi-arid areas of the world, moisture and rainfall amount varies considerably in different seasons, structures like small buildings and highways constructed on expansive soils are encountered with periodic swelling and shrinkage cycles (Basma, 1996). Cracks and breakups are formed due to swelling of expansive clays in roads, pavements, building foundations, irrigation systems, slab-on-grade members channel and reservoir linings, sewer lines and water lines (Çokça, 2001). In the United States, structures seated on expansive soils cause an estimated cost of more than 15 billion dollars due to damage caused from the soil (Al-Rawas, 2006).

Nearly 600 million tons of fly ash is produced each year in all around the world. In Turkey, 11 power station plants are in operation namely; Afşin-Elbistan, Çatalağzı, Çayırhan, Kangal, Kemerköy, Orhaneli, Seyitömer, Soma, Tunçbilek, Yatağan and Yeniköy. The amount of fly ash produced in each year in these power plants is averagely 16 million ton by the year 2006 (Turker et al., 2009). Although, in many countries rate of utilization of fly ash in civil engineering applications (mainly in cement production) reaches upto eight percent of the total produced amount, in Turkey only a small amount is used. Therefore in Turkey, studies related to utilization of fly ash are needed for the reduction of environmental problems and financial loss due to the fly ash deposition in disposal sites (Alkaya, 2009).

Expansive soils' swelling potential can be fully eliminated or at least decreased by using some methods. One of the most widely used stabilization

method is adding some chemicals to soil (Chen, 1975). Fly ash's benefit in stabilizing the soil has been proved in the recent studies. Fly ash causes many important environmental problems such as land, air, and water pollution and using fly ash for soil stabilization is a good way to handle the waste problem of fly ash (Nalbantoğlu, 2004).

Determination of swell potential of expansive soils is generally done by one cycle of wetting although it has been shown that behavior of expansive soils is considerably affected by the number of wetting-drying cycles. One should take the effects of number of cycles on the swelling and shrinking behavior of expansive soils into consideration since continuous wetting-drying cycles are observed in soils in nature as a result of environmental effects (Tawfiq and Nalbantoğlu, 2009). Changes in the swelling behavior of natural expansive soils due to wetting-drying cycles are well documented but studies performed to see the influence of cyclic wetting and drying on the swelling behavior of chemically stabilized soils are insufficient. The long-term behavior of foundations and earth structures should be assessed, employing chemically stabilized soils, by performing such a study (Rao et al., 2001).

1.2 Aim of the Study

There are lots of studies concerning the effect of chemical additives (lime, fly ash) on the swell potential of expansive clays. However, the long-term performance of chemical additives on reducing the swell potential of expansive clays is studied by only a few researchers. The aim of this study is to investigate the effect of cyclic-wetting on the swell potential of an expansive soil treated by Class C Fly Ash.

1.3 Scope of the Study

In the scope of this thesis, a literature review on expansive clays is given Chapter 2. In Chapter 3, literature review on Fly Ash is presented. Previous

studies related to cyclic-swell shrink behaviour of natural and chemically stabilized expansive clays are given in Chapter 4. In Chapter 5, 6 and 7 the experimental works, discussions of the test results and conclusions are presented respectively.

CHAPTER 2

LITERATURE REVIEW

2.1 Expansive Soils

2.1.1 Clay Mineralogy

The swelling phenomenon is related to the clay hydration but it is not necessarily mean that all clays should swell with water (Foster,1954). In the chemical treatment, procedures of stabilizer selection which are reported in the literature depend on plasticity index (PI) properties, soil type and particle size (Hausmann, 1990). However, stabilizing the soils of similar plasticity properties with the same chemical additive and dosage does not ensure that their engineering behaviour will be similar. The original mineralogical composition of the soils and the chemical reactions between chemical additives and clay materials can cause the difference in distinct treated soil behaviours. As a result, it is an important step to incorporate the clay mineralogy along with other soil properties including gradation and plasticity index in the stabilization design methodology (Chiottori, 2008). In order to understand the engineering behaviour of fine grained soils, one should study clay mineralogy in the first step (Wan et al., 2002).

Clay can be defined by considering both the size and class of minerals. Constituents of a soil smaller than a particular size, generally 0.002 mm (2 μm) refer to clay in engineering classifications. Or as a mineral term, clay refers to specific clay minerals which are distinguished by a net negative electrical charge, plasticity when mixed with water, small particle size, and high weathering resistance (Mitchell, 2005). Most clay minerals involve an aluminium-hydroxyl octahedron and a silicon-oxygen tetrahedron as basic

structural units (see Figure 2.1). Both units have valence imbalances which result in net negative charges. Therefore, the basic units combine to form sheet structures and they do not exist in isolation. The sharing of oxygen ions to form a silica sheet is the way of combination of the tetrahedral units. The octahedral units combine by the sharing of hydroxyl ions to form a gibbsite sheet. The gibbsite sheet is electrically neutral whereas the silica sheet retains a net negative charge (Craig, 2004). Stacking of these sheets on top of each other with different ions bonding them together forms various clay minerals (Oweis and Khera, 1998). The synthesis pattern of clays is given in Figure 2.2.

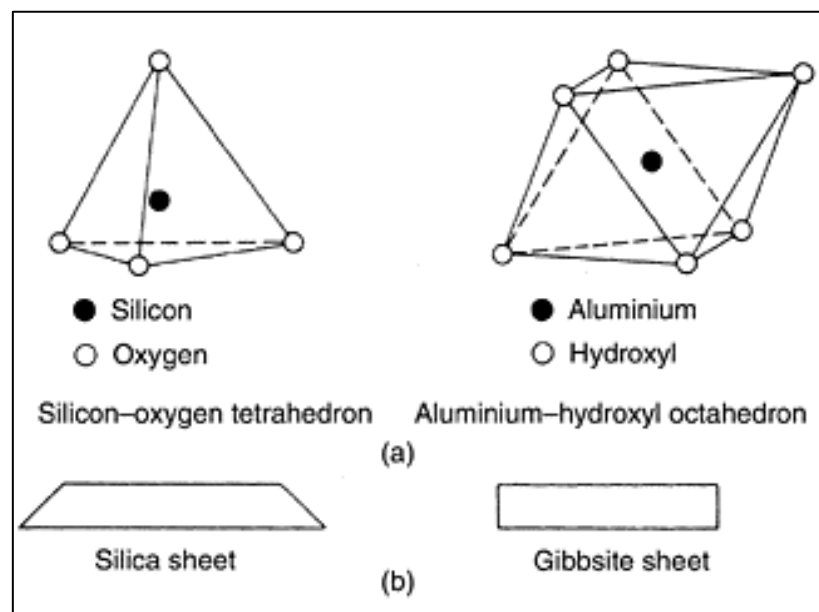


Figure 2.1 Basic Unit of Clay Minerals (Craig, 1997)

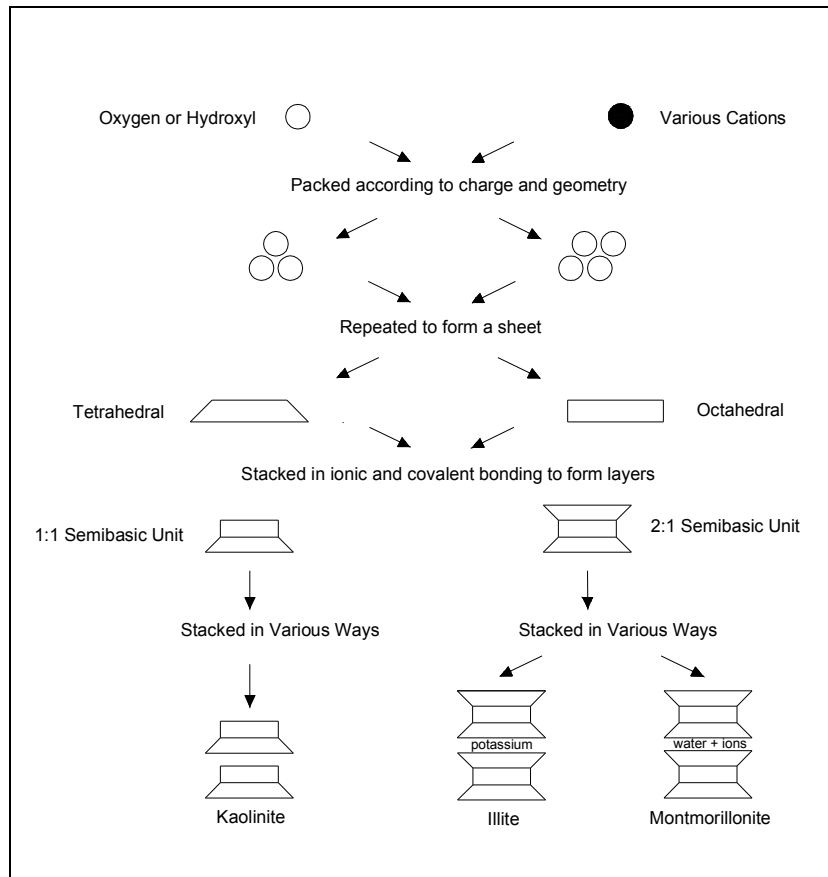


Figure 2.2 Synthesis pattern of Clay Minerals (modified from Mitchell, 2005)

Crystalline structures (Kaolinite, Illite, and Montmorillonite) could be taken into account when dividing clay minerals into three main groups.

2.1.1.1 Kaolinite

A single sheet of silica and a single sheet of gibbsite are combined by relatively strong hydrogen bonding to form kaolinite (Craig, 2004).

Kaolinite yields hydraulic conductivity of a value greater than or equal to 10^{-6} cm/s. It also has a low activity and low liquid limit (Oweis and Khera, 1998). Separation of the layers of Kaolinite is very difficult since they are combined by strong hydrogen bonds. Thus, it is relatively stable and water cannot

penetrate between the layers. As a result of this, little swell of kaolinite is shown on wetting by water (Koteswara, 2011). Structure and scanning electron micrograph of Kaolinite are given in Figures 2.3 and 2.4, respectively.

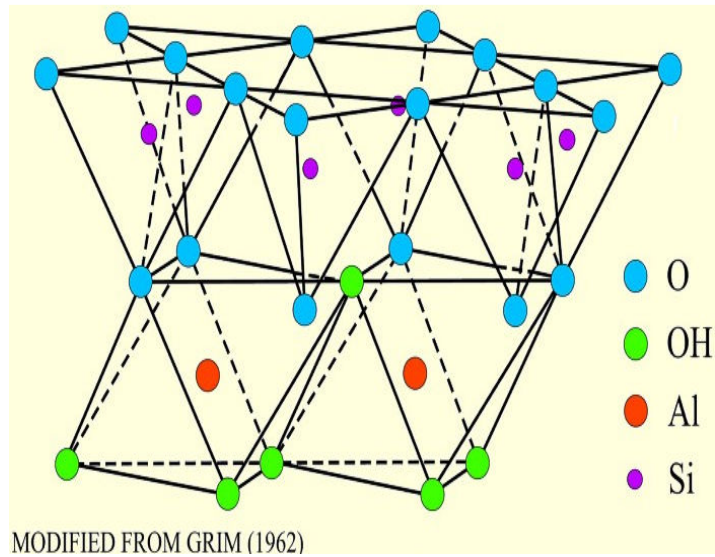


Figure 2.3 Structure of Kaolinite (USGS, 2001)

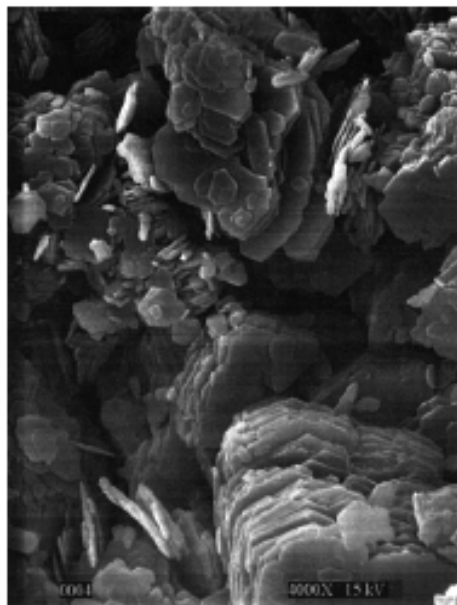


Figure 2.4 Scanning Electron Micrograph of Kaolinite (Murray, 2007)

2.1.1.2 Illite

Illite has basic structure which consists of a gibbsite sheet between and combined with two sheets of silica. Partial substitution of silicon by aluminium is seen in the silica sheet. Bonding that links the combined sheets together is relatively weak since non-exchangeable potassium ions are present between the sheets (Craig, 2004). The cation bond of illite is stronger than the water bond of montmorillonite and weaker than the hydrogen bond of kaolinite (Koteswara, 2011).

Illite's hydraulic conductivity is equal to or smaller than 10^{-7} cm/s and it has a higher liquid limit than kaolinite (Oweis and Khera, 1998). Illite can be expansive but problems posed by them are generally not significant (Nelson and Miller, 1992). Structure and scanning electron micrograph are given in Figures 2.5 and 2.6, respectively.

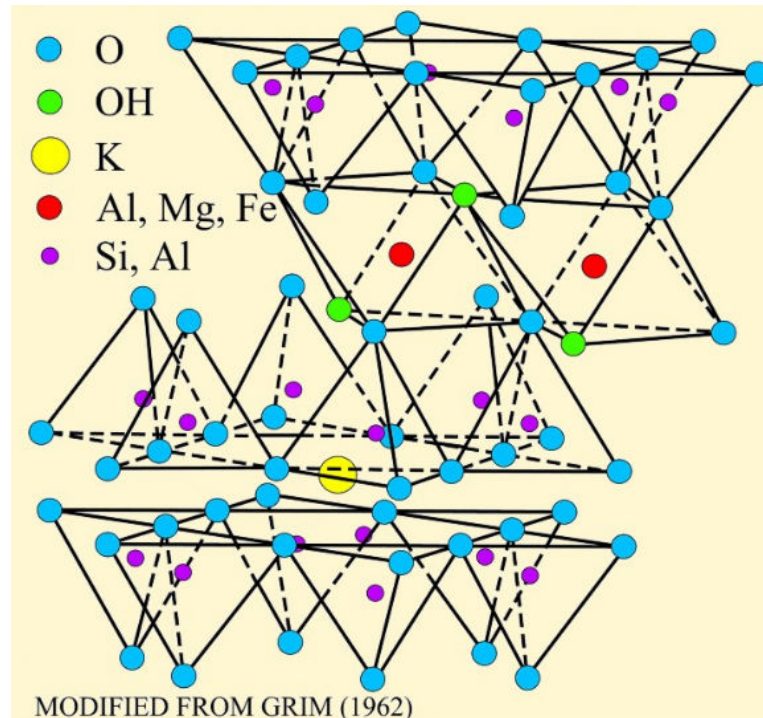


Figure 2.5 Structure of Illite (USGS, 2001)

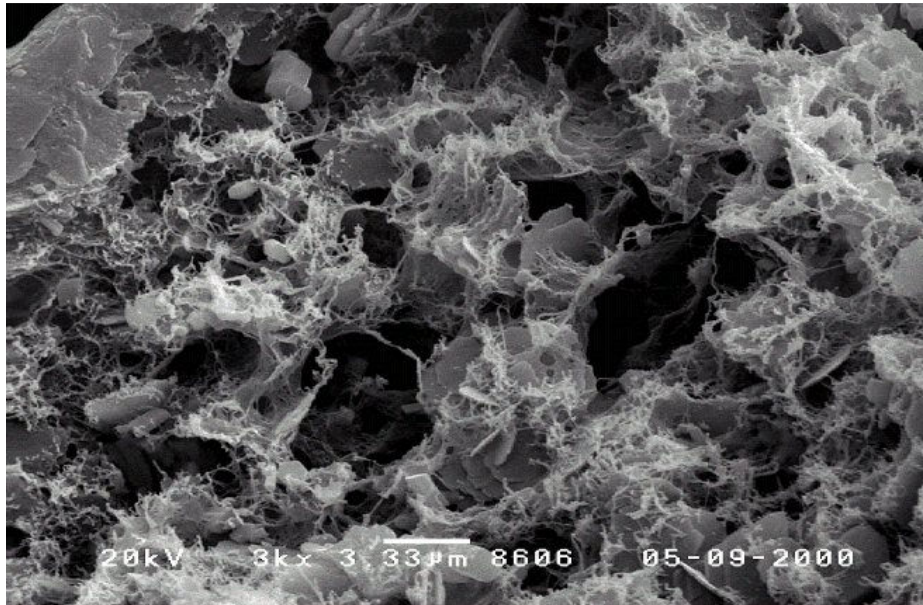


Figure 2.6 Scanning Electron Micrograph of Illite (source: <http://webmineral.com/specimens/picshow.php?id=1284&target=Illite>)

2.1.1.3 Montmorillonite

Montmorillonite is a member of the smectite group. It is formed in marine waters or from weathering of volcanic ash under poor drainage conditions (Oweis and Khera, 1998). Its basic structure is same with illite. Partial substitutions of aluminium by magnesium and iron; and silicon by aluminium are seen in the gibbsite and silica sheets, respectively. A very weak bond, resulted from being occupied of the spaces between combined sheets by exchangeable cations (other than potassium) and water molecules, is formed in the montmorillonite structure (Craig, 2004). The mentioned bond is due to exchangeable cations and Van der Waals forces. Since the bond is very weak, it can be broken by water or other cationic or polar organic fluids which enter between the sheets. An important amount of charge deficiency is observed due to extensive substitution of silica and alumina. The layers yield much smaller particles with a very large specific surface and expand much as a result of easy entrance of water between them. In this clay group, montmorillonite has the highest liquid limit, activity, and swelling potential

(Oweis and Khera, 1998). Structure and scanning electron micrograph of montmorillonite are illustrated in Figures 2.7 and 2.8, respectively.

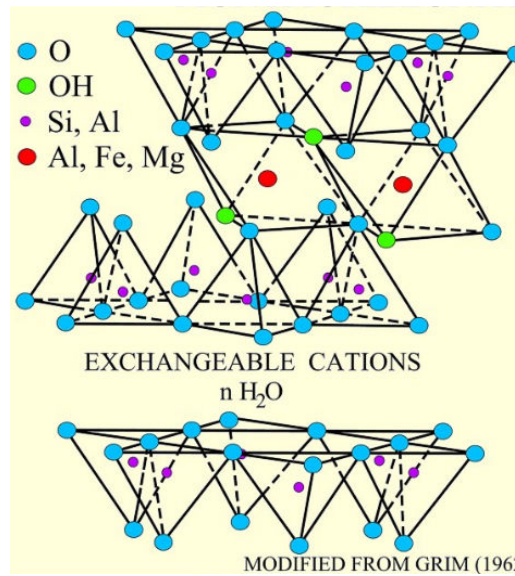


Figure 2.7 Structure of Montmorillonite (USGS, 2001)

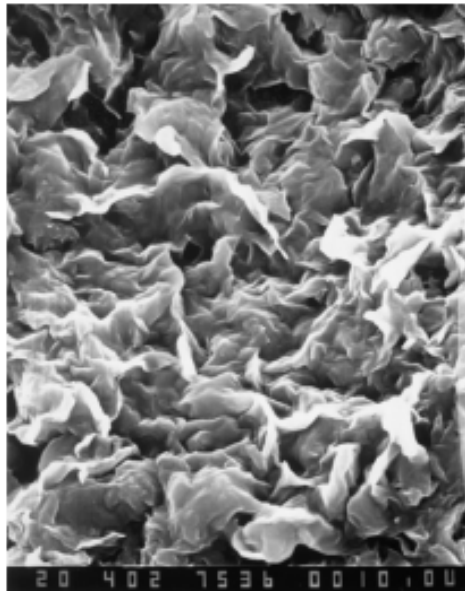


Figure 2.8 Scanning Electron Micrograph of Sodium Montmorillonite (Murray, 2007)

2.1.2 Factors Influencing Swelling

According to Nelson and Miller (1992), swelling mechanism of expansive clays is complex and is influenced by some factors. Many of these factors also affect physical soil properties (such as plasticity and density) or are affected by them. Shrink-swell potential of a soil is considered to be influenced by the factors which can be considered in three different groups. These groups can be listed as follows:

- **Soil Characteristics:** Characteristics of soil by which the basic nature of the internal force field is influenced.
- **Environmental Factors:** Changes that may occur in the internal force system can be influenced by some environmental factors. These factors also influence the shrink-swell potential of a soil.
- **State of Stress**

The aforementioned factors are given in Tables 2.1, 2.2 and 2.3, in short.

Table 2.1 Soil Properties that influence shrink-swell potential
(Nelson and Miller, 1992)

Clay Mineralogy	Montmorillonites, vermiculites, and some mixed layer minerals cause volume changes. Although Illites and Kaolinites are usually nonexpansive, these minerals cause volume changes when particle sizes are extremely fine
Soil Water Chemistry	Swelling is decreased by the increase in cation concentration and cation valence. For example, Mg^{+2} cations in the soil water would result in less swelling than Na^{+} ions.
Soil Suction	Soil suction is an independent effective stress variable, represented by the negative pore pressure in unsaturated soils. Soil suction is related to saturation, gravity, pore size and shape, surface tension, and electrical and chemical characteristics of the soil particles and water.
Plasticity	In general, soils that exhibit plastic behavior over wide ranges of moisture content and that have high liquid limits have greater potential for swelling and shrinking. Plasticity is an indicator of swell potential.
Soil Structure and Fabric	Flocculated clays tend to be more expansive than dispersed clays. Cemented particles reduce swell. Fabric and structure are altered by compaction at higher water content or remolding. Kneading compaction has been shown to create dispersed structures with lower swell potential than soils statically compacted at lower water contents.
Dry Density	Higher densities usually indicate closer particle spacings, which may mean greater repulsive forces between particles and larger swelling potential.

Table 2.2 Environmental Conditions that influence shrink-swell potential
(Nelson and Miller, 1992)

Initial Moisture Conditioning	A desiccated expansive soil will have a higher affinity for water, or higher suction, than the same soil at higher water content, lower suction
Climate	Amount and variation of precipitation and evapotranspiration greatly influence the moisture availability and depth of seasonal moisture fluctuation. Greatest seasonal heave occurs in semiarid climates rather than those with pronounced, short wet periods
Groundwater	Shallow water tables provide a source of moisture and fluctuating water tables contribute to moisture
Drainage and manmade water sources	Surface drainage features, such as ponding around a poorly graded house foundation, provide sources of water at the surface; leaky plumbing can give the soil access to water at greater depth.
Vegetation	Trees, shrubs, and grasses deplete moisture from the soil through transpiration, and cause the soil to be differentially wetted in areas of varying vegetation
Permeability	Soils with higher permeabilities, particularly due to fissures and cracks in the field soil mass, allow faster migration of water and promote faster rates of swell
Temperature	Increasing temperatures cause moisture to diffuse to cooler areas beneath pavements and buildings

Table 2.3 Stress Conditions that influence shrink-swell potential
(Nelson and Miller, 1992)

Stress History	An overconsolidated soil is more expansive than the same soil at the same void ratio, but normally consolidated. Repeated wetting and drying tend to reduce swell in laboratory samples, but after a certain number of wetting-drying cycles, swell is unaffected.
In Situ Conditions	The initial stress state in a soil must be estimated in order to evaluate the probable consequences of loading the soil mass and/or altering the moisture environment therein. The initial effective stress can be roughly determined through sampling and testing in a laboratory, or by making in situ measurements and observations
Loading	Magnitude of surcharge load determines the amount of volume change that will occur for a given moisture content and density. An externally applied load acts to balance interparticle repulsive forces and reduces swell
Soil Profile	The thickness and location of potentially expansive layers in the profile considerably influence potential movement. Greatest movement will occur in profiles that have expansive clays extending from the surface to depths below the acting zone. Less movement will occur if expansive soil is overlain by nonexpansive material or overlies bedrock at a shallow depth

2.2 Soil Stabilization

2.2.1 Chemical Stabilization

The soil may be removed and replaced with a competent fill where the soil layer that has expansive characteristics is shallow. The structure is articulately designed to withstand the expected heave or appropriate soil treatment is carried out to reduce the heave magnitude in the case where the expansive layer extends to a larger depth. Removal of the soil and an articulate design of the structure are expensive works to carry out. Therefore, a practical and economical approach, stabilization of soil, becomes an attractive alternative in various cases (Al-Mhaidib and Al-Shamrani, 1996). The oldest and widespread method of ground improvement is using chemical admixtures for soil stabilization (Chen, 1975). To stabilize expansive soils, generally, lime, cement and fly ash are used as admixtures. Physical and chemical conditions of the natural soil, workability of agent, economic and safety constraints, and specific conditions of the construction are the factors that affect the application of these agents (Fang, 1991).

2.2.2 Lime Stabilization

Stabilizing subgrade soil by using lime is a well-known method all over the world for a long time (Chen, 1975). Three basic chemical reactions occur when lime and pozzolonic clays are mixed in presence of water. These reactions are cation exchange and flocculation-agglomeration, cementation (pozzolanic reaction) and carbonation (Fang, 1991).

2.2.2.1 Cation Exchange and Flocculation-Agglomeration

The replacement of univalent sodium (Na^+) and hydrogen (H^+) ions of soil with divalent (Ca^{2+}) calcium ions of lime results in cation exchange and flocculation-agglomeration reactions. Clay content and plasticity is bound by these reactions. Agglomeration reaction of lime and soil is used to destroy collapsible characteristics of some silts (Fang, 1991).

2.2.2.2 Cementation or Pozzolanic Reactions

Soil-lime pozzolonic reactions are the ones which occur between lime, water, and soil silica and alumina to form cementing material types. In nature, sources of alumina and silica may possibly be clay minerals, quartz, feldspars, micas, and other silicates or alumino-silicate minerals, either crystalline or amorphous. The clay minerals are crucial sources because lime is effective as a stabilizer only in soils which contain clay. Sufficient addition of lime to a soil results in an increase in the pH of the soil-lime mixture. Hence, the solubility of silica, alumina, and clay minerals is also increased. Therefore, these materials become available for reacting with lime. A simplified qualitative representation of some typical soil-lime reactions are presented below. (Walker et al, 1992)



2.2.2.3 Carbonation

Carbonation is seen when the lime added to soil draws CO_2 from air or soil to form CaCO_3 instead of reacting with soil. This situation is observed when excessive amount of lime is added or insufficient amount of pozzolonic clay presents in the soil. CaCO_3 is a plastic material and increases the soil

plasticity. It also binds lime so that reactions between lime and pozzolanic materials can not occur. Therefore, beneficial results are not produced in the case of addition of excessive lime (Fang, 1991).

2.2.3 Fly Ash Stabilization

Fly ash is obtained by collecting the fine residues stemmed from the burning of pulverized coal in thermal power plants (Ji-Ru and Xing, 2002).

It is endeavoured to make use of fly ash as much as possible since this helps in abating the disposal problems. Low unit weight, low compressibility and pozzolanic reactivity are the properties which make fly ash an important agent for geotechnical engineering. Pozzolanic property makes fly ashes a valuable stabilizing agent for soils. The pozzolanic reactivity of fly ash is affected by its reactive silica, free lime content, fineness, carbon content and iron (Sivapullaiah et al., 1998). Although for lime treatment of soils, pozzolanic reactions depend on the aluminous and siliceous materials provided by soil, for class C fly ash, the calcium oxide of the fly ash can react with the aluminous and siliceous materials of the fly ash itself (Şenol, 2003). Treatment of expansive soils by using fly ash is shown to be appropriate in the previous studies (Sivapullaiah et al., 1998; Nalbantoğlu & Güçbilmez, 2001; Çokça, 2001; Ji-Ru and Xing, 2002; Nalbantoğlu, 2004; Phanikumar and Sharma, 2007; Zha et al., 2008).

CHAPTER 3

FLY ASH

3.1 General

Ever increasing demand for electricity is met by burning large quantities of coal in thermal power plants. A residue consisting of inorganic mineral constituents and partially-burned organic matter remains after the combustion of coal. The inorganic mineral constituents form ash of which 80% is fly ash (Sivapullaiah et al., 1998).

Recycling of by-products and wastes becomes an increasingly important problem for the near future day by day. Considerable amount of coal fly ash is produced in Turkey and it is accepted as one of the major wastes (Erol et al, 2006). In Turkey, 11 thermal power plants are in operation namely; Afşin-Elbistan, Çatalağzı, Çayırhan, Kangal, Kemerköy, Orhaneli, Seyitömer, Soma, Tunçbilek, Yatağan and Yeniköy. The amount of fly ash produced in each year in these power plants is averagely 16 million tons by the year 2006 (Turker et al., 2009).

Deposition of these wastes could cause air, water and soil pollution that have negative impacts on human health. Representative figure showing coal ash pollution chain prepared by Greenpeace (2010) is given below (Figure 3.1).

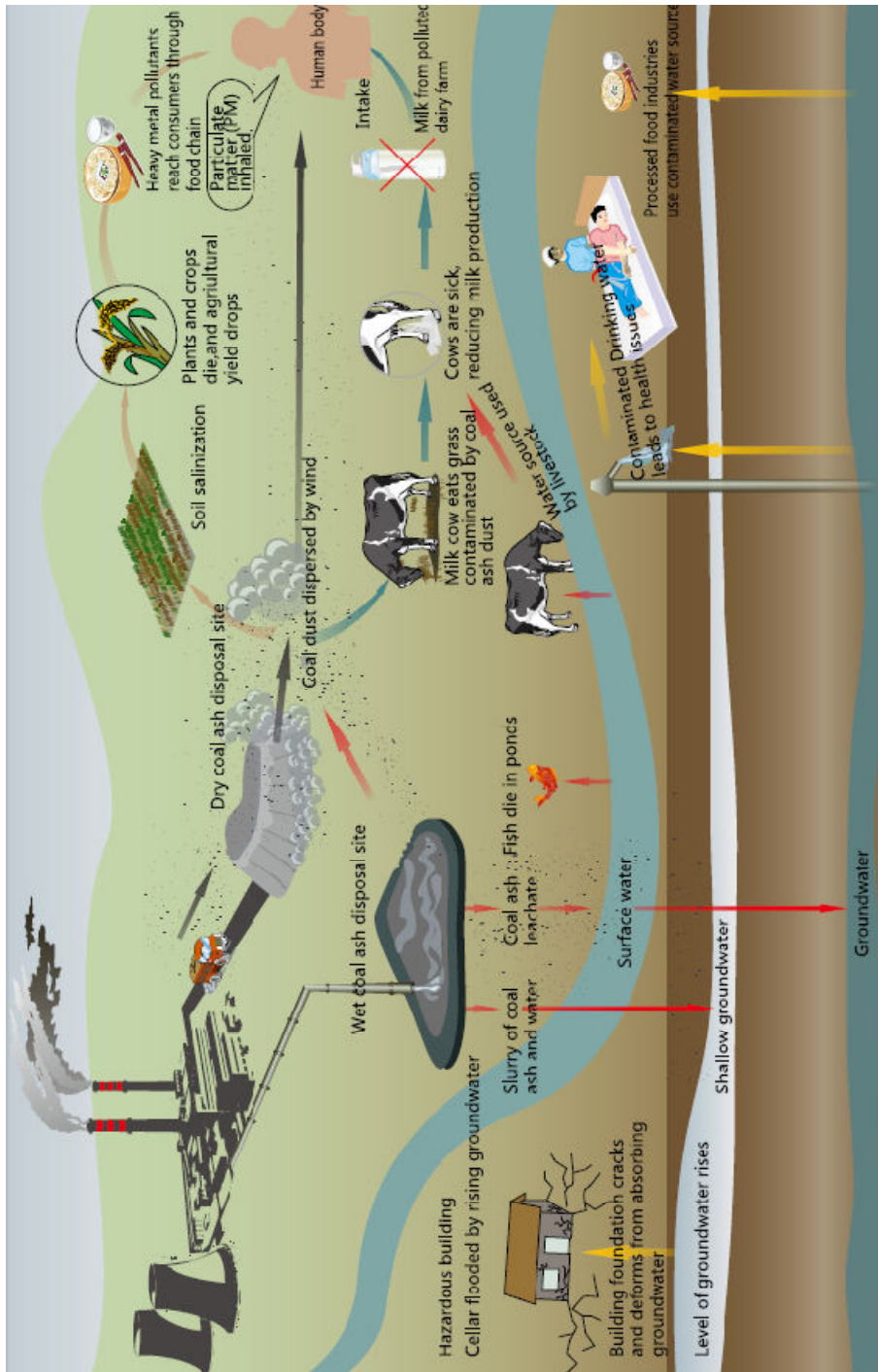


Figure 3.1 Coal Ash Pollution Chain (Greenpeace,2010)

3.2 Factors that influence Fly Ash Properties

The fly ash properties are influenced by several factors and it could change in the same power plant even in the same day because of the change in loading conditions (Görhan, 2009). The primary affecting factors include the coal source and boiler & emission control design. The mineralogy and specific fly ash sources' properties are affected by these factors (Mackiewicz and Ferguson, 2005).

3.2.1 Coal Source

The type and amount of inorganic matter within the coal and the constituents within the fly ash are dictated by the coal source. The produced ash does not show self-cementing properties since bituminous and many lignite coals have low concentrations of calcium compounds. Typically, higher concentrations of calcium carbonate is observed in subbituminous coals and the produced fly ash contains 20 to 30% calcium compounds (Mackiewicz and Ferguson, 2005).

3.2.2 Boiler and Emission Control Design

As the chemical constituents of a particular fly ash are dictated by the coal source, crystalline compounds existing in fly ash are also highly influenced by boiler and emission control design as well as plant operation. The rate at which the fused particles are cooled dictated the fly ash hydration characteristics. The inorganic matter existing in the coal is fused and transported from the combustion chamber during combustion. These small particles are suspended in the exhaust gases. Rapid cooling of the mentioned particles results in a noncrystalline (glassy) or amorphous fly ash structure. Whereas, when the particles are cooled at a slower rate, the structure of the produced fly ash is more crystalline. As the self-cementing characteristics of the fly ash is provided by the crystalline compounds, the degree of crystallinity, which in

turn determines the specific fly ash sources' hydration characteristics, is influenced by the boiler and emission control design as well as plant operation (Mackiewicz and Ferguson, 2005).

3.3 Classification of Fly Ashes

According to ASTM C-618-08a (Standard Specification for Coal Fly Ash and Raw or Calcined Natural Pozzolan for Use in Concrete), fly ashes are divided into two classes. These classes are named as Class F and Class C and they are explained below.

- **Class F:** Production of Class F fly ash is typically made by burning bituminous coal or anthracite. It can also be produced from lignite and subbituminous coal. Pozzolanic properties are exhibited by this class of fly ash but it has no self-cementing properties. This material can be used for many soil stabilization applications by adding some activators (lime etc.) into fly ash to obtain cementitious properties.
- **Class C:** Typically, burning of lignite or subbituminous coal results in Class C type of fly ash. This class can also be produced from anthracite or bituminous coal. Total calcium content, expressed as calcium oxide (CaO), of this type of fly ash is more than 10%. In addition to having pozzolonic properties, Class C fly ash also has some cementitious properties.

In this study, Fly Ash taken from Soma Thermal Power Plant is used.

3.4 Soma Thermal Power Plant

Soma Thermal Power Plant is located in Manisa Province, Soma District. It is 90 and 130km away from Manisa and İzmir respectively (Direskeneli, 2007). With an installed capacity of 1034 MW, Soma thermal power plant consumes 30,000 tons of low-quality lignite obtained from the reserves of Soma basin

and approximately 12,000 tons of fly ash is produced per day. Conveyor belts which are nearly 10 km in length are utilized to transport the solid waste to the disposal site. Spreading of ash by wind is prevented by damping the solid waste by using nozzle on the conveyor. Furthermore, water is added to the waste at the disposal site so that a slurry pond is formed. Approximately 7 liters of water is needed to sluice 1 kg of coal ash obtained from the Soma thermal power plant (Baba and Kaya, 2003).

In Turkey, ponds are not frequently used since they require considerable amount of area and they cause water quality deterioration of sluicing waters. However, Soma thermal power plant has a large ash pond. This pond is used as the ultimate waste disposal site (Figure 3.2) (Baba and Kaya, 2003).



Figure 3.2 Ash Disposal Site of Soma Thermal Power Plant
(Baba and Kaya, 2003)

Soma Fly Ash is generally classified as Class C according to ASTM C618-08a. The scanning electron micrograph of Soma Fly ash is shown in Figure 3.3.

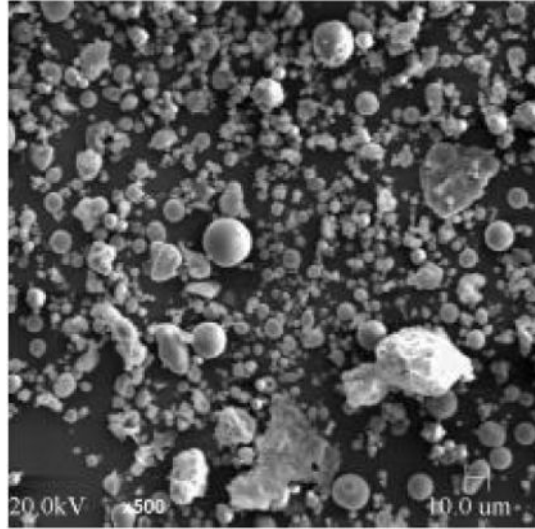


Figure 3.3 Scanning Electron Micrograph of Soma Fly Ash (Çelik, 2004)

3.5 Utilization of Fly Ash

Solid waste disposal is a costly procedure thus an increased awareness of using beneficial technologies has been seen recently (Santos, 2011). In many areas such as; waste stabilization, mining applications, soil modification, cement-concrete-grout production (as a pozzolan and admixture) and road construction, fly ash can be utilized. Fly ash production and utilization is increasing every year in USA. Graphs that show the annual production and usage amounts of fly ash (Figure 3.4) and the annual percent usage (Figure 3.5) values between the years 1980-2009, prepared by utilizing the data that was published in 2011 by the American Coal Ash Association (ACAA). According to this data, fly ash production increased from 48.30 million tons to 63.00 million tons, fly ash usage increased from 6.82 million tons to 24.72 million tons and percent usage increased from 13.3 % to 39.2 %.

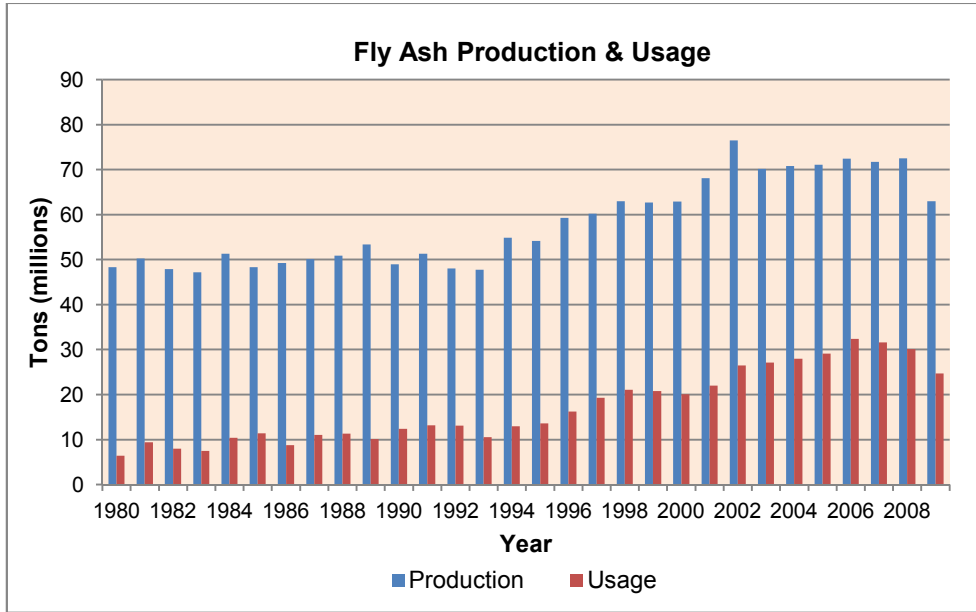


Figure 3.4 Fly Ash production and utilization statistics for USA
(adapted from American Coal Ash Association, 2011)

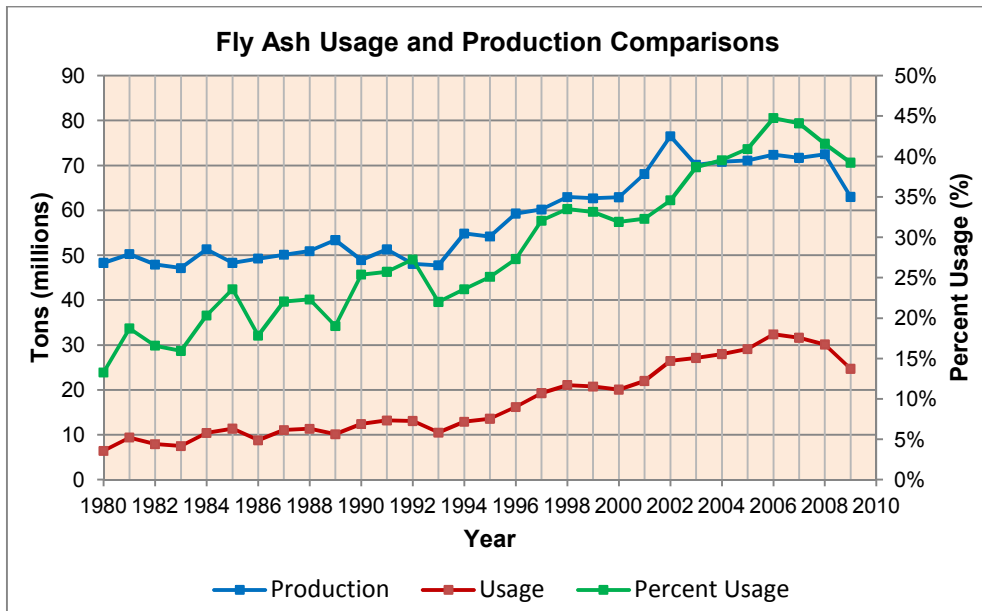


Figure 3.5 Fly Ash production and utilization comparison for USA
(adapted from American Coal Ash Association, 2011)

Also share of fly ash usage in different areas in USA by the year 2009 are tabulated in Table 3.1. This table is prepared again by utilizing the data that was published in 2011 by the American Coal Ash Association (ACAA). In this table percent utilization values are calculated in two different ways by means of using total fly ash usage (24.72 millions tons) and total production (63 million tons) amounts.

Table 3.1 Utilization of Fly Ash by 2009 in USA (ACAA, 2011)

Utilization Area	Utilization (million tons)	Percent Utilization (%) (based on)	
		Total Usage	Total Production
Concrete/Concrete Products /Grout	9.80	39.64	15.55
Blended Cement/ Raw Feed for Clinker	2.44	9.86	3.87
Flowable Fill	0.26	1.07	0.42
Structural Fills / Embankments	4.65	18.80	7.38
Road base / Sub-base	0.20	0.80	0.32
Soil Modification / Stabilization	0.67	2.71	1.06
Blasting Grit/ Roofing Granules	0.05	0.19	0.08
Mining Application	2.15	8.69	3.41
Waste Stabilization / Solidification	3.52	14.22	5.58
Agriculture	0.10	0.42	0.16
Aggregate	0.09	0.35	0.14
Miscellaneous / Other	0.80	3.25	1.27
Total	24.72	100%	39.24%

According to this data, by the year 2009, 2.71 % of the total used and 1.06 % of the total produced fly ash was utilized for soil stabilization in USA.

CHAPTER 4

PREVIOUS STUDIES ON CYCLIC SWELL-SHRINK BEHAVIOUR OF SOILS

4.1 General

In the previous studies two methods have been used for determining the cyclic swell-shrink behavior of expansive soils. These are the full swell-full shrink and full swell-partial shrink (Güney et al., 2007)

Full Swell-Full Shrink: Samples are allowed to swell until the primary swell completed or no more swell is observed, and dried fully or until the water content comes below the shrinkage limit.

Full Swell-Partial Shrink: Samples are allowed to swell until the primary swell completed or no more swell is observed, and dried to their initial moisture content.

4.2 Studies on Nonstabilized Soils

Day, (1994) performed cyclic swell-shrink tests on silty clay soil with liquid and plastic limits of 46% and 24%, respectively. Full swell-full shrink tests were conducted where the soils were allowed to dry below their shrinkage limit. The author found out that full swell-full shrink cycles caused an increase in swell potential and this increase was explained by destruction of the flocculated structure of clay and formation of more expansive and permeable soil having a dispersed structure.

In the study performed by Al-Homoud et al, (1995), expansive characteristics of soils which were exposed to swell-shrink cycles were investigated. Tests were conducted on six different soils with liquid, plastic, and shrinkage limits varying between 65-90%, 15-40% and 10-20%, respectively. During the experiments full swell-partial shrink method were used. The results showed that as the number of cycle increases, swell potential decreases. Furthermore, it was noted that first cycle caused the maximum reduction in swelling potential and swell percent reached to equilibrium after conducting 4-5 cycles. The authors explained the swell reduction with the soil particles' rearrangement.

Basma, (1996) studied on four different soils to determine the effect of cyclic swell-shrink on expansive soils. Both partial and full shrink methods were applied. For partial shrink, samples were allowed to dry at room temperature, and for full shrink, samples were exposed to sunlight. The results of the experiments showed that an increase in the swell potential was observed after full shrink and a decrease was seen after partial shrink. Swell potential came to a constant value at the end of 4-5 cycles. Apart from the other researchers, Basma (1996) performed ultra sound investigation test on samples, and found out that void ratio of samples that were exposed to full shrink cycles increased and that of ones which were exposed to partial shrink cycles decreased.

Doostmohammadi et al, (2009) investigated the effect of cyclic wetting – drying on swelling potential and swelling pressure of mudstone composed of sediments with silt and clay sized particles. Full swell-full shrink tests were applied on samples and the results showed that both swell potential and pressure increased. The tested samples were taken from an area where the hydroelectric power plant called Masjed-Soleiman had been constructed. Power house of that project intersected with mudstone interlayers. In order to monitor the swell pressure on concrete linings, during construction of the power house, total pressure cells were installed behind linings. Records were taken during six years period to evaluate the cyclic swell-shrink behavior of mudstone (Figure 4.1). The results of the laboratory and field tests were consistent in showing an increase in swell potential after cyclic wetting-drying.

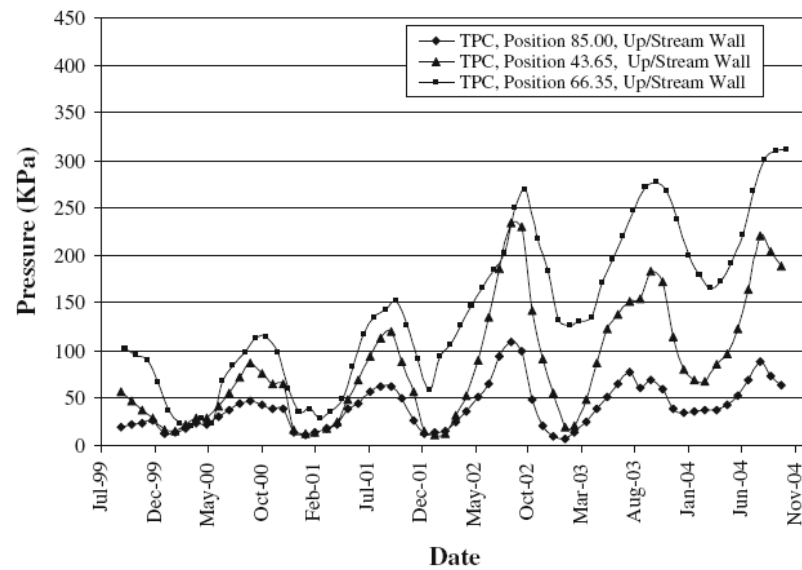


Figure 4.1 Total pressure cells data for the Power House linings of Masjed-Soleiman Hydroelectric Power Plant Project (Doostmohammadi, 2009)

Tawfiq & Nalbantoğlu, (2009), studied the effect of the cyclic wetting and drying on the swelling behavior of a natural expansive soil with liquid limit and plasticity index values of 64% and 36%, respectively. During the experiments both full swell-full shrink and full swell-partial shrink methods were applied. Results of the experiments showed that swell potential increased after full swell-full shrink cycles and decreased after full swell-partial shrink cycles. Authors explained the swell potential increase after full shrink cycles with the decrease in the water content and development of macro cracks at the end of the second cycle that allowed water to penetrate into soil pores. Also, swell potential decrease due to partial shrink method was explained by the high water content existing before the wetting procedure. For the full swell –full shrink and full swell-partial shrink cycles swell potential come into equilibrium after the fifth and the first cycle, respectively (Figure 4.2).

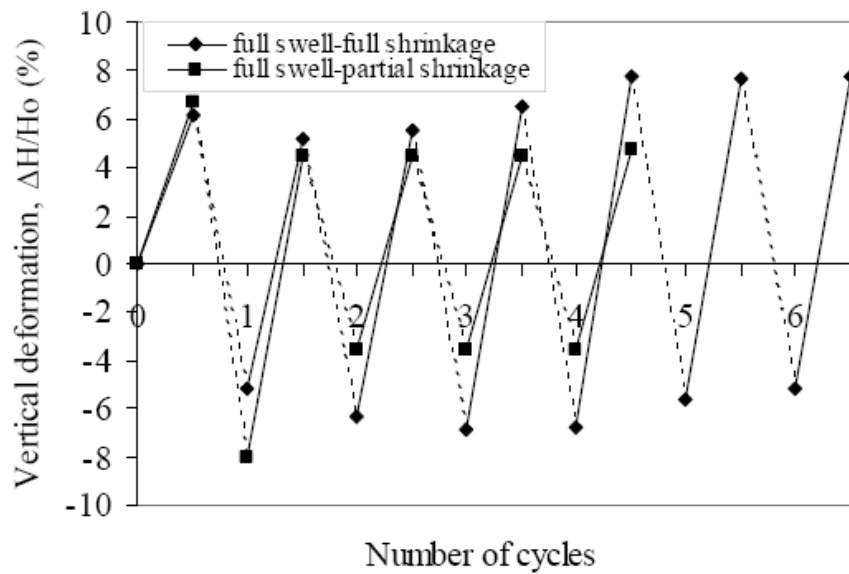


Figure 4.2 Effect of full swell-full shrink and full swell-partial shrink on swell potential of an expansive soil (Tawfiq & Nalbantoğlu, 2009)

Tripathy & Rao, (2009) carried out cyclic swell–shrink tests under 50 kPa of surcharge pressure on a compacted expansive clay with liquid limit and plasticity index of 100% and 58%, respectively. In this study, both of the shrinkage methods were used as that of Tawfiq & Nalbantoğlu, (2009) studies. Increase in swell potential was observed after full shrink cycles even after the first cycle and swell potential decreased for partial shrink cycles. Swell potential came into equilibrium after five or more cycles.

Türköz, (2009) conducted tests on an expansive soil obtained by mixing different percentages of bentonite with high plasticity Silty Clay to determine the effect of wetting-drying on microstructure. Samples were allowed to swell fully and than dried to shrinkage limit. Only the swell values were presented in the study. Swell percentages could not be presented due to the deformations occurred on the surface of samples during drying. The results showed that after each cycle, swell amount decreased. The reduction was explained by the flocculation of particles.

In addition to these researchers, the studies of Popesco (1980) and Osipov et al. (1987) on nonstabilized soils showed that full swell-full shrink cycles caused an increase in the swelling potential of soils and also the studies of Chen (1965), Chen et al. (1985) and Dif and Blumel (1991) showed that reduction occurred in swelling potential of expansive soils that exposed to full swell-partial shrink cycles (Basma, 1996).

The summary of the swell-shrink procedures applied by different researchers to see the effect of wetting-drying cycles on swelling properties of non-stabilized expansive soils is presented in Table 4.1

The previous studies indicate that there occurs an increase in swelling potential of expansive soils that were exposed to full swell-full shrink cycles. A reduction in swell potential is seen for the soils that were exposed to full swell-partial shrink cycles.

Table 4.1 Swell-Shrink Procedures applied on nonstabilized expansive soils in previous studies by different researchers

Authors	Swell-Shrink Method	Swell Procedure	Shrinkage Procedure
Day,(1994)	F _{Sw} -F _{Sh} *	At least until primary swell completed (1.5 days)	Exposed to sunshine at summer (2.5 days)
Al-Homoud et al, (1995)	F _{Sw} -P _{Sh} **	At least until primary swell completed (at least 40 hrs)	Dried at laboratory environment (1 day)
Basma, (1996)	F _{Sw} -P _{Sh}	Until full swell completed (24 hours)	Dried at room temperature (1 day)
	F _{Sw} -F _{Sh}		Exposed to sunshine (1.5 days)

Table 4.1 Swell-Shrink Procedures applied on nonstabilized expansive soils in previous studies by different researchers (continued)

Authors	Swell-Shrink Method	Swell Procedure	Shrinkage Procedure
Doostmohammadi et al, (2009)	F _{Sw} -F _{Sh}	Until full swell completed	Dried at 40°C until reaching of a constant strain value
Tawfiq & Nalbantoğlu, 2009	F _{Sw} -P _{Sh}	Until full swell completed (4 days)	Dried at 40±3°C) (3 days and 8 days for partial and full shrinkage)
	F _{Sw} -F _{Sh}		
Tripathy & Rao, (2009)	F _{Sw} -P _{Sh}	Until full swell completed (3 days)	Dried at 40±5°C (0.5- 1.0 day)
	F _{Sw} -F _{Sh}		Dried at 40±5°C (4 days)
Türköz (2009)	F _{Sw} -F _{Sh}	Until 91% of full swell completed (1 day)	Dried at 105 °C (1 day)

*Full Swell-Full Shrink ** Full Swell-Partial Shrink

4.3 Studies on Stabilized Soils

Rao et al, (2001) studied the effect of wetting-drying cycles on the lime-treated soil's index properties. Hydrometer and Atterberg limit tests were applied to lime-treated soil. Hydrated lime was used in the experiments with the percentages 2%, 4% and 7%. Full swell-full shrink method was used and specimens were exposed to 20 wetting – drying cycles during the tests. At the end of the experiments, clay content and liquid limit increased and plastic limit and shrinkage limit of treated samples decreased (Figures 4.3 and 4.4). The author explained the corresponding increase and reduction in the index properties by breakdown of cementation and flocculation of particles and by the increase in the thickness of diffuse double layer.

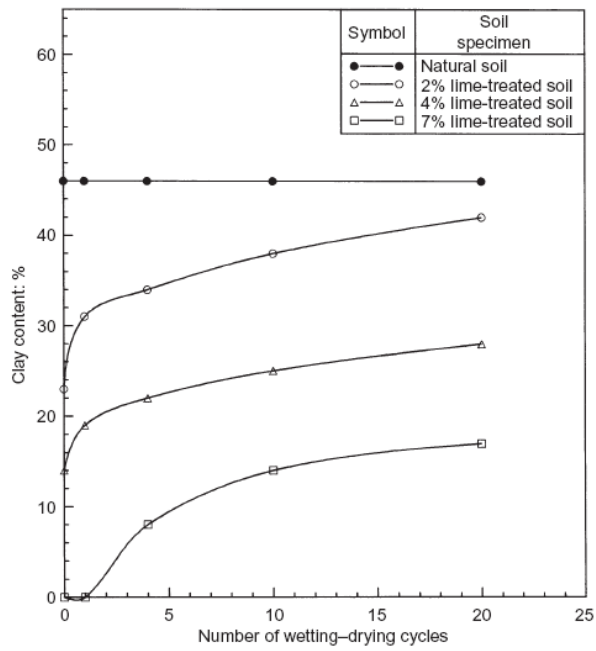


Figure 4.3 Effect of wetting-drying cycles on clay content of lime treated soils (Rao, 2001)

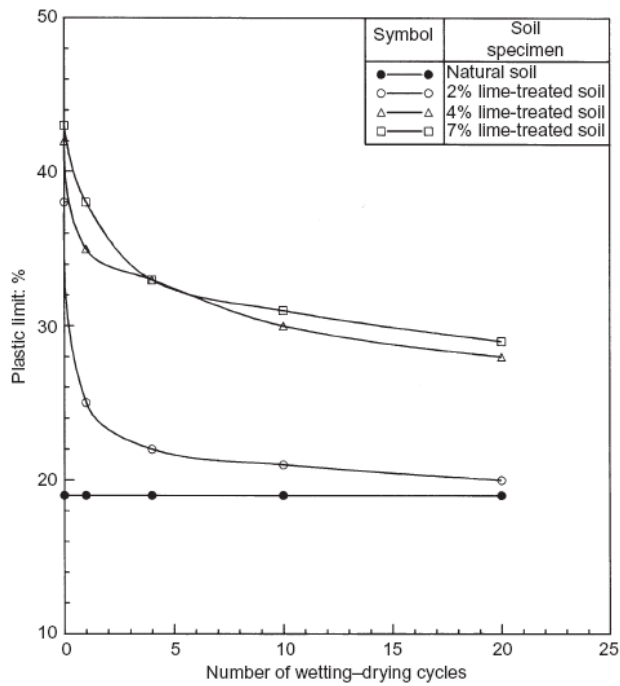


Figure 4.4 Effect of wetting-drying cycles on plastic limit of lime treated soils (Rao, 2001)

Another study was also performed by Rao et al, (2001) on lime-treated expansive soils. This time, the effect of cyclic wetting – drying cycles on swell potential of lime treated expansive soils was investigated. Full swell-full shrink method was used as in the previous study. The results of the experiments indicated that the effect of lime treatment was partially reduced after four wetting-drying cycles.

Güney et al, (2007) also conducted cyclic swell – shrink tests to determine the long term behavior of lime-treated clayey soils. During the tests, samples were dried to their initial moisture content. Tests were carried out on three different soils. During the study two different proportions of lime; 3% and 6%, were used. Properties of the materials that were used in this study are presented in Table 4.2.

Table 4.2 Properties of the materials used in Güney et al, (2007) studies.

Sample	Liquid Limit (%)	Plastic Limit (%)	Plasticity Index (%)	Shrinkage Limit (%)
Soil A	385	35	350	23
Soil A + 3L	360	45	315	26
Soil A + 6L	255	57	198	29
Soil B	168	28	140	27
Soil B+ 3L	160	37	123	30
Soil B + 6L	140	45	95	35
Soil C	115	45	70	25
Soil C + 3L	104	49	55	41
Soil C + 6L	103	50	53	58

At the end of the tests, swell potential of Soils A and B reduced in the first cycle and reached to equilibrium after the fourth cycle. However, swell potentials of 3% and 6% lime treated soils increased (Figure 4.5).

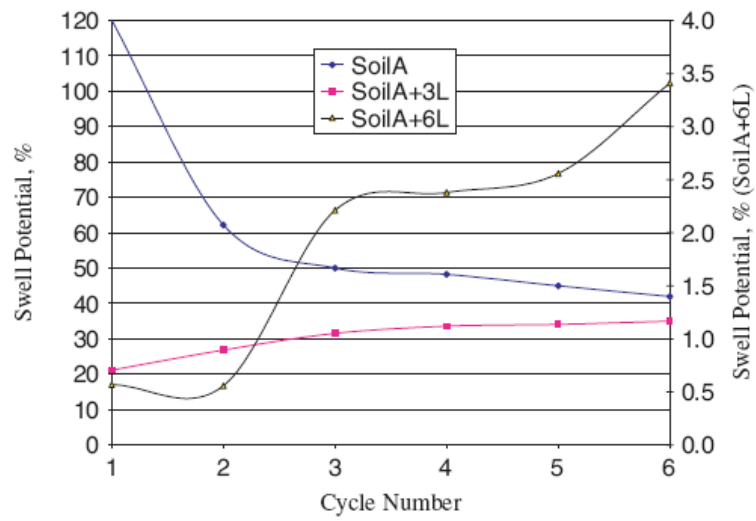


Figure 4.5 Change of Swell Percent for Soil A and lime treated Soil A. (Güney et al, 2007)

Soil C and lime treated Soil C samples showed similar behaviour at the end of the test. For all of the specimens, swelling percent decreased after wetting and drying cycles (Figure 4.6).

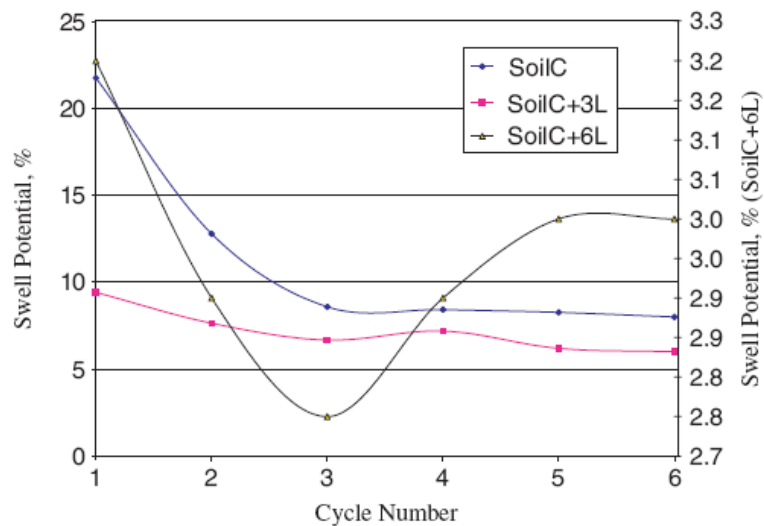


Figure 4.6 Change of Swell Percent for Soil C and lime treated Soil C. (Güney et al, 2007)

Rao A. & Rao M., (2008) investigated the effect of cyclic drying-wetting on the swelling behavior of expansive soil stabilized by using fly ash cushions (Figure 4.7) that were treated with cement and lime. Full swell-full shrink procedure was applied during the tests. Reduction in swell potential was observed at the end of the tests. The reduction in swell potential increased with an increase in cushion thickness. Also fly ash cushions treated with cement showed more reduction in heave compared to the ones treated with lime. Swell potential reached to equilibrium after three and four cycles for the fly ash cushions treated with cement and lime, respectively.

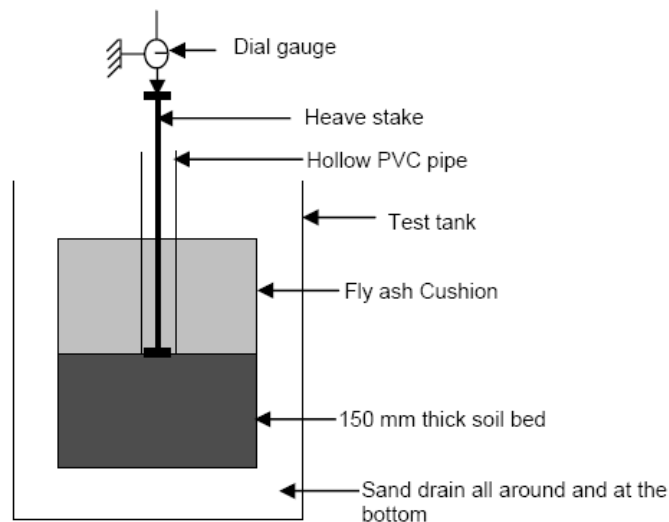


Figure 4.7 Experimental set up used in Rao A.& Rao M.,(2008) studies

In the study performed by Akcanca & Aytekin, (2011), effects of wetting – drying cycles on the lime treated samples prepared by mixing sand and bentonite in different percentages were investigated. Only swell pressure tests were performed and samples were allowed to dry until their moisture content reaches to a value slightly smaller than their initial moisture content. Test results showed that there was a partial loss of the beneficiary effect of chemical treatment (Figure 4.8).

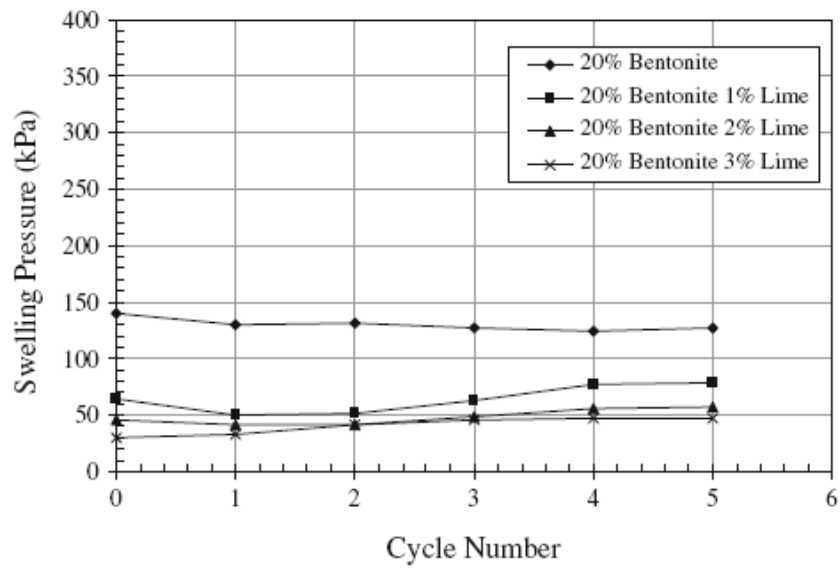


Figure 4.8 Cyclic swell-shrink behavior of samples containing 20% bentonite treated with lime (Akcanca & Aytikin, 2011)

Kalkan, (2011) studied the effect of cyclic swell-shrink on natural expansive clay samples stabilized by silica fume. During the experiments full swell-partial shrink procedures were applied. An improvement in the durability of treated samples against wetting-drying was observed at the end of the tests. Furthermore, the results of the experiments showed that as the percent of the stabilizer increased, swell potentials of samples reached to equilibrium more rapidly (Figure 4.9).

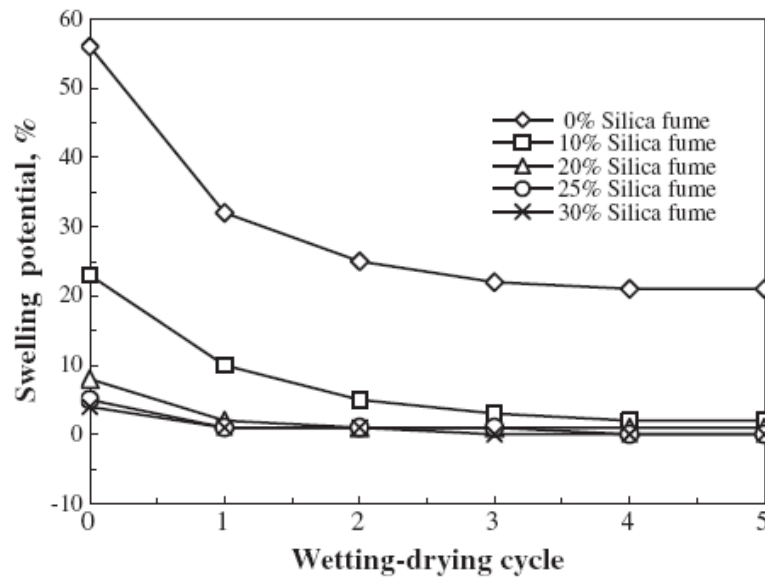


Figure 4.9 Cyclic swell-shrink behavior of expansive soil stabilized with silica fume (Kalkan, 2011)

The summary of the swell-shrink procedure of the authors that studied the effect of wetting-drying cycles on swelling properties of stabilized expansive soils is presented in Table 4.3.

Table 4.3 Swell-Shrink Procedures applied on stabilized expansive soils in previous studies by different researchers

Authors	Swell-Shrink Method	Swell Procedure	Shrinkage Procedure	Additive Type (Percent (%))	Conclusion
Rao et al. (2001)	F _{Sw} -F _{Sh}	Until full swell completed (2 days)	Dried at 45°C by a hot circulator (2 days)	Lime (2%,4% and 7%)	Swell Potential and Clay Content increased
Güney et al. (2007)	F _{Sw} -P _{Sh}	At least until primary swell completed (60 hours)	Air-dried at 24°C until initial moisture content reached	Lime (3% and 6%)	Swell Potential increased for two treated samples and decreased for one
Rao A. & Rao M., (2008)	F _{Sw} -F _{Sh}	Until there was no change in dial gauge for 3 consecutive day	Until there was no change in thickness for 3 consecutive day	Fly Ash Cushions (treated with lime and cement)	Swell Potential decreased
Akcanca & Aytekin, (2011)	F _{Sw} -P _{Sh}	Until swelling pressure reached (7 days)	Dried at 35±5°C to a moisture content a little bit below initial moisture content (1 day)	Lime (1%,2% and 3%)	Swell Pressure increased
Kalkan, (2011)	F _{Sw} -P _{Sh}	Untill full swell completed (over 2 days)	Air-dried at 22°C until initial moisture content reached (5 days)	Silica Fume (10%,20%,25 and 30%)	Swell Potential decreased

The previous studies on stabilized expansive soils show that although beneficiary effect of silica fume and fly ash cushions in reducing the swell potential was preserved after cyclic swell-shrink cycles, that of lime was partially lost mostly. However, in the studies conducted by Güney et al. (2007) on three different soils treated with same lime type and percentages, the swell potentials of two lime treated soil increased whereas a decrease in swell potential observed in the remaining one. Therefore, there could be a decrease or an increase in the swell potential after cyclic-swell shrink tests for lime treated soils. In short, further studies should be conducted on chemically treated expansive soils for better estimation of the long-term behavior.

CHAPTER 5

EXPERIMENTAL WORKS

5.1 Purpose

The aim of this study is to investigate the effects of addition of Class C Fly Ash on atterberg limits, grain size distribution, swell percentage and then to investigate the effect of cyclic swell-shrink on swell percentage of an expansive soil stabilized by Class C Fly Ash.

5.2 Materials

Bentonite, kaolinite, Class C fly ash, lime and sand were used in this study.

Bentonite: Na-Bentonite was used in this study, which was the product of Karakaya Bentonite Factory, located in Ankara (Figure 5.1).

Kaolinite: Kaolinite was product of Kale Maden Industrial Raw Materials Industry & Trade Co. This material was grounded into fine grains in METU Civil Engineering Department Transportation Laboratory and sieved through # 40 sieve before usage (Figure 5.1).

Fly Ash: Class C Fly Ash from Soma Thermal Power Plant was utilized. It was taken from Ilion Cement Construction Industry and Trade Co. as a bagged material (dry). This material sieved through # 40 sieve before usage (Figure 5.1). Specific gravity of Fly Ash is 2.56. Minealogical composition of Fly Ash was determined by X-Ray diffraction method performed in General Directorate

of Mineral Research and Exploration (Appendix A). Chemical analysis of the Fly Ash is presented in Table 5.1.

Lime: Hydrated lime was taken from Baştaş Cement Trade Inc. This material passed through # 40 sieve before usage (Figure 5.1). Specific gravity of Lime is 2.52. Chemical contents of lime that obtained from supplier is given in Table 5.1.

Sand: Sand with a gradation smaller than 0.425mm (passing through #40 sieve) was used.

Table 5.1 Chemical Composition of Fly Ash and Lime

Composition (%)	Fly Ash	Lime
SiO ₂ (Silica)	38.10	0.58
Al ₂ O ₃ (Alumina)	16.55	0.38
TiO ₂ (Titanium Dioxide)	0.70	*
Fe ₂ O ₃ (Ferric Oxide)	4.10	0.11
CaO (Calcium Oxide)	31.45	67.76
MgO (Magnesium Oxide)	1.35	2.20
Na ₂ O (Sodium Oxide)	0.35	*
K ₂ O (Potassium Oxide)	1.40	*
P ₂ O ₅ (Phosphorus Oxide)	0.20	*
MnO (Manganese Oxide)	0.10	*
Loss on Ignition	0.45	*

*Not determined



Figure 5.1. Views from Materials (1-kaolinite, 2-bentonite, 3-fly ash, 4-lime)

Free lime content ($\text{Ca}(\text{OH})_2$) of the fly ash and lime was also determined as it is one of the main factors that affects pozzolonic activity. Tests were performed according to ASTM C 25 at Chemical Engineering Department laboratory in METU. The procedure of the test is summarized below;

Sucrose solution was prepared by dissolving 40 g sugar in 100 ml CO_2 -free water and several drops of 4% phenolphthalein indicator and 0.1 N NaOH added to this solution until the colour turns into faint pink.

Sample sieved through #50 sieve and 2.804 g of sample, was mixed with 100 ml sucrose solution and 40 ml CO_2 -free water (Figure 5.2).

Mixture was allowed to stand for 15 minutes for reactions and it was swirled at 5 minutes intervals

After 15 minutes 4 -5 drops of 4% phenolphthalein indicator added to mixture.

Finally, mixture was titrated with 1.0 N HCl until the pink colour disappeared for 3 secs.



Figure 5.2.View from mixtures before titration

Free lime content could be calculated by using the formula given below;

$$\text{Free lime content (Ca(OH)}_2\text{), \%} = N \times V \times 3.704 / W$$

N: normality of acid solution (1)

V: standard HCl (1.0 N), ml

W: weight of sample, g (2.804 g)

Free lime content of fly ash and lime found as 16.5% and 56.0% respectively by using the method and formula described above.

5.3 Preparation and Properties of Test Samples

Expansive soil (Sample A) used in this study was prepared in laboratory environment by mixing kaolinite and bentonite. Composition of the kaolinite and bentonite was 85% and 15% respectively by dry weight of sample. Firstly, Sample A was pre-tested to see if the prepared sample had swelling potential, then to investigate the effect of Fly Ash as stabilizer, maximum pre-determined percentage of Fly Ash (20%) was added to Sample A. At the end of the tests it was understood that Sample A had a high swelling potential (63%) and fly ash was an effective chemical additive. Also, lime was added to Sample A to compare the effectiveness of fly ash as a stabilization agent. Samples were obtained by mixing Sample A with different percentages of Fly Ash varying from 5% to 20% and lime changing between 1% and 5% (by dry weight of soil). Also sand was used as an inert material and added with percentage of 5% to Sample A to see the effect of fly ash and lime as a stabilizer. The compositions of specimens used in this study are presented in Table 5.2.

Before the preparation of samples, kaolinite was air-dried, grounded and then all materials oven-dried at 45 °C for one day. After that the materials were sieved through #40 sieve. Then predetermined amount of each material was put into bowl and mixed with a plastic spoon. After mixing, materials were sieved through #30 sieve two times to obtain a well mixed, homogenous sample.

Table 5.2 Composition of Prepared Specimens

Sample	Bentonite-Kaolinite	Fly Ash	Lime	Sand
A	100	-	-	-
5% FA	95	5	-	-
10% FA	90	10	-	-
15% FA	85	15	-	-
20% FA	80	20	-	-
1% L	99	-	1	-
3% L	97	-	3	-
5% L	95	-	5	-
5% S	95	-	-	5

Then 10% water by dry weight of sample was added to mixed materials. As 150 g materials were used to obtain samples, only 15 g water was needed. However, during the mixing process, some of the water evaporated, so rather than using 15 g water, 20 g water was used each time to obtain a sample with water content, $w=10\%$. After mixing with water, materials that stuck to each other were separated by hand and sieved through # 30 sieve until all the materials passed (Figure 5.3).

Finally, the sample was put into plastic bag and allowed to wait one day in desiccator to have homogeneous water distribution. For the cured samples of 5% fly ash, samples that were prepared according to above procedure, were kept 7 days and 28 days in the desiccators, that was put into moisture room with a 70% moisture and 22-25 °C temperature.

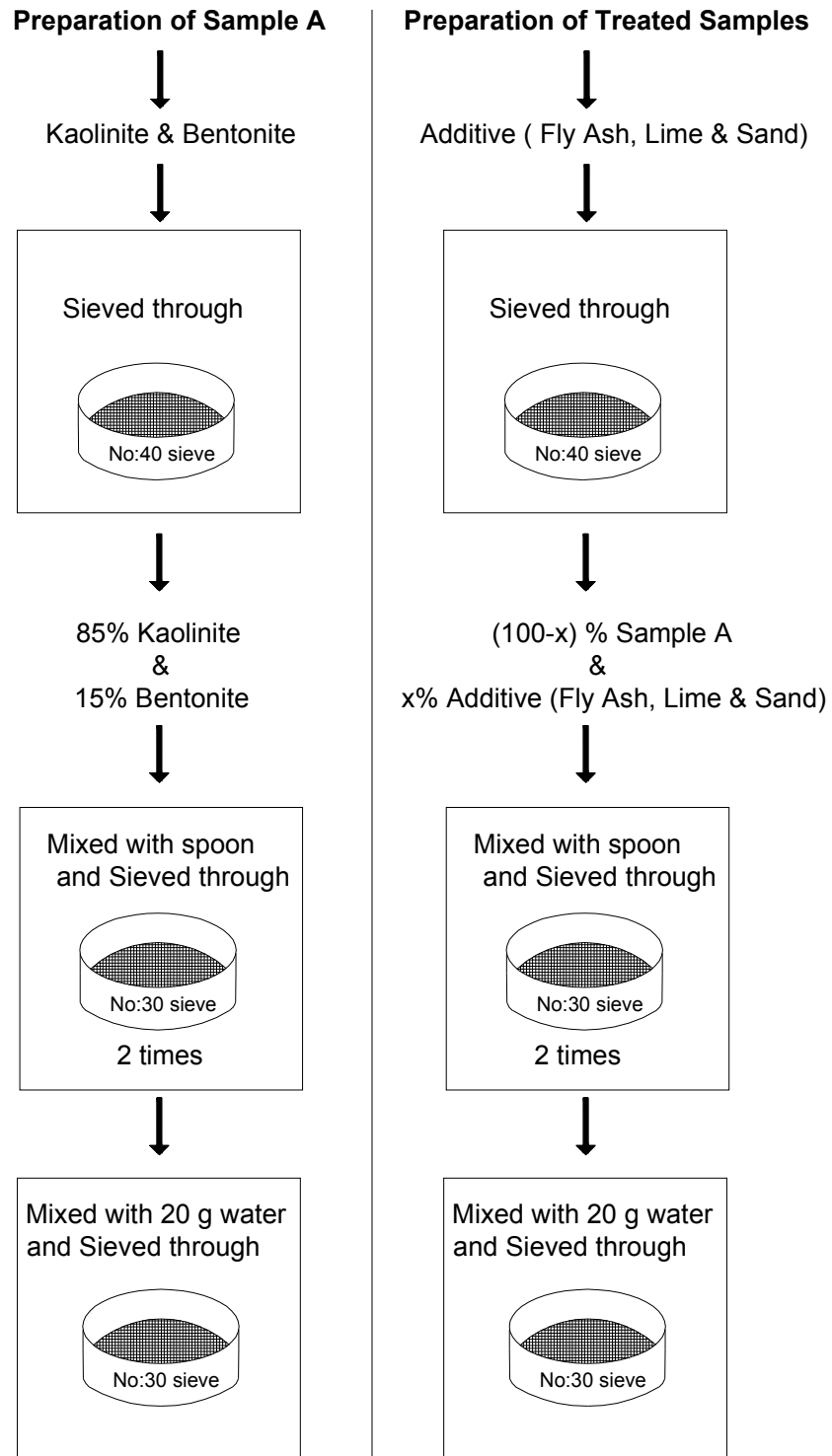


Figure 5.3. Preparation of Samples

5.4 Properties of Samples

Atterberg limits; namely liquid limit (LL), plastic limit (PL), plasticity index (PI) and shrinkage limit (SL) tests, hydrometer tests and specific gravity tests were performed on the samples to determine the index properties. Liquid limit, plastic limit and plasticity index were determined according to ASTM D4318, and shrinkage limit, specific gravity and hydrometer tests were performed according to ASTM D427, ASTM D854 and ASTM D422 respectively.

Grain size distribution curves of fly ash and lime could not be determined by hydrometer tests due to the rapid settling of the material to the bottom of the flask. However, this problem was not encountered for the fly ash or lime treated samples. Rapid settlement of fly ash could be explained by the formation of crystals due to the reaction within fly ash, occurred with the addition of water (Figure 5.4).



Figure 5.4. Crystals formed in fly ash during the hydrometer test

Effect of additives on specific gravity, liquid limit, plastic limit, plasticity index, shrinkage limit, linear shrinkage, and shrinkage index (SI=LL-SL) are presented in Figure 5.5, 5.6, 5.7, 5.8, 5.9, 5.10 and 5.11.

Grain Size distribution curves for fly ash and lime treated samples are presented in Figure 5.12 and 5.13 respectively.

Soil classification of the samples was made according to the Unified Soil Classification System (USCS). Soil Classes were determined by entering liquid limit and plasticity index values to the plasticity chart (Figure 5.14).

Activity values of samples were determined by dividing plasticity index (PI) values to the clay percent.

Swelling potentials of samples were estimated by using PI, clay percentages and classification chart recommended by Seed et al. (1962) (Figure 5.15).

Properties of samples are summarized in Table 5.3

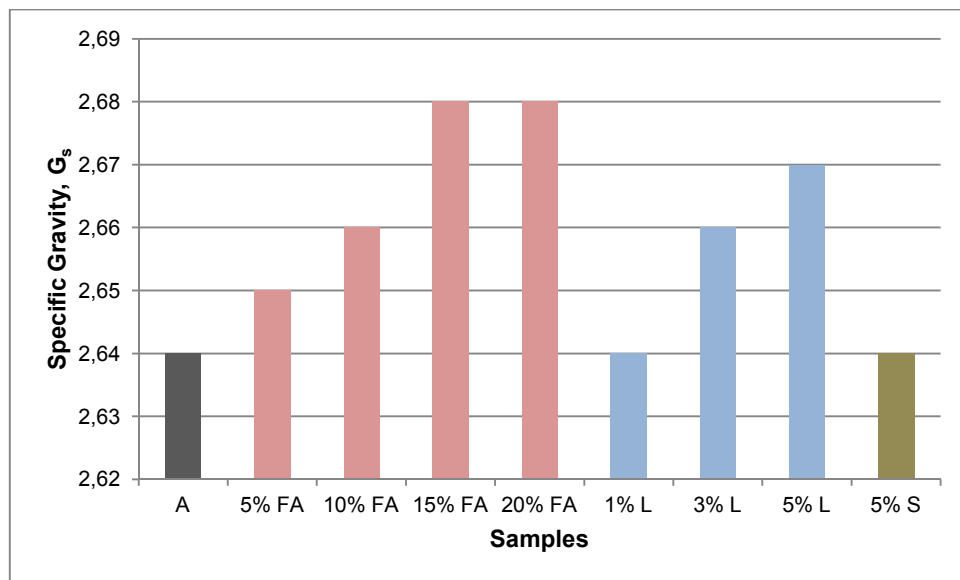


Figure 5.5 Effect of Addition of Fly Ash, Lime and Sand on Specific Gravity (G_s) of the Samples

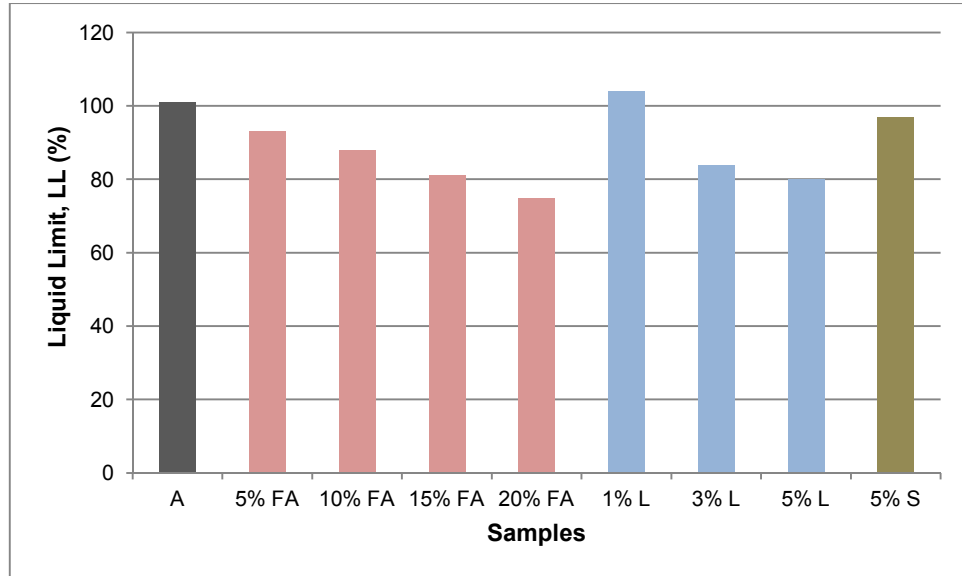


Figure 5.6 Effect of Addition of Fly Ash, Lime and Sand on Liquid Limit (LL) of the Samples

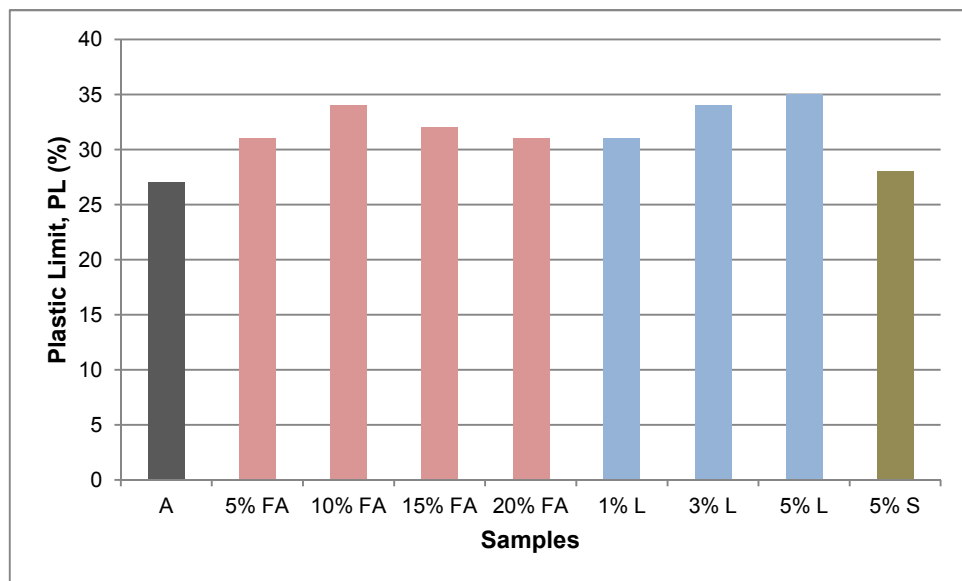


Figure 5.7 Effect of Addition of Fly Ash, Lime and Sand on Plastic Limit (PL) of the Samples

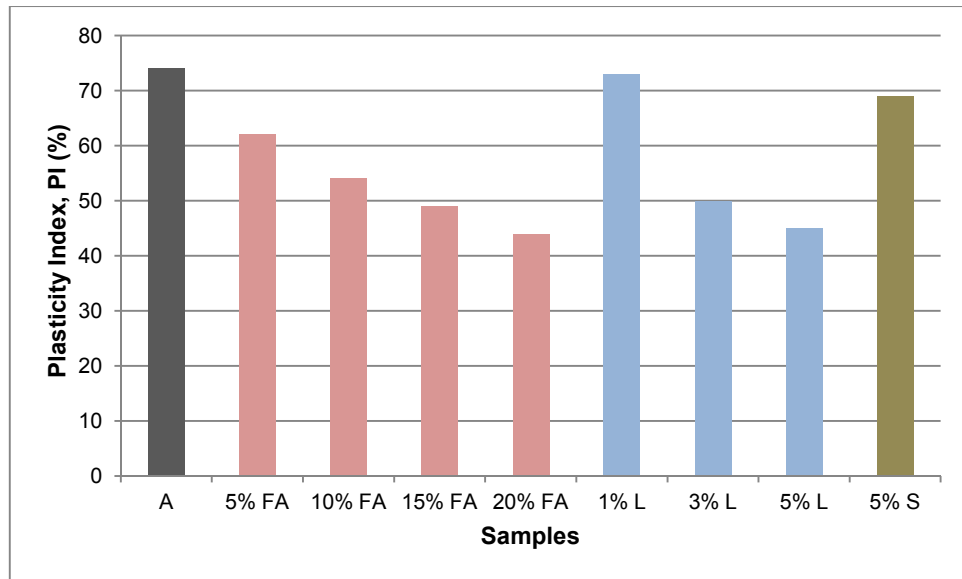


Figure 5.8 Effect of Addition of Fly Ash, Lime and Sand on Plasticity Index (PI) of the Samples

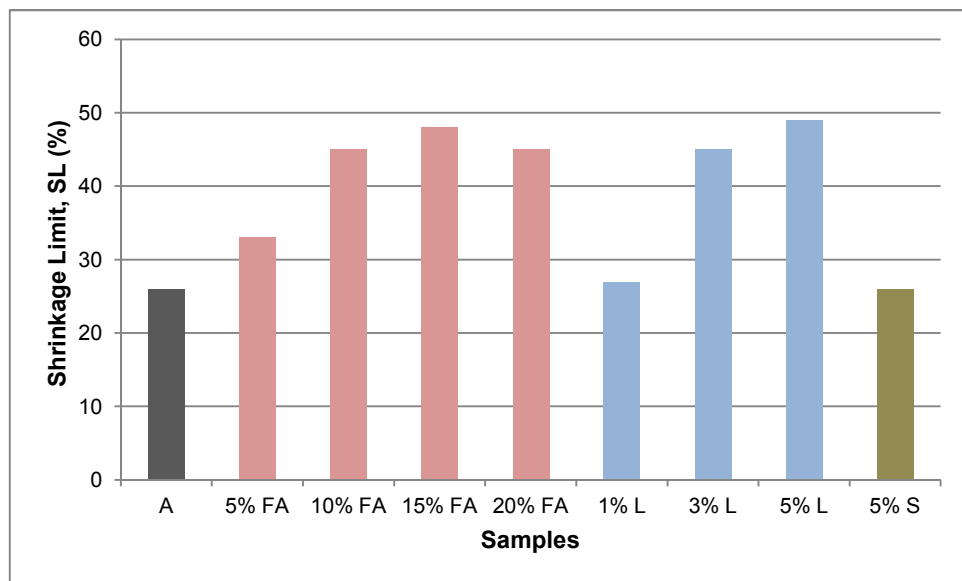


Figure 5.9 Effect of Addition of Fly Ash, Lime and Sand on Shrinkage Limit (SL) of the Samples

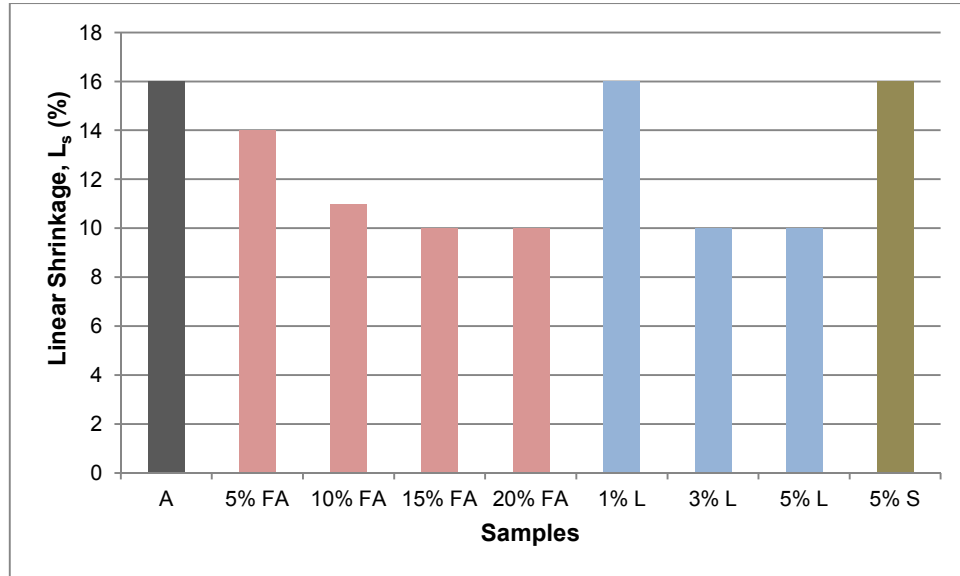


Figure 5.10 Effect of Addition of Fly Ash, Lime and Sand on Linear Shrinkage (L_s) of the Samples

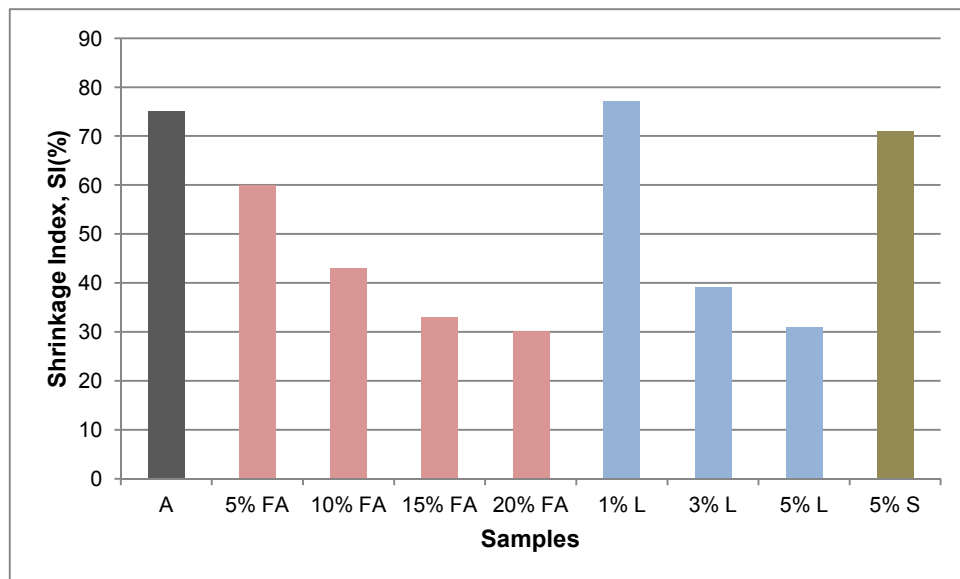


Figure 5.11 Effect of Addition of Fly Ash, Lime and Sand on Shrinkage Index (SI) of the Samples

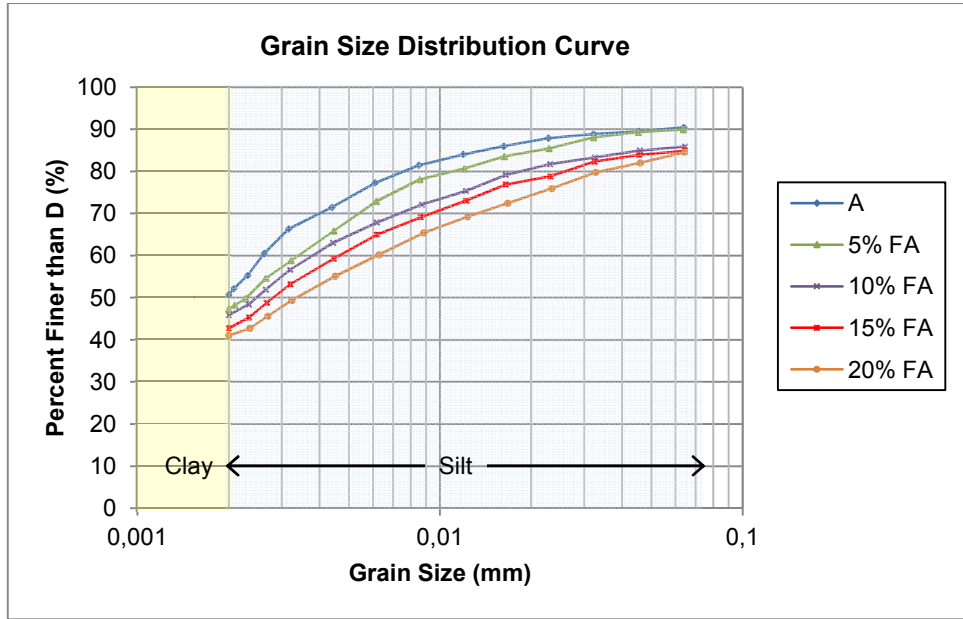


Figure 5.12 Grain Size Distribution Curves for Sample A and Fly Ash Treated Samples

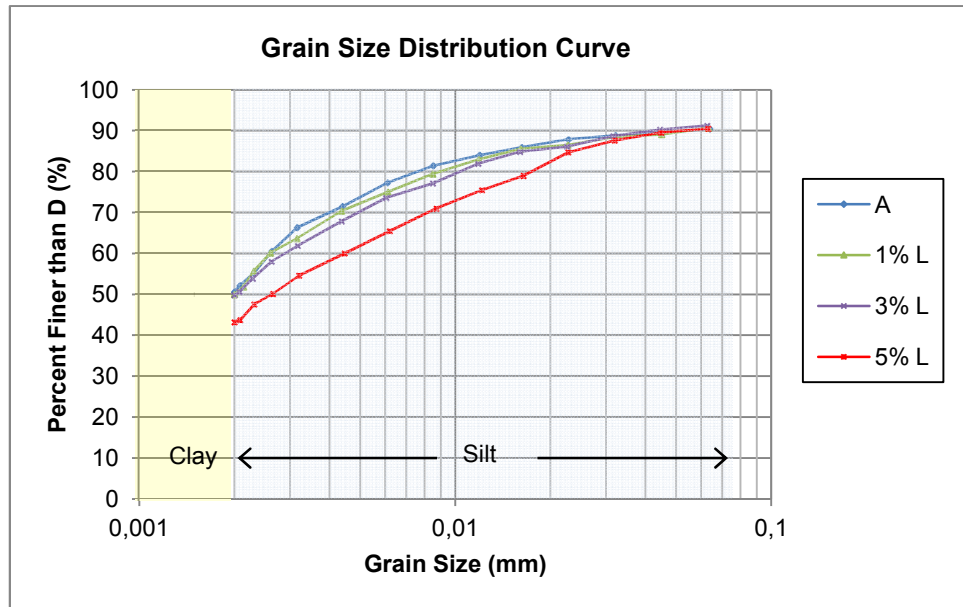


Figure 5.13 Grain Size Distribution Curves for Sample A and Lime Treated Samples

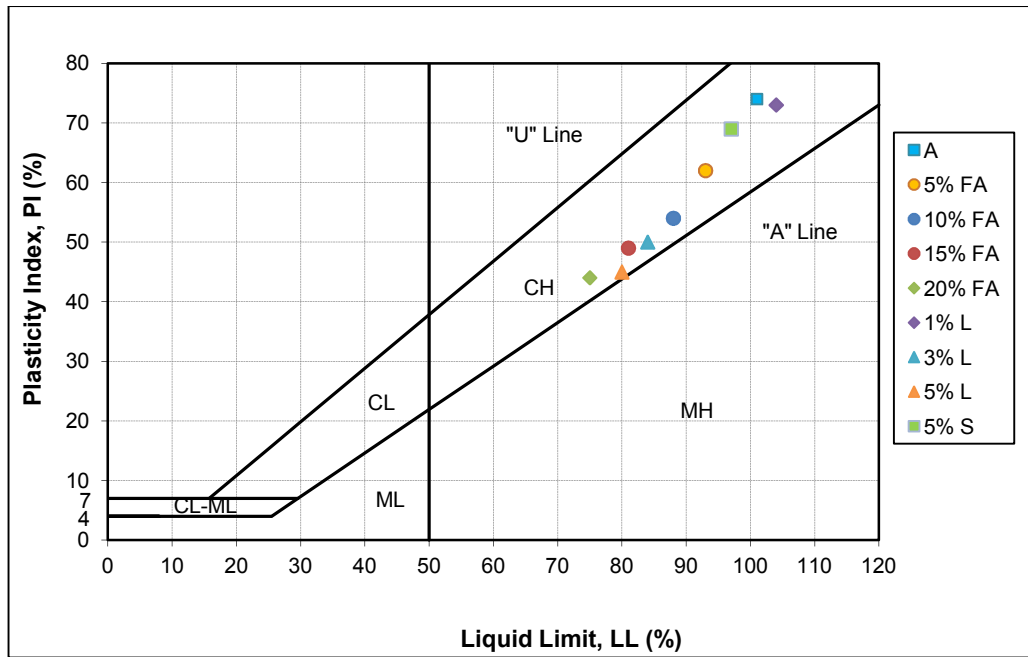


Figure 5.14 Plasticity Chart

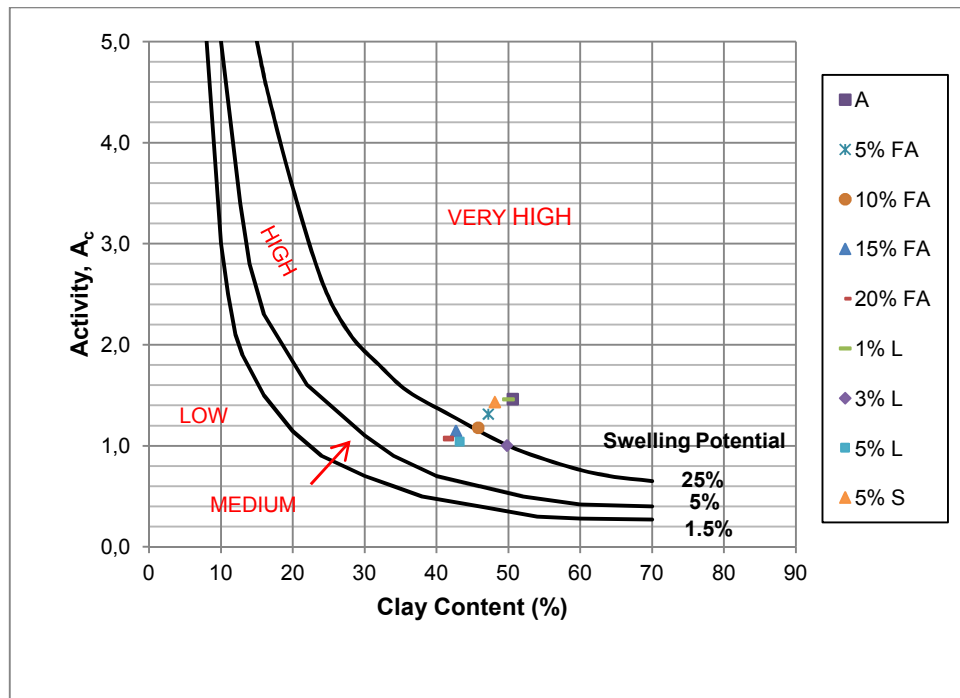


Figure 5.15 Swelling Potential Classification Chart (after Seed et al., 1962)

Table 5.3 Properties of Samples

Sample	Clay (%)	Silt (%)	G _s	LL (%)	PL (%)	PI (%)	SL (%)	L _s (%)	SI (%)	Soil Classification	A _c	Swelling Potential (Seed et al,1962)
A	50.6	49.1	2.64	101	27	74	26	16	75	CH	1.46	Very High
5% FA	47.2	51.4	2.65	93	31	62	33	14	60	CH	1.31	Very High
10% FA	45.8	51.7	2.66	88	34	54	45	11	43	CH	1.18	High-Very High
15% FA	42.7	53.7	2.68	81	32	49	48	10	33	CH	1.15	High
20% FA	41.0	54.1	2.68	75	31	44	45	10	30	CH	1.07	High
1% L	50.0	49.7	2.64	104	31	73	27	16	77	CH	1.46	Very High
3% L	49.8	49.9	2.66	84	34	50	45	10	39	CH	1.00	High-Very High
5% L	43.2	56.3	2.67	80	35	45	49	10	31	CH	1.04	High
5% S	48.1	46.7	2.64	97	28	69	26	16	71	CH	1.43	Very High

G_s: Specific Gravity, LL: Liquid Limit, PL: Plastic Limit, PI: Plasticity Index

SL: Shrinkage Limit, L_s: Linear Shrinkage, SI: Shrinkage Index, A_c: Activity

5.5 Procedures for Cyclic Swell and Shrink Tests

5.5.1 Compaction of Specimens

Samples were compacted directly into consolidation rings statically with a dry density of 1.64 g/cm^3 (bulk density of 1.80 g/cm^3) by the help of a hydraulic jack (Figure 5.16). Before compaction, vaseline was applied to inner surface of the ring to prevent sticking of particles during drying.

Static compaction was performed in one step, as the compaction of samples in layers resulted in more cracks after swell-shrink cycles even if threaded surface formed at the end of the static compaction step of each layer. At the end of the static compaction, samples with 19.1 mm height and diameter equal to or slightly larger than 63.5 mm were obtained. After compaction, bottom of the samples was trimmed by means of a steel ruler to open the pores.

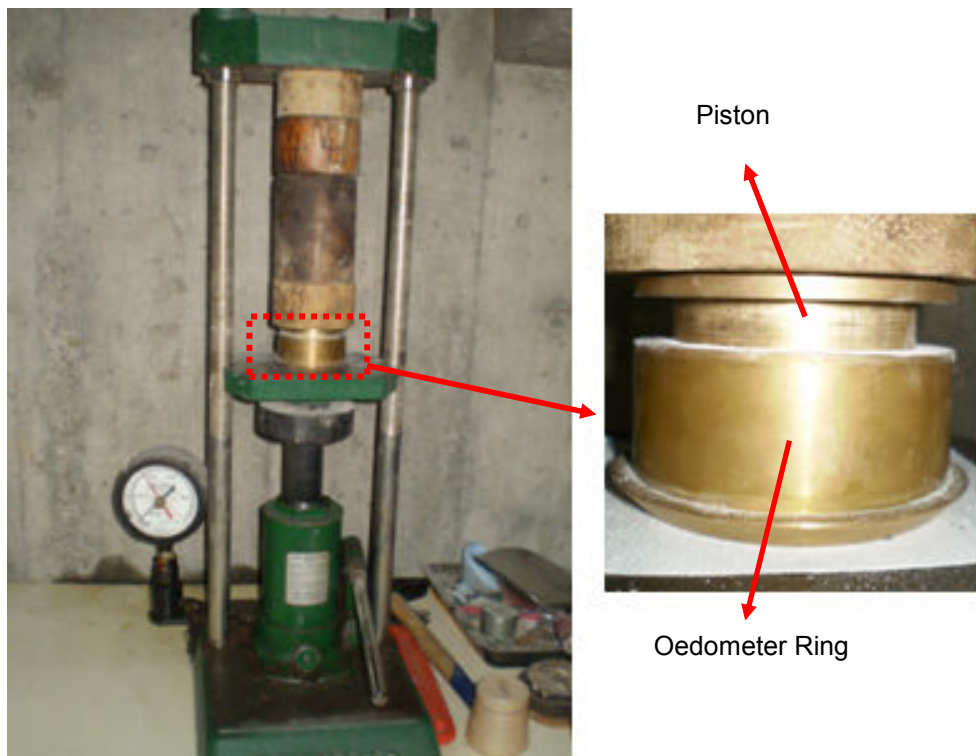


Figure 5.16 A View from Static Compaction

5.5.2 Cyclic Swell – Shrink Tests

Free swell tests were performed for determining the swell potential of samples according to ASTM D-4546. The procedure of the test was as follows; firstly porous stone was placed on the oedometer, then sample, which was compacted in the consolidation ring as explained in Section 5.5.1, was placed in the oedometer after placing filter papers on top and bottom of it. After that another porous stone placed at the top of the sample (Figure 5.17).

Then, the oedometer was put into a pot and mounted and the initial reading of dial gauge was recorded (Figure 5.18). The sample was inundated by filling the pot with water and pouring water through standpipes. Distilled water was used to eliminate ion effects during testing. Swelling of the sample started right after the inundation of water. The sample was allowed to swell freely under a pressure of nearly 1.35 kPa caused by the dead weight of the cap of the oedometer. Deflection values were recorded at least until the primary swell was completed. After the completion of swelling, the water in the pot was poured and the oedometer was dismantled. Then the sample was taken and weighed.

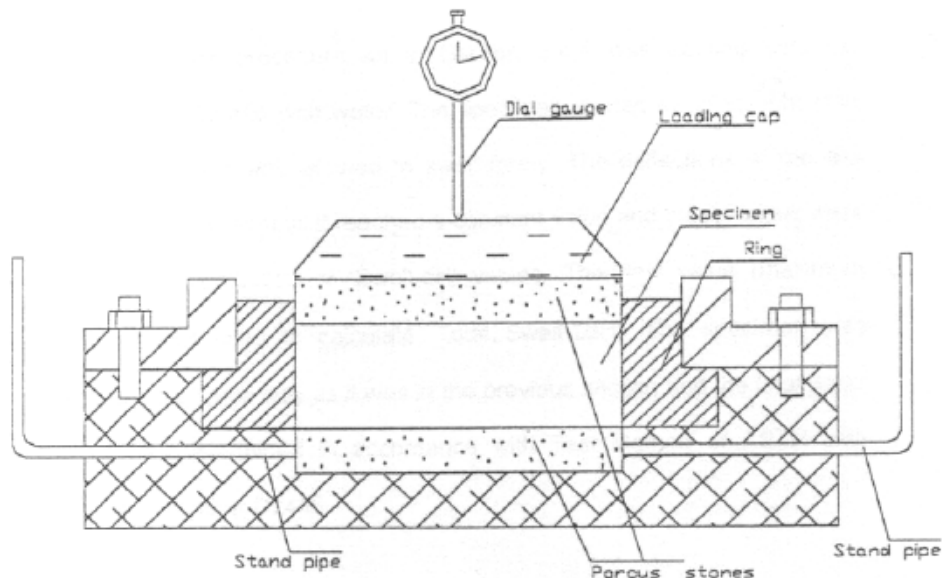


Figure 5.17 Free Swell Test Setup Drawing (İpek, 1998)



Figure 5.18 View from Oedometers during testing

During shrinkage procedure, the samples were allowed to air-dry at least four hours and then put into oven that had a fixed temperature of $45 \pm 5^\circ \text{C}$ and allowed to shrink until they reached to their initial water content. As the initial water content of the samples were smaller than their shrinkage limit, this procedure is named as full shrinkage method. The reason of choosing this temperature was to make samples dry as quickly as possible and also this was a representative temperature for the climates in arid and semi-arid regions where expansive soils mostly exists.

Weight of the samples was controlled from time to time to understand if they reached to their initial water content or not. When the samples were dried until their initial water content, they were taken from the oven and their heights were determined by means of a digital caliper with an accuracy of 0.01mm (Figure 5.19) and volume of the samples were determined by using mercury similar to shrinkage limit test (Figure 5.20). Then the samples were allowed to wait in the desiccator for nearly two hours not to make them to expose rapid temperature difference.



Figure 5.19 Measuring height with digital caliper



Figure 5.20 Measuring volume with mercury

Occurrence of excessive cracks in samples after drying was the most severe problem faced during the experiments. Mercury could not be used to determine the volume of the samples for which excessive cracks occurred (mainly for 3%, 5% lime treated samples). Volume of those samples was determined by measuring the diameter and height of the sample with caliper.

However, at this time height of the sample was measured after placing sample into the ring and gently pushing from the top to make the cracks closed.

Finally samples were again put into oedometers and allowed to swell freely. These procedures were repeated five times to determine the long-term behavior of unstabilized and stabilized samples.

Swell percentage was determined by three different ways.

1) Axial swell was calculated to determine the increase or decrease in swell potential at the end of each cycle, using the formula given below:

Axial Swell (%) = $\Delta H_i / H_{id} * 100$ where;

ΔH_i = Height difference between dry and wet state in a cycle

H_{id} = Height at dry state

2) As the samples also shrunk laterally, volumetric swell was calculated to determine the increase or decrease in swell potential at the end of each cycle, using the formula given below:

Volumetric Swell (%) = $\Delta V_i / V_{id} * 100$ where;

ΔV_i = Volume difference between dry and wet state in a cycle

V_{id} = Volume at dry state

3) Volumetric swell was also calculated by using the initial volume rather than using dry volume of soil in each cycle to determine the effect of cyclic-wetting with respect to initial condition by the formula stated below:

Volumetric Swell (%) = $\Delta V / V_0 * 100$ where;

ΔV = Change in initial volume (V_0) of the sample at the end of each cycle

V_0 = Initial volume of the sample

5.5.3 Test Results

Free swell values of Sample A and treated samples were shown in Figure 5.21.

Axial swell, volumetric swell with respect to dry volume at the beginning of each cycle and volumetric swell with respect to initial volume is presented in Figure 5.22, 5.23 and 5.24 for Sample A and fly ash treated samples, in Figure 5.24, 5.25 and 5.26 for Sample A and lime treated samples, in Figure 5.27, 5.28 and 5.29 for Sample A and samples containing 5% additive and in Figure 5.30, 5.31 and 5.32 for 0 day, 7 days and 28 days cured samples of 5% fly ash treated samples respectively. Swell versus Time graphs are presented in Appendix B.

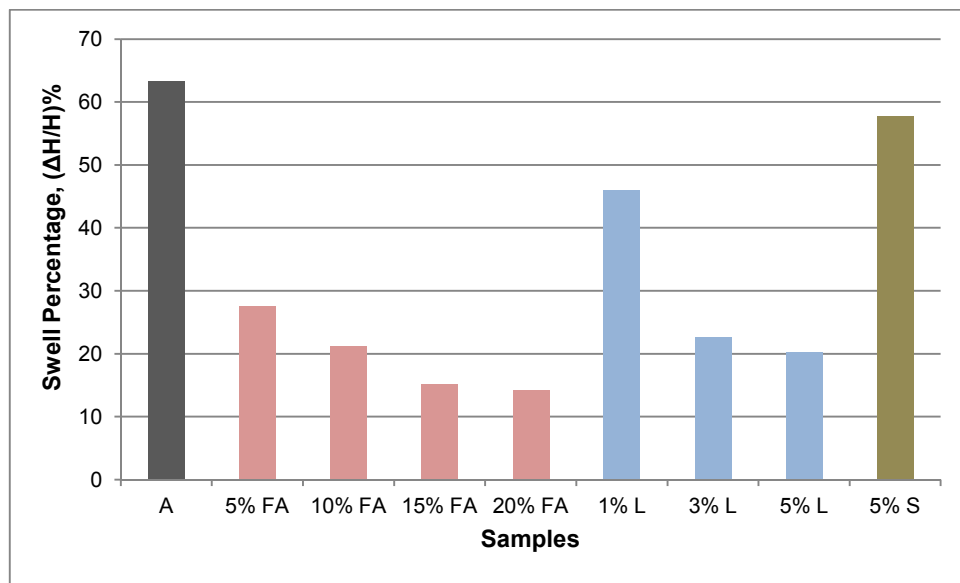


Figure 5.21 Effect of Addition of Fly Ash, Lime and Sand on Free Swell of the Samples

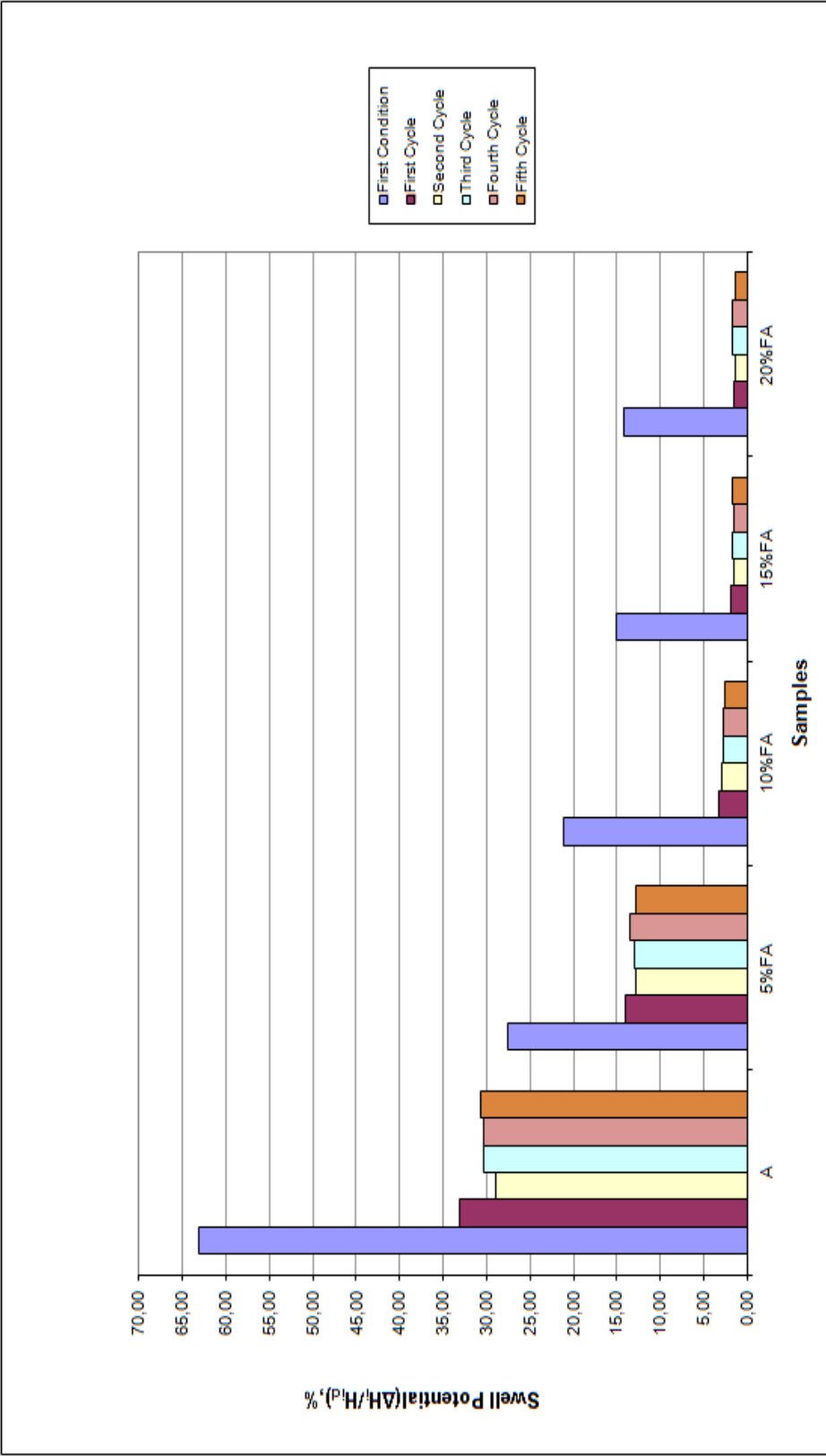


Figure 5.22 Axial Swell Potential of Sample A and Fly Ash Treated Samples

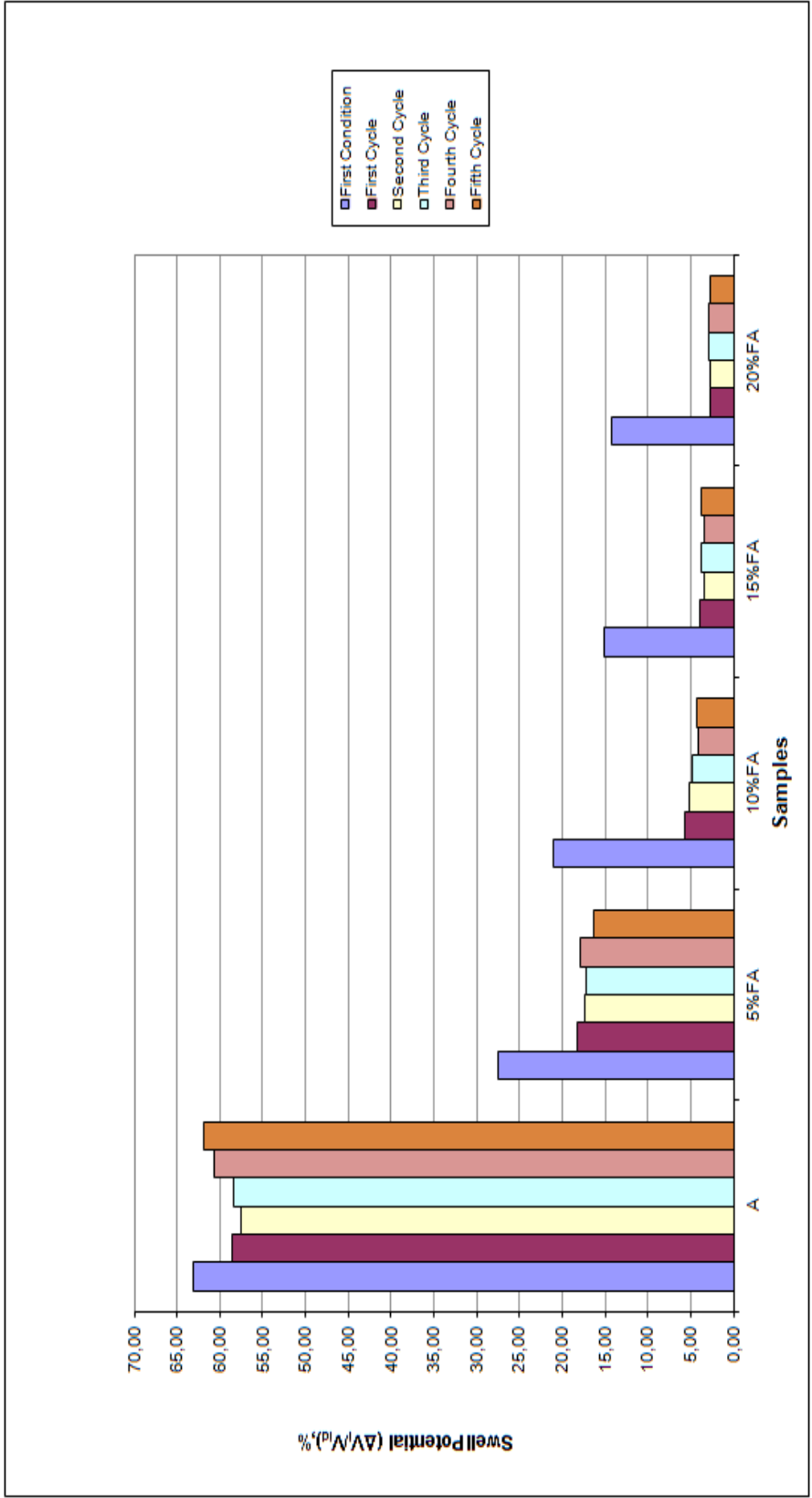


Figure 5.23 Volumetric Swell Potential of Sample A and Fly Ash Treated Samples with respect to dry volume at the beginning of each cycle

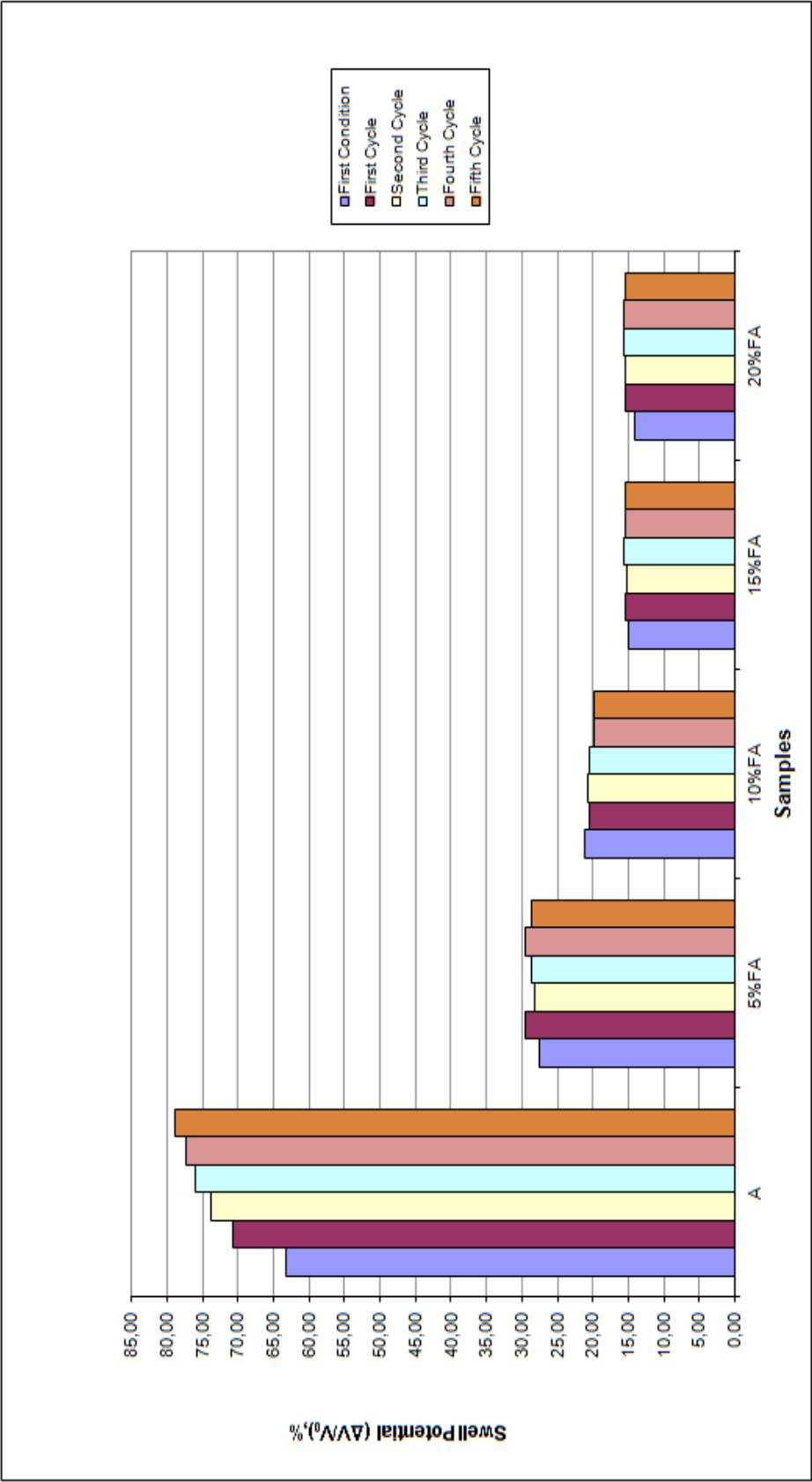


Figure 5.24 Volumetric Swell Potential of Sample A and Fly Ash Treated Samples with respect to initial volume

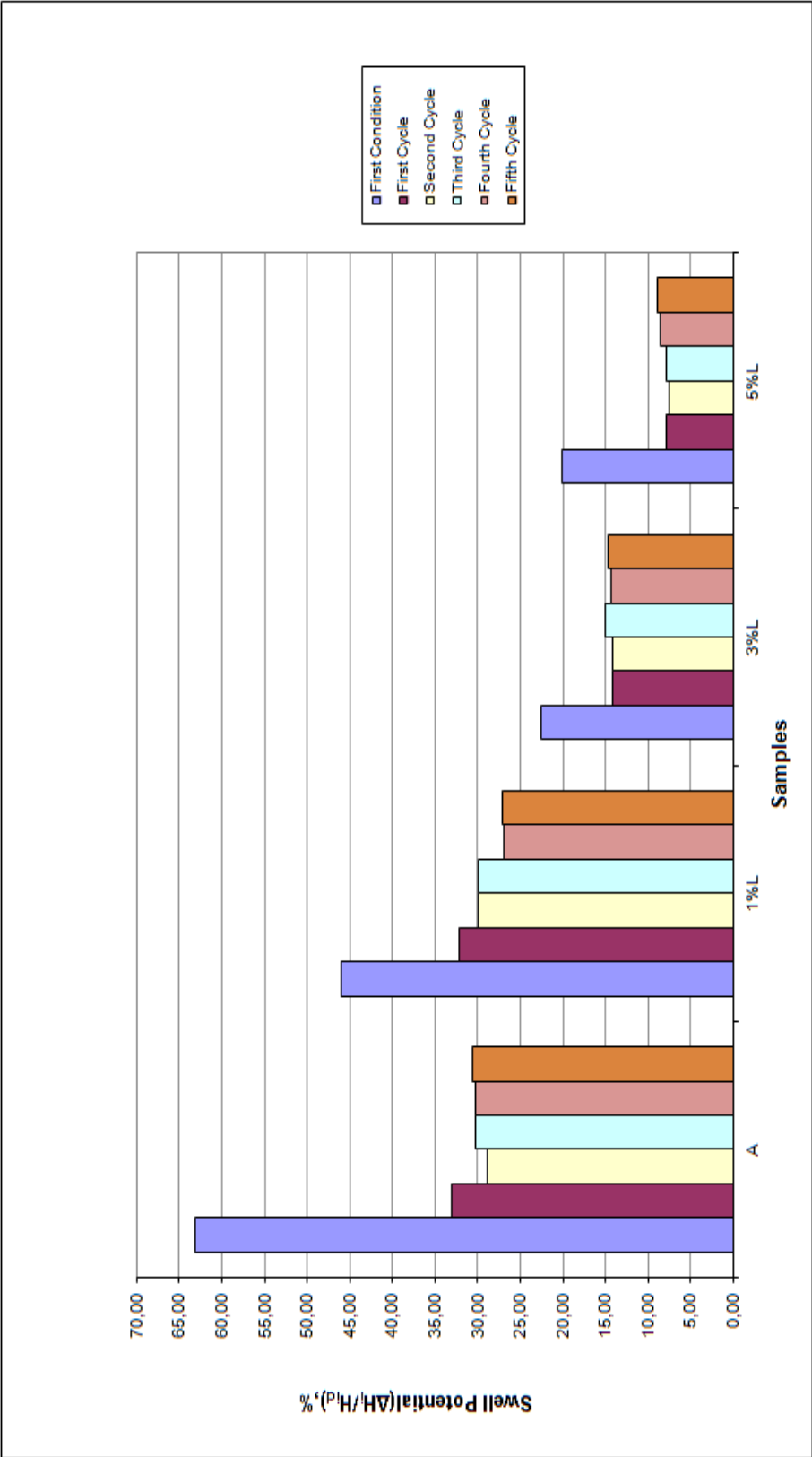


Figure 5.25 Axial Swell Potential of Sample A and Lime Treated Samples

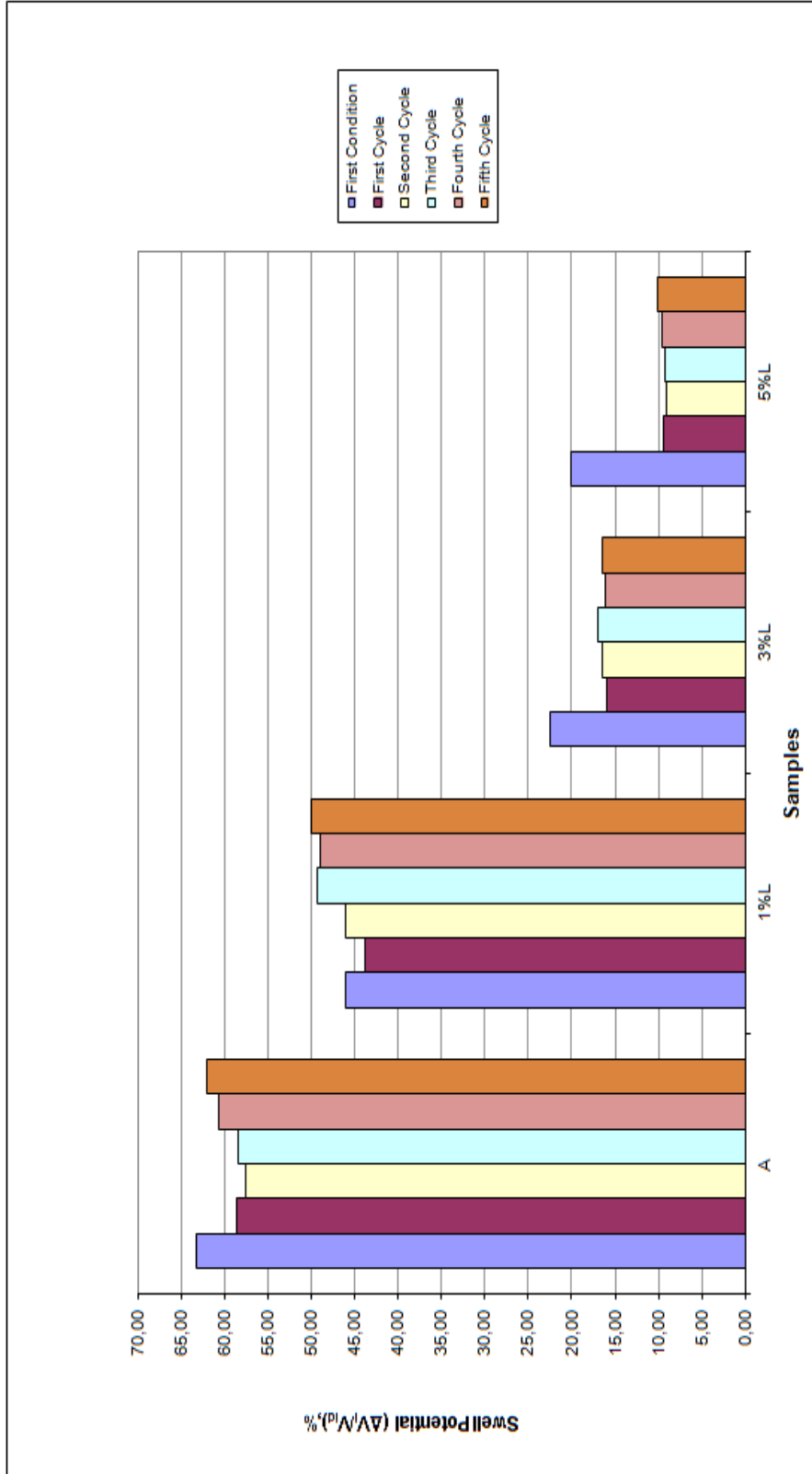


Figure 5.26 Volumetric Swell Potential of Sample A and Lime Treated Samples with respect to dry volume at the beginning of each cycle

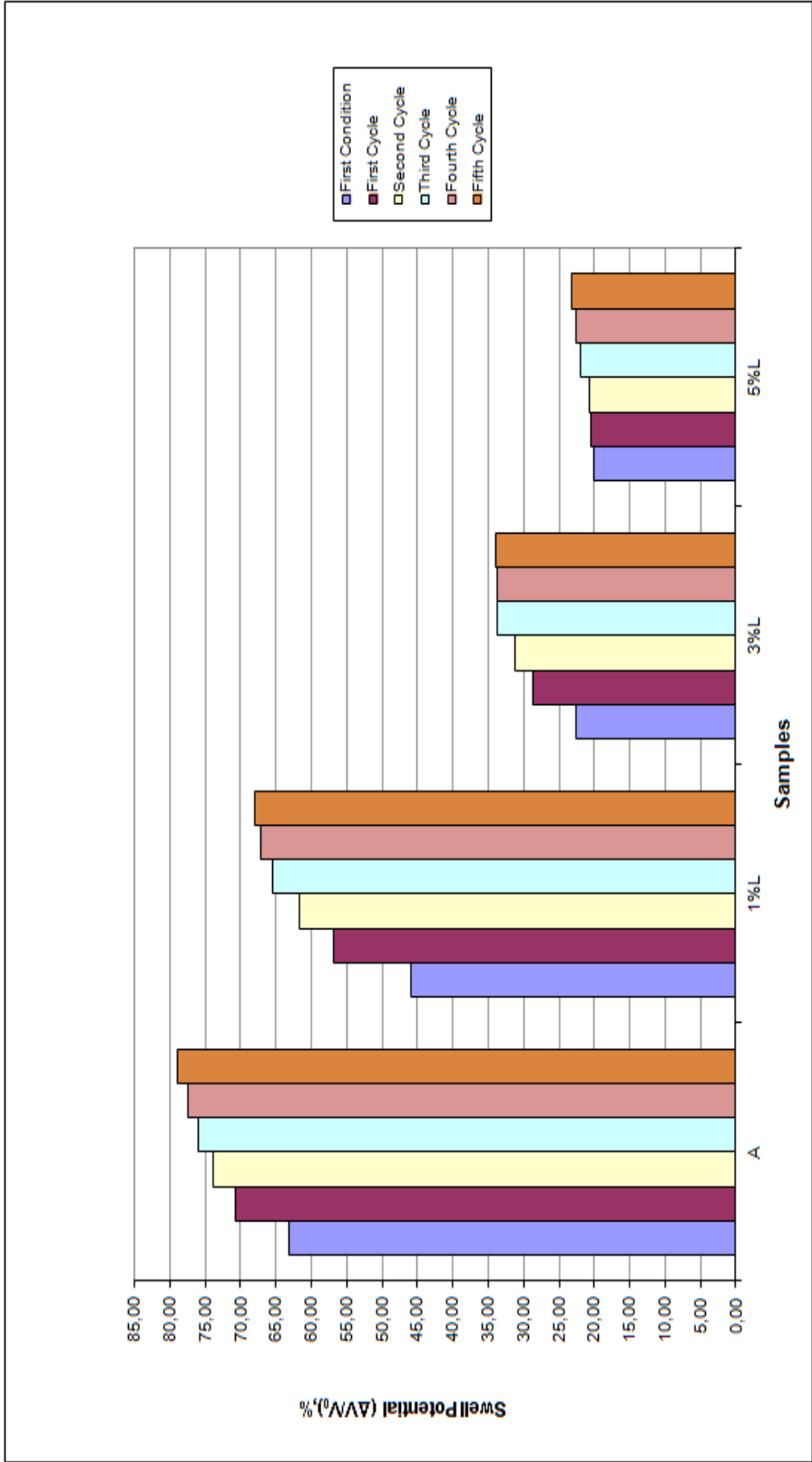


Figure 5.27 Volumetric Swell Potential of Sample A and Lime Treated Samples with respect to initial volume

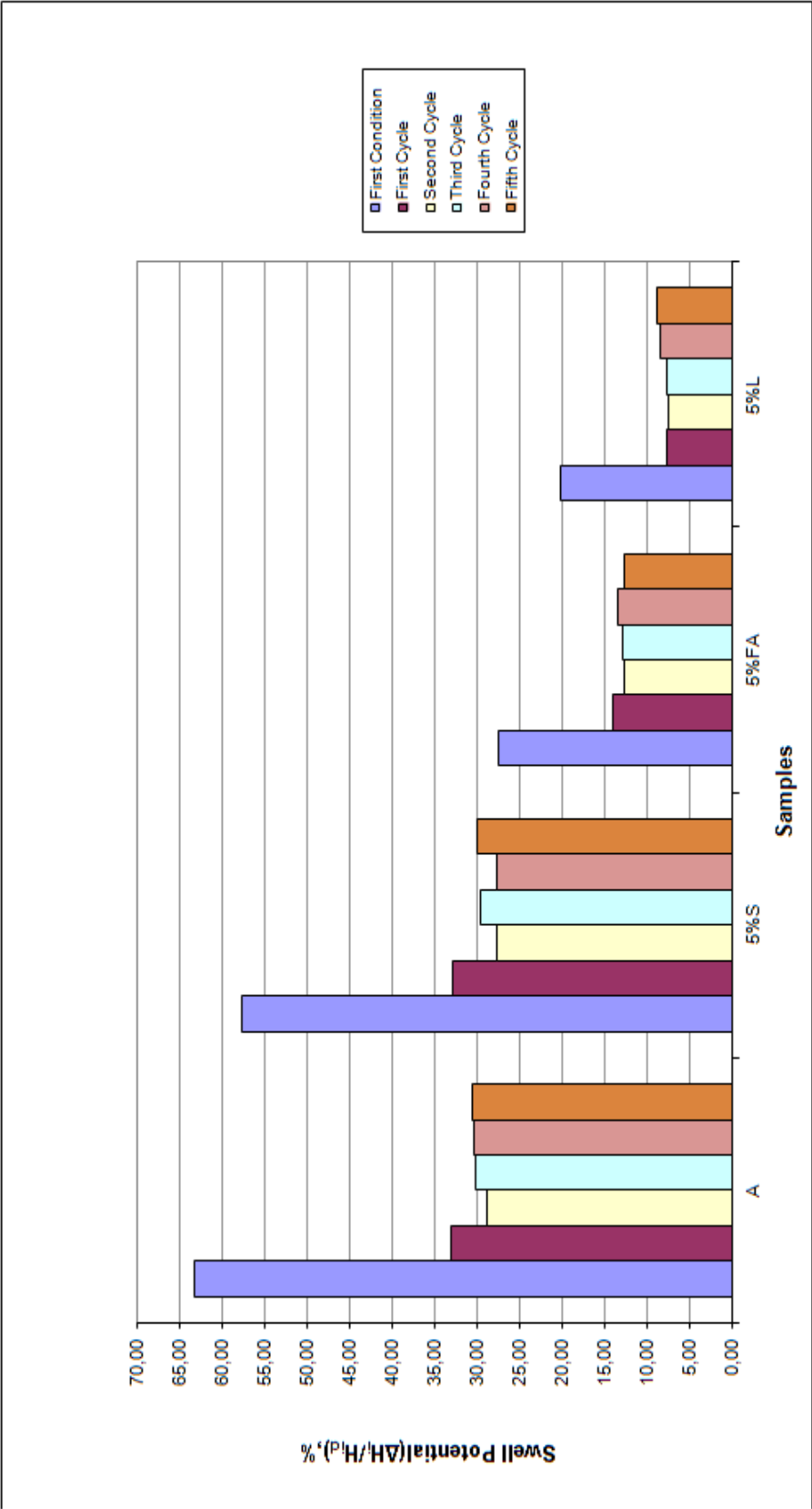


Figure 5.28 Axial Swell Potential of Sample A and Samples containing 5% Additives

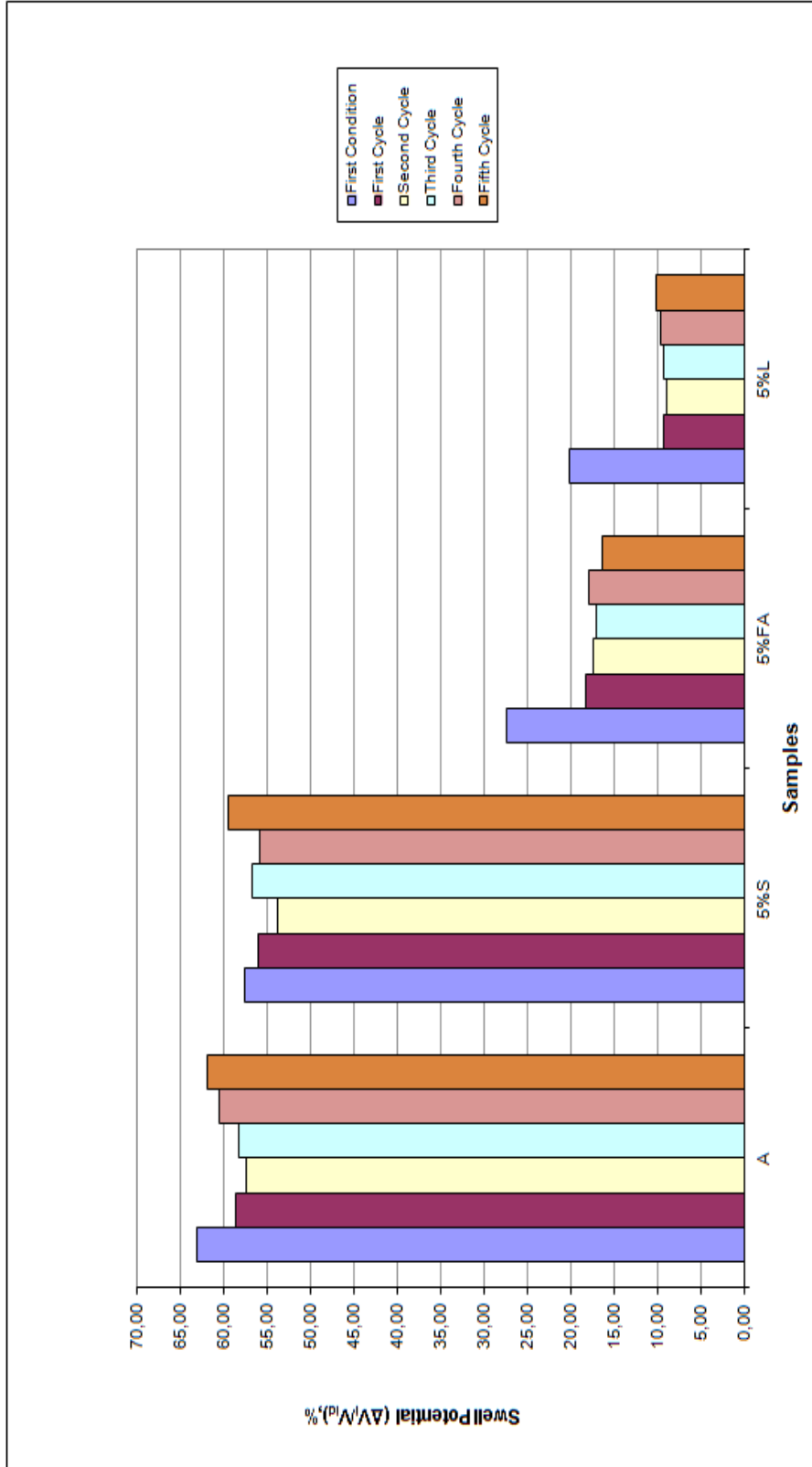


Figure 5.29 Volumetric Swell Potential of Sample A and Samples containing 5% Additives with respect to dry volume at the beginning of each cycle

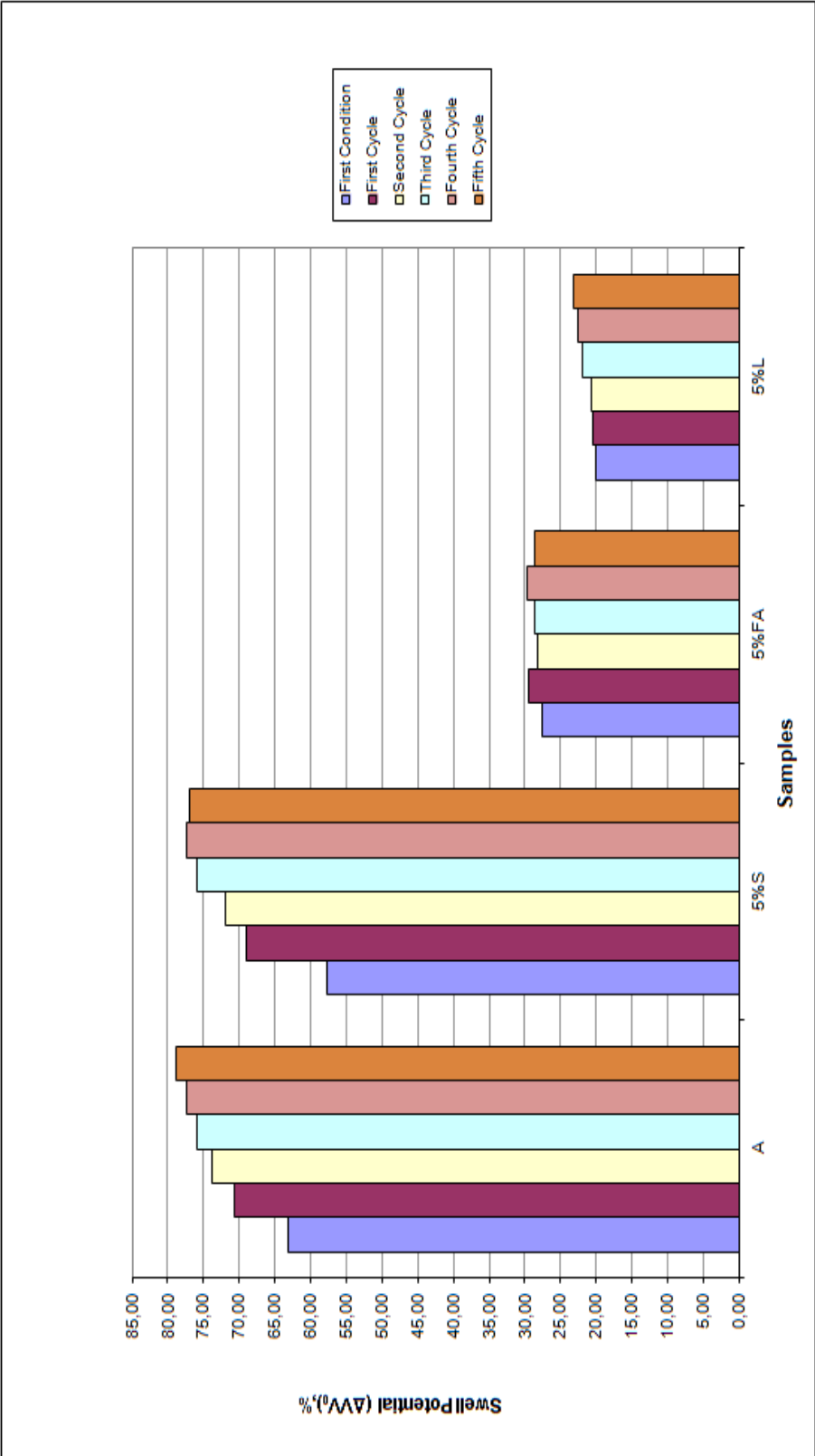


Figure 5.30 Volumetric Swell Potential of Sample A and Samples containing 5% Additives with respect to initial volume

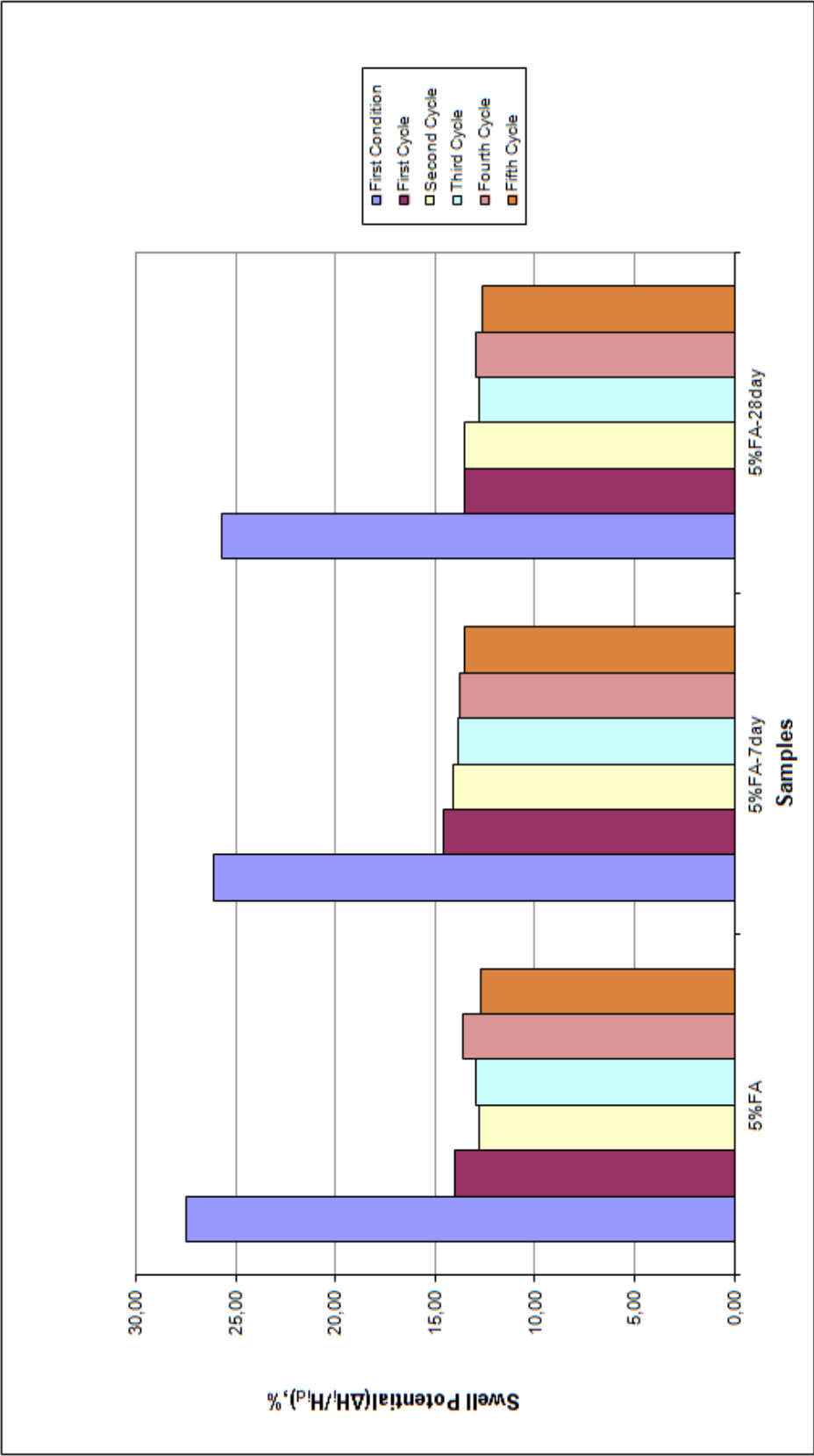


Figure 5.31 Axial Swell Potential of 5% fly ash added Samples with and without curing

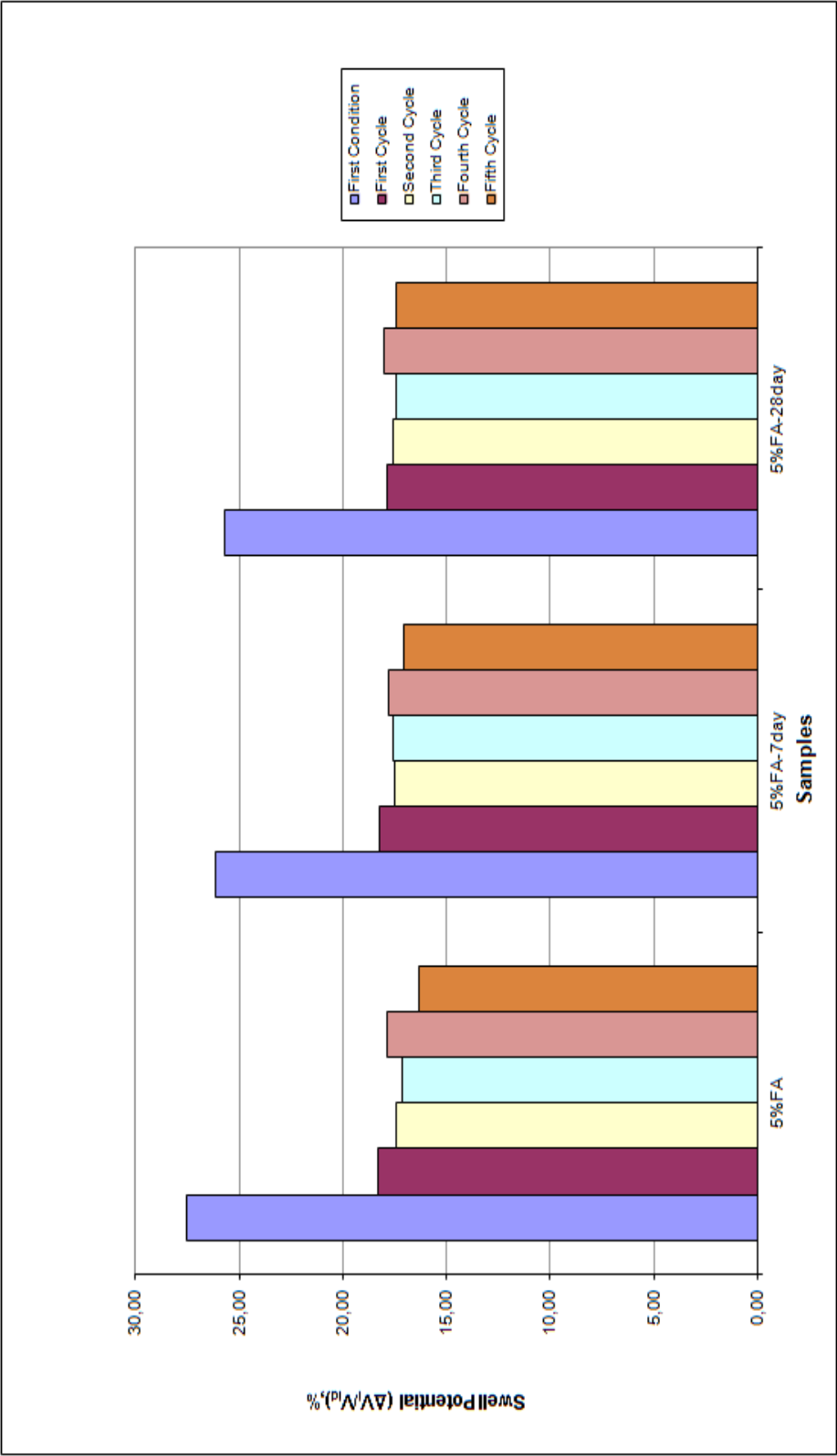


Figure 5.32 Volumetric Swell Potential of 5% fly ash added Samples with and without curing with respect to dry volume at the beginning of each cycle

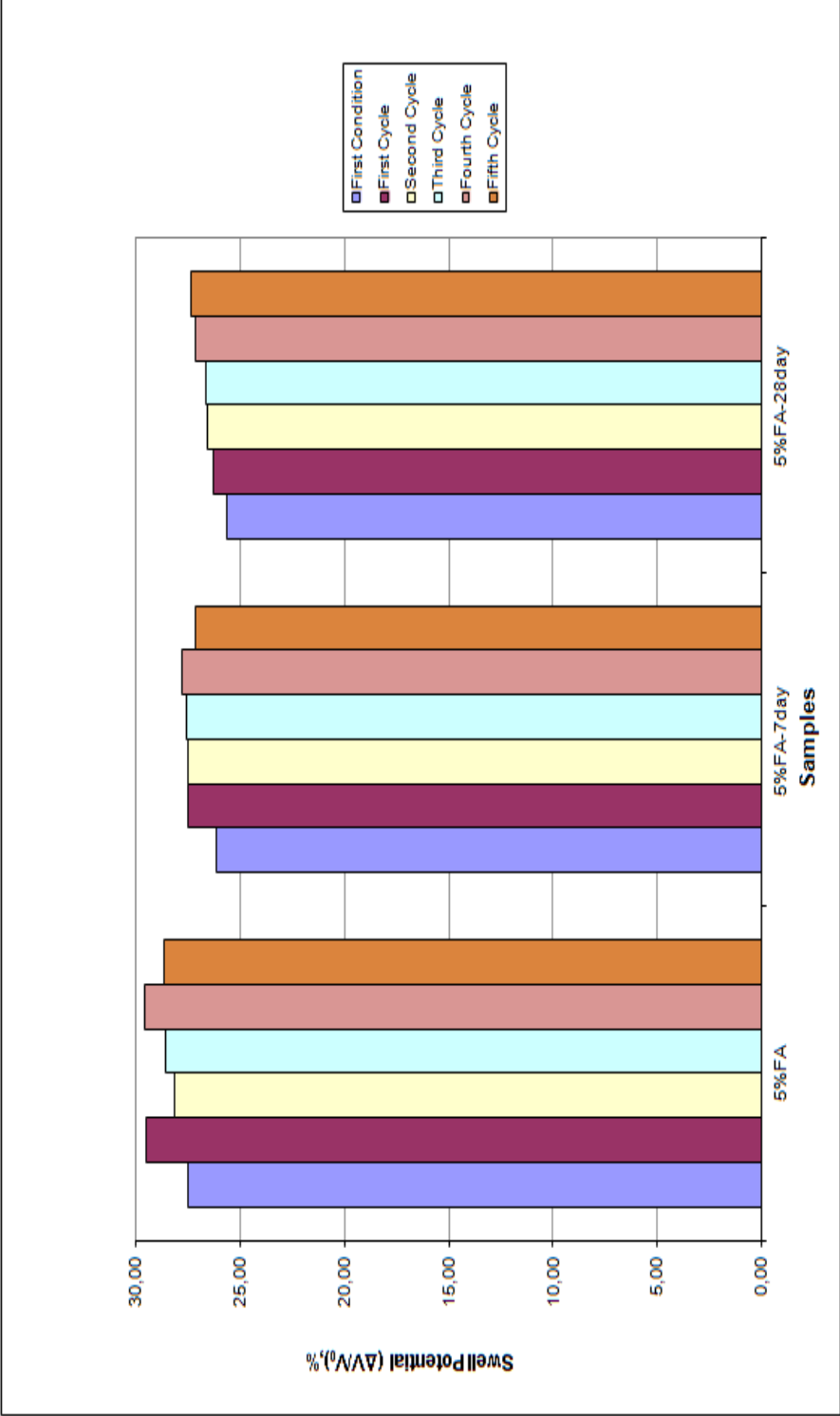


Figure 5.33 Volumetric Swell Potential of 5% fly ash added Samples with and without curing with respect to initial volume

5.6 SEM - EDX Analysis

Scanning Electron Microscope (SEM) is a microscope that forms images by using electrons rather than using light. SEM analysis gives valuable information about the microstructure of soils and change in microstructure for chemically treated soils.

In this study, SEM analysis was performed at METU Central Laboratory and during analysis QUANTA 400F Field Emission Scanning Microscope was used. It is a high resolution electron microscope with a resolution of 1.2 nm. The used voltage and magnification factor varied between 10-20kV and 3000-20000 respectively during the analysis. The samples, chosen for SEM analysis was tabulated in Table 5.4. Before the analysis all the samples were dried at 45°C as the water vapour harms the microscope. Then the samples were exposed to vacuum and covered with gold and palladium as the soil samples are insulant.

Table 5.4 Samples chosen for SEM Analysis

Sample	Condition
A	Before applying cycles (after compaction)
	After 5 swell-shrink cycles
5% FA	Before applying cycles (after compaction)
	After 5 swell-shrink cycles
20% FA	Before applying cycles (after compaction)
	After 5 swell-shrink cycles
3%L	Before applying cycles (after compaction)
	After first condition (dry state of first cycle)
5%L	Before applying cycles (after compaction)
	After 5 swell-shrink cycles

To see the effect of swell-shrink cycles on microstructure, samples were analysed both right after compaction and after being exposed to 5 swell-shrink cycles except for the 3%L treated sample. The aim of analysing 3%L after first condition (dry state of first cycle) was to determine the reason for high swelling amount in the first cycle. SEM images of samples are given in Figures 5.34 - 5.41.

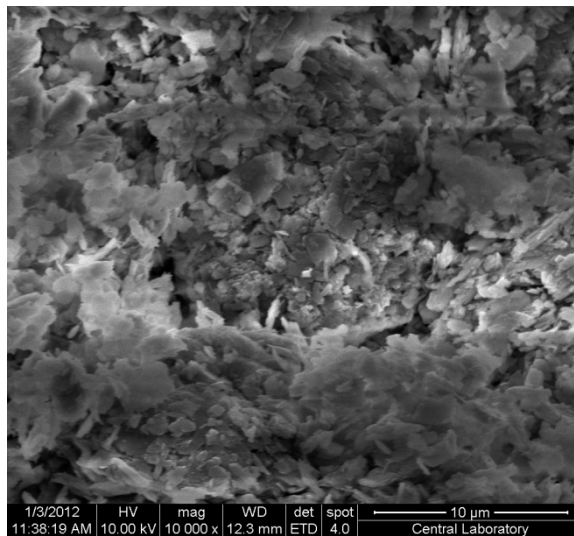


Figure 5.34 SEM image of Sample A after compaction (magnification factor=10000)

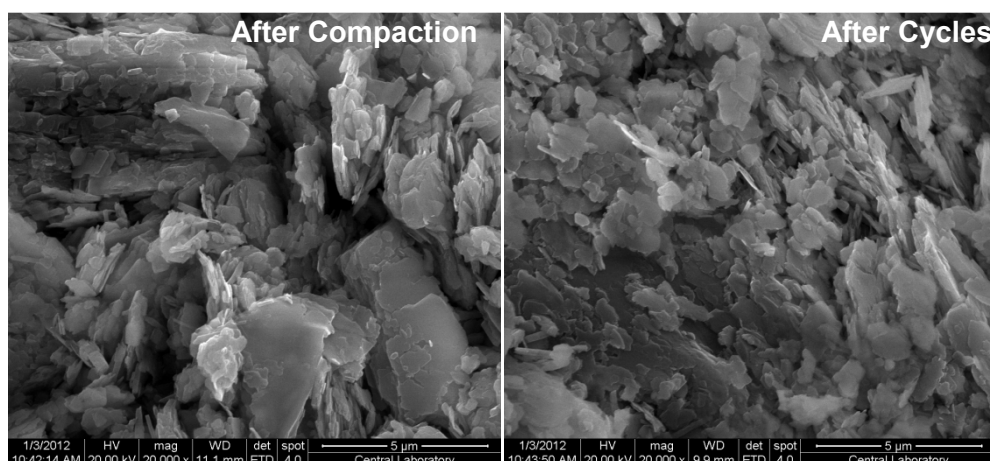


Figure 5.35 SEM images of Sample A after compaction and cycles (magnification factor=20000)

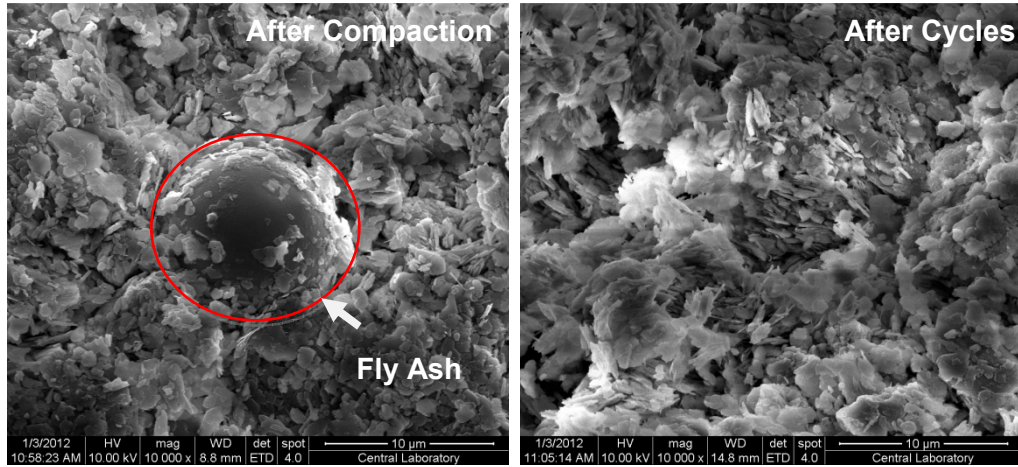


Figure 5.36 SEM images of 5%FA treated sample after compaction and cycles (magnification factor=10000)

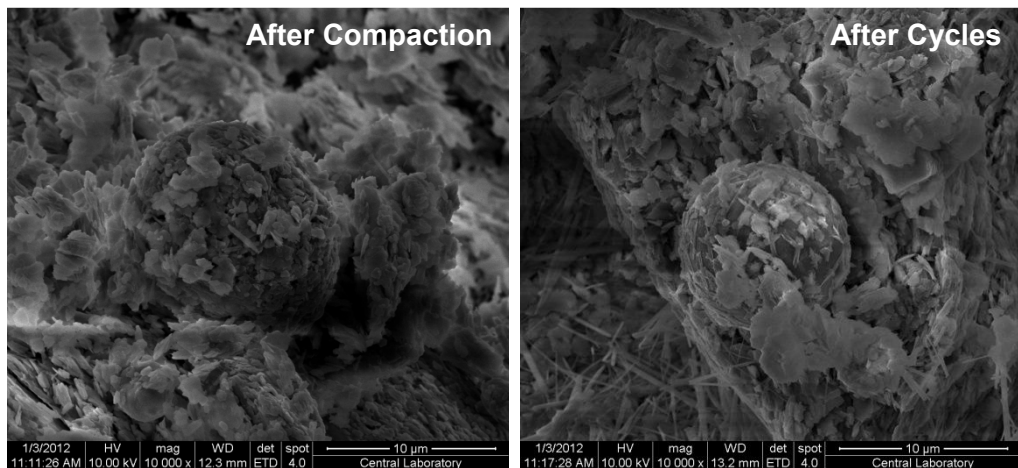


Figure 5.37 SEM images of 20%FA treated sample after compaction and cycles (magnification factor=10000)

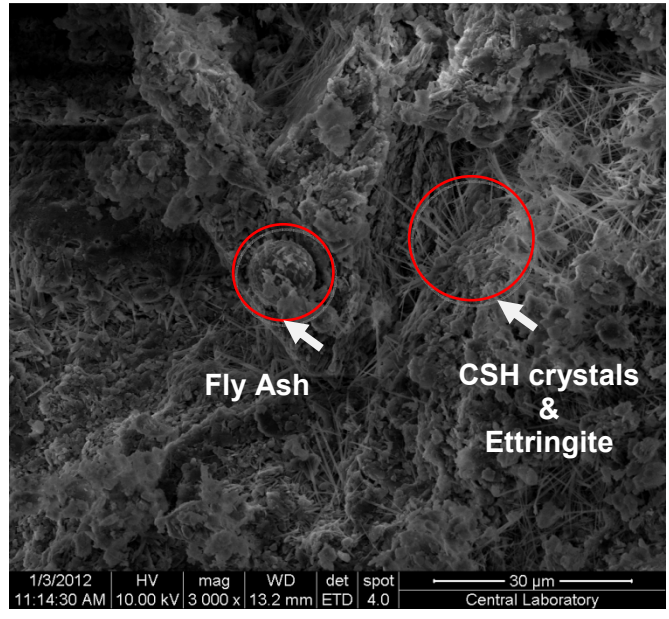


Figure 5.38 SEM images of 20%FA treated sample after cycles (magnification factor=3000)

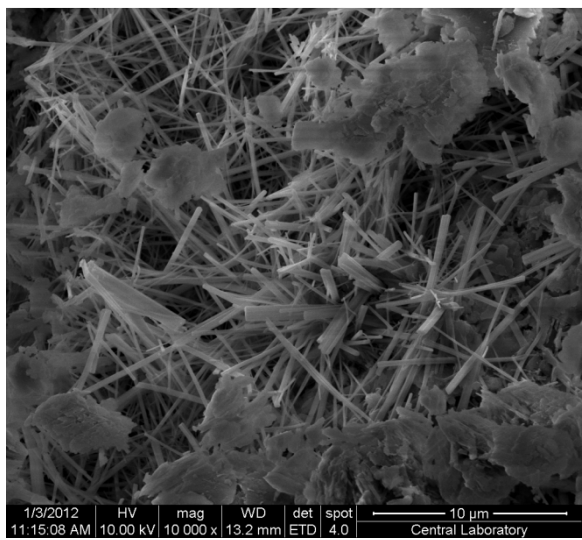


Figure 5.39 SEM images of Calcium Silicate Hydrate crystals (CSH) and Ettringite formed within 20%FA treated sample after cycles (magnification factor=10000)

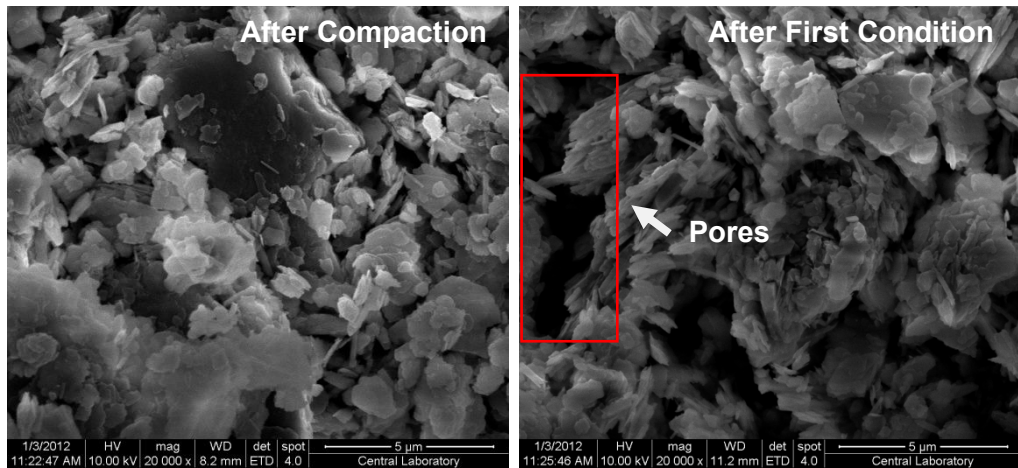


Figure 5.40 SEM images of 3%L treated sample after compaction and first condition (at dry state of first cycle) (magnification factor=20000)

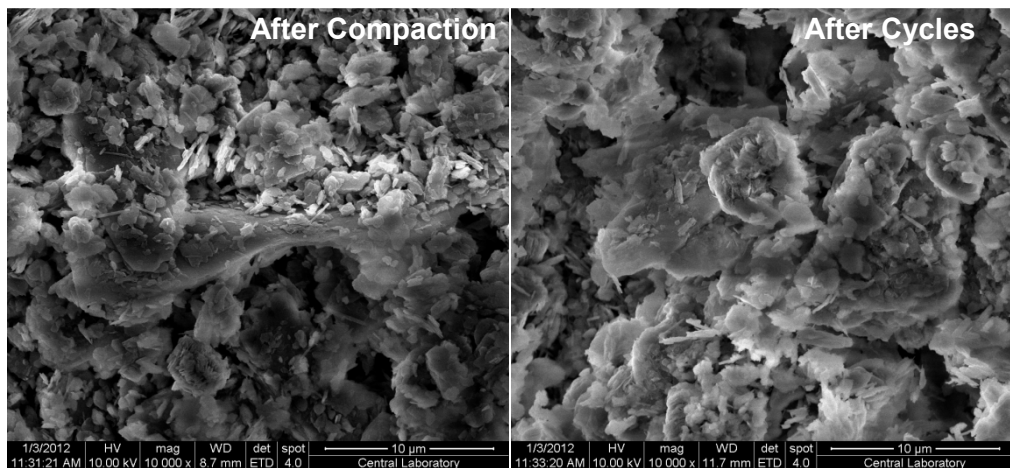


Figure 5.41 SEM images of 5%L treated sample after compaction and cycles (magnification factor=10000)

Also Energy Dispersive X-Ray (EDX) analysis which gives information about the chemical characterization (elements) of a material, was performed on 5%FA (after compaction) and 20%FA (after cycles) treated samples to detect the fly ash in these samples (Figures 5.36 and 5.38). EDX diagrams of the fly ash which is in the 5%FA (after compaction) and 20%FA samples (after cycles) are presented in Figure 5.42 and Figure 5.43 respectively.

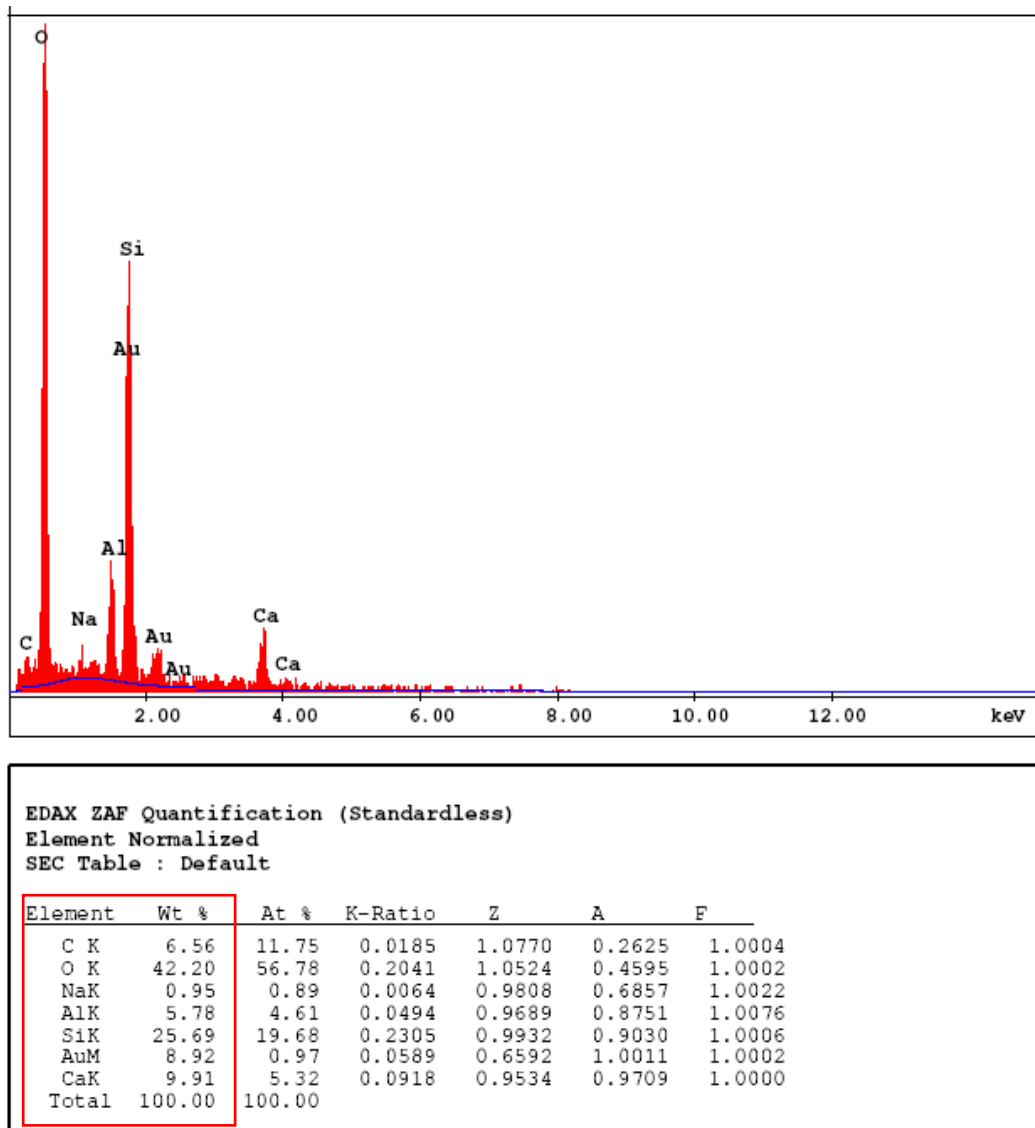
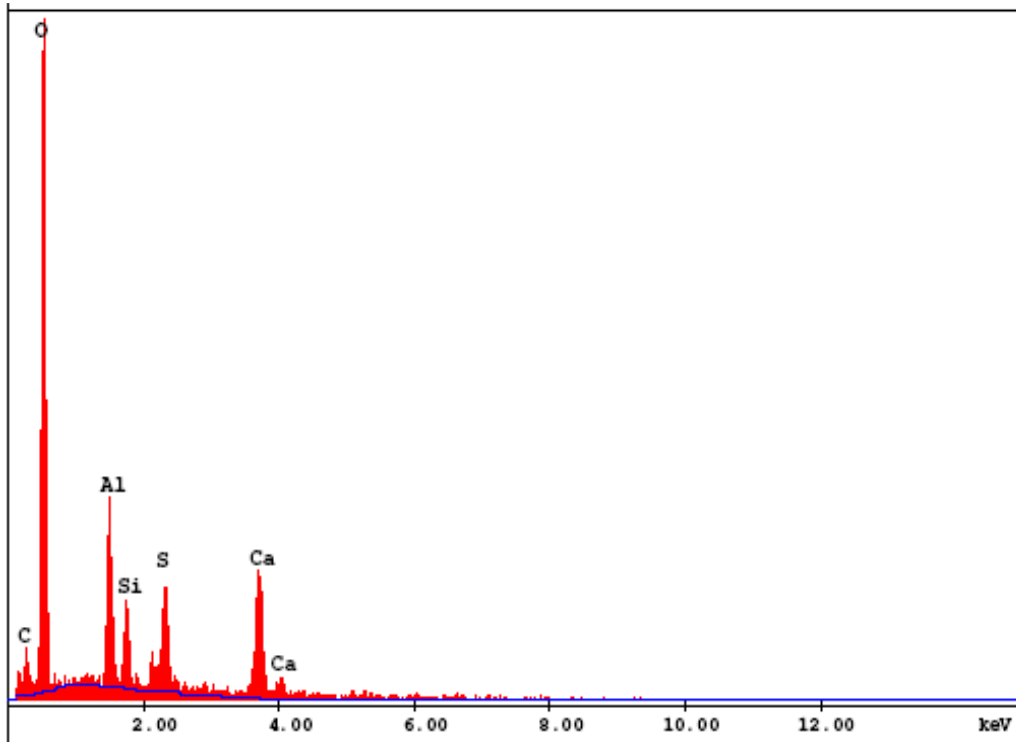


Figure 5.42 EDX Diagram of fly ash within the 5%FA treated sample (after compaction)



EDAX ZAF Quantification (Standardless)
 Element Normalized
 SEC Table : Default

Element	Wt %	At %	K-Ratio	Z	A	F
C K	5.65	9.81	0.0199	1.0617	0.3316	1.0006
O K	46.78	61.01	0.1935	1.0376	0.3987	1.0001
AlK	8.77	6.79	0.0735	0.9528	0.8759	1.0035
SiK	5.10	3.79	0.0449	0.9778	0.8954	1.0040
S K	8.15	5.30	0.0753	0.9642	0.9517	1.0068
CaK	25.55	13.30	0.2369	0.9360	0.9904	1.0000
Total	100.00	100.00				

Figure 5.43 EDX Diagram of fly ash within the 20%FA treated sample (after cycles)

CHAPTER 6

DISCUSSION ON TEST RESULTS

6.1 Effect of Additives on Grain Size Distribution

In ASTM D422, it is recommended to take hydrometer readings continually upto 4 hours and take final reading 24 hours from the start of the test. However, according to final readings, percent finer than 0.0014mm, seemed to increase with the addition of fly ash and lime. However, such an increase was unreasonable. The reason for that is the gradual decrease in percent passing values for the determined grain sizes, after 4 hours for Sample A. This gradual decrease could be explained by the hydration of bentonite. Therefore, percent passing values for the diameters smaller than 0.002 mm (clay sized particles) was not shown on the grain size distribution curves (Figure 5.12 & 5.13). Also continuous readings were taken upto 10 hours rather than 4 hours to better estimate the clay fraction.

After the hydrometer tests, it was found out that with the addition of stabilizers grain size distribution curve of Sample A shifted to coarser side (except for the particles smaller than 0.0014mm) (Figures 5.12 & 5.13). However, grain size distribution curves of 1% and 3% lime treated samples were not altered much (Figure 5.13). This shifting could be explained by the addition of silt-sized particles to Sample A and also by the flocculation of particles due to the chemical reactions.

6.2 Effect of Additives on Specific Gravity

Specific gravity of Sample A, fly ash and lime was found as 2.64, 2.56 and 2.52 respectively. As the specific gravity of Sample A is higher than that of fly ash and lime, it was expected that addition of stabilizers would decrease the specific gravity of Sample A. However, the test results were not as expected (Figure 5.5). Specific gravity remained same for 1% lime treated sample, and increased with the increase in lime content. For fly ash treated samples, specific gravity increased even for minimum percentage addition, 5%. With the increase in fly ash percentage, specific gravity also increased and remained same after 15% fly ash and found as 2.68 for both 15% and 20% added samples. Specific gravity remained same for the 5% sand treated samples. Increase in specific gravity for lime and fly ash treated samples could be caused by the pozzolonic reactions occurred due to high calcium content of lime and fly ash. Same trend was also observed in the study conducted by Çetiner, (2004) for the lime treated soils. The results of the tests and the specific gravity values calculated by mass basis are tabulated in Table 6.1. Specific gravity of expansive soil and lime was 2.51 and 2.76 respectively.

Table 6.1 Specific gravity values obtained in Çetiner, (2004) study

Sample	Specific Gravity (G_s)		Difference in G_s
	Measured	Calculated	
Expansive Soil	2.51	-	-
1% L	2.53	2.51	0.02
3% L	2.54	2.52	0.02
5% L	2.56	2.52	0.04
8% L	2.57	2.53	0.04

The difference in measured and calculated specific gravity values could be due to the pozzolonic reactions.

6.3 Effect of Additives on Liquid Limit

Liquid Limit values remained nearly same for 1% lime added sample and decreased for the remaining ones (Table 6.2). Liquid limit values of the treated samples also decreased with the increase in stabilizers percentage (Figure 5.6). Addition of 5% and 20% fly ash to Sample A reduced the liquid limit by 7.9 % and 25.7% respectively (Table 6.2). Same trend was also observed for lime treated samples and although addition of 1% lime did not change the liquid limit of Sample A, considerable amount of reduction observed for 3% and 5% added samples (Table 6.2). Liquid limit reduction of samples could be explained by addition of non-plastic material to Sample A and also flocculation of particles due to the reactions.

Table 6.2 Percent Changes in Specific Gravity (G_s), Liquid Limit (LL), Plastic Limit (PL), Plasticity Index (PI), Shrinkage Limit (SL), Linear Shrinkage (L_s), Shrinkage Index (SI) and Activity (A_c)

Sample	Percent change in							
	G_s	LL	PL	PI	SL	L_s	SI	A_c
A	0.0	0.0	0.0	0.0	0.0	0.0	0.0	0.0
5% FA	+0.4	-7.9	+14.8	-16.2	+26.9	-12.5	-20.0	-10.3
10% FA	+0.8	-12.9	+25.9	-27.0	+73.1	-31.3	-42.7	-19.2
15% FA	+1.5	-19.8	+18.5	-33.0	+84.6	-37.5	-56.0	-21.2
20% FA	+1.5	-25.7	+14.8	-40.5	+73.1	-37.5	-60.0	-26.7
1% L	0.0	+3.00	+14.8	-1.4	+3.8	0.00	+2.7	0.0
3% L	+0.8	-16.8	+25.9	-32.4	+73.1	-37.5	-48.0	-31.5
5% L	+1.1	-20.8	+29.6	-39.2	+88.5	-37.5	-58.7	-28.8
5% S	0.0	-4.0	+3.7	-6.8	0.0	0.0	-5.3	-2.1

“+”: increase, “-”: decrease

6.4 Effect of Additives on Plastic Limit

Plastic Limit values of Sample A increased with the addition of fly ash, lime and sand (Table 6.2). Plastic limit values of the samples increased with increasing amount of lime. However, for fly ash added samples maximum plastic limit value was obtained for 10% fly ash added sample and plastic limit values started to decrease with the increase in fly ash content. While addition of 10% fly ash increased the plastic limit by 25.9 %, increase for 20% fly ash treated sample was only 14.8%. Maximum increase observed for the 5% lime treated sample and minimum for 5% sand with the percent increase 29.6 and 3.7 respectively (Table 6.2).

6.5 Effect of Additives on Plasticity Index

Plasticity Index values of Sample A decreased with the addition of fly ash, lime and sand (Table 6.2). However, reduction for 1% lime treated sample was ignorable (1.4%). Addition of stabilizers in other percentages resulted in considerable variations in plastic limit. Maximum reduction observed for 5% lime and 20% fly ash treated samples with percent decrease 39.2% and 40.5% respectively (Table 6.2). Reduction in plasticity index of treated samples could be explained by addition of non-plastic material to Sample A and also flocculation of particles due to the chemical reactions.

6.6 Effect of Additives on Shrinkage Limit

Shrinkage limit remained nearly same for 5% sand added sample and increased by the addition of other stabilizers (Table 6.2). Increase in shrinkage limit for the 1% lime treated sample was ignorable (3.8%). Considerable increase observed for 3% and 5% lime treated samples with percent increase 73.1% and 88.5% respectively (Table 6.2). For the fly ash treated samples minimum and maximum increase was obtained for the sample that contains 5% and 15% fly ash respectively. It could be stated that the threshold value for

fly ash added samples was 10% and shrinkage limit did not change much after addition of more fly ash. Robinson and Thagesen, (2004) stated that sufficient water is needed for hydration and pozzolonic reactions to occur, also pozzolonic reactions proceed very slowly for the temperatures below 20-25°C and the rate of reaction increases for the temperatures above 25-30°C. Therefore, water and temperature are the two important factors that affect the reactions for chemically stabilized samples. As the water and temperature increases, rate of reactions increases. In the shrinkage limit test, samples were prepared with water content higher than liquid limit (Table 5.3) and allowed to dry at 105°C. So, such a high increment in shrinkage limit could be explained by these reactions which resulted in rapid setting of samples that caused less volume change.

6.7 Effect of Additives on Linear Shrinkage

Linear Shrinkage of Sample A did not change with the addition of 1% lime and 5% sand (Table 6.2). Maximum reduction was observed for the samples that were stabilized with 15% and 20% fly ash and 3% and 5% lime. The decrease in the linear shrinkage values for those samples was 37.5% (Table 6.2). Linear shrinkage values were concurrent with shrinkage limit values.

6.8 Effect of Additives on Shrinkage Index

Shrinkage Index values slightly increased for 1% lime treated sample however, this increase was ignorable (2.7%) (Table 6.2). Shrinkage index also did not vary much for 5% sand added sample. For the other treated samples, shrinkage index decreased dramatically. Maximum reduction was observed for 20% fly ash and 5% lime treated samples with the percent decrease values 60.0% and 58.7% respectively (Table 6.2).

6.9 Effect of Additives on Activity

Activity remained same for 1% lime treated sample and decreased significantly for other lime and fly ash treated samples (Table 6.2).

6.10 Effect of Additives on Swell Percentage

Swell percentage of Sample A decreased with the addition of stabilizer (Table 6.3). This reduction could be explained by replacement of some percent of expansive material with non-expansive material and chemical reactions.

Addition of 5% fly ash decreased the swell potential of Sample A by 56.0% and maximum percent reduction in swell percentage was 77.5% which was observed for 20% fly ash treated sample (Table 6.3). Effect of addition of 15% or 20% fly ash not differed much by means of swell percentage. Such a high reduction in swell percentage is due to the high calcium content of Soma Fly Ash.

For lime treated samples, percent reduction in swell percentage was 27.0%, 64.4% and 68% for 1%, 3% and 5% lime treated samples respectively. Swell percentages of 10% fly ash, 3% lime and 5% lime treated samples were nearly same (Table 6.3).

Minimum reduction in swell percentage was obtained for the 5% sand treated sample. However, this was an expected result since sand is an inert material. So it may be stated that addition of 5% non-swelling material to Sample A reduces swell percent by 8.7%. 5% fly ash and 5% lime addition to Sample A, reduces swell percent by 56% and 68%, therefore $56 - 8.7 = 47.3\%$ and $68 - 8.7 = 59.3\%$ reduction in swell percent is due to the chemical reactions.

Also it could be stated that, chart provided by Seed et al., (1962) is successful at predicting the swelling potential of soils (Table 5.3) considering the results of the swelling tests (Table 6.3).

Table 6.3 Swell Percentages and Percent Change in Swell Percentage with the addition of stabilizers

Sample	Swell Percentage (%)	Percent Change in Swell Percentage (%)
A	63.2	0
5% FA	27.5	-56.0
10% FA	21.1	-66.6
15% FA	15.1	-76.0
20% FA	14.2	-77.5
1% L	46.0	-27.0
3% L	22.5	-64.4
5% L	20.2	-68.0
5% S	57.7	-8.7

“-”: decrease

6.11 Effect of Curing on Swell Percentage

Swell percentages of 5% fly ash treated samples were obtained as 27.5 %, 26.2% and 25.7 % for no cured, 7 days cured and 28 days cured conditions (Figure 5.32). Change in swell percent was ignorable. Robinson and Thagesen, (2004) stated that sufficient water is needed for hydration and pozzolonic reactions to occur, also pozzolonic reactions proceed very slowly for the temperatures below 20-25°C and the rate of reaction increases for the temperatures above 25-30°C. As pozzolonic (long term) reactions depend on water and temperature, low water content (10%) and temperature (22-25°C) could be the reason of such a low reduction in swell percentage. Also as all of the samples waited one day in the desiccator before compaction to allow water distribute homogenously, this may also cause some pozzolonic reactions to occur.

6.12 Effect of Cyclic Swell-Shrink on Swell Percentages of Samples

Axial swell percentages of samples after each cycle are tabulated in Table 6.4

Table 6.4. Axial swell percentages ($\Delta H_i/H_{id}$) of samples at the end of each cycle

Samples	Swell Percentages (%)					
	First Condition	First Cycle	Second Cycle	Third Cycle	Fourth Cycle	Fifth Cycle
A	63.2	33.0	28.9	30.3	30.3	30.7
5% FA	27.5	14.0	12.8	13.0	13.6	12.8
10% FA	21.1	3.2	3.0	2.8	2.7	2.6
15% FA	15.1	1.9	1.6	1.7	1.6	1.6
20% FA	14.2	1.6	1.3	1.7	1.6	1.3
1% L	46.0	32.2	30.0	29.9	27.0	27.0
3% L	22.5	14.2	14.5	15.0	14.3	14.6
5% L	20.2	7.8	7.6	7.8	8.5	9.0
5% S	57.7	32.9	27.7	29.7	27.8	30.0

Axial swell percentages were calculated by dividing height difference between dry and wet state in a cycle (ΔH_i) to height at dry state (H_{id}) (Table 6.4). For all samples, swell percentages decreased at the first cycle and nearly remained same or slightly increase or decrease in the successive cycles. This reduction in axial swell percentage could be explained by the increase in height of samples and decrease in swelling after first drying state (Appendix B). Addition of 10, 15 and 20 % fly ash provided the maximum advantage and nearly same swell percentages were obtained for 15% and 20% fly ash treated samples.

Volumetric swell percentages of samples with respect to volume at dry state of each cycle are tabulated in Table 6.5

Table 6.5. Volumetric swell percentages ($\Delta V_i/V_{id}$) of samples at the end of each cycle

Samples	Swell Percentages (%)					
	First Condition	First Cycle	Second Cycle	Third Cycle	Fourth Cycle	Fifth Cycle
A	63.2	58.6	57.5	58.4	60.6	62.0
5% FA	27.5	18.3	17.4	17.2	17.9	16.4
10% FA	21.1	5.7	5.2	4.9	4.0	4.3
15% FA	15.1	4.0	3.5	3.7	3.5	3.8
20% FA	14.2	2.8	2.8	2.9	2.9	2.7
1% L	46.0	43.9	46.2	49.4	49.0	50.0
3% L	22.5	16.0	16.5	16.9	16.2	16.5
5% L	20.2	9.4	9.1	9.3	9.6	10.1
5% S	57.7	56.2	53.9	56.7	55.9	59.5

Volumetric swell percentages were calculated by dividing volume difference between dry and wet state in a cycle (ΔV_i) to volume at dry state (V_{id}) (Table 6.5). For the samples except for Sample A, 1% lime and 5% sand treated samples, swell percentages decreased at the first cycle and nearly remained same or slightly increase or decrease in the successive cycles. However, any significant change in swell potential was not observed for Sample A, 1% lime and 5% sand treated samples. Reduction in volumetric swell percentage for fly ash and lime treated samples (except for 1%) could be the result of such a high increase in shrinkage limit (Table 6.2) and also pozzolanic reactions.

Volumetric swell percentages of samples also calculated with respect to initial volume. The results are tabulated in Table 6.6

Table 6.6. Volumetric swell percentages ($\Delta V/V_0$) of samples with respect to initial volume

Samples	Swell Percentages (%)					
	First Condition	First Cycle	Second Cycle	Third Cycle	Fourth Cycle	Fifth Cycle
A	63.2	70.6	73.8	76.0	77.4	78.9
5% FA	27.5	29.5	28.2	28.6	29.6	28.7
10% FA	21.1	20.5	20.8	20.5	19.9	19.8
15% FA	15.1	15.4	15.1	15.6	15.4	15.5
20% FA	14.2	15.4	15.4	15.7	15.7	15.3
1% L	46.0	56.8	61.6	65.6	67.2	67.9
3% L	22.5	28.6	31.3	33.7	33.7	34.0
5% L	20.2	20.5	20.8	21.9	22.7	23.2
5% S	57.7	69.0	72.0	75.9	77.3	77.0

Volumetric swell percentages were also calculated by dividing change in initial volume (ΔV) of the sample at the end of each cycle to initial volume (V_0) to determine the effect of cyclic-wetting with respect to initial conditions (Table 6.6).

For Sample A, volumetric swell percentage increased after first cycle and increase in swell percentage continued for the successive cycles, however rate of increase was reached to equilibrium after third cycle.

For fly ash treated samples, swell percentage with respect to initial volume was not differed much after wetting-drying cycles. The observed increases were due to the micro cracks developed during drying.

Volumetric swell percentages of 1% lime and 5% sand treated samples increased after the first cycle and reached to equilibrium after fourth cycle .

For the 3% lime treated sample, an increase in swell percentage was observed after the first cycle and swell percentage reached to equilibrium at

the end of the third cycle. Increase in swell percentage of 3% lime treated sample could be the result of the change in the microstructure of sample after wetting-drying cycle that caused macro cracks at the drying periods of successive cycles and allowed water to enter pores of sample easily during swelling (Figure 6.1).



Figure 6.1. Views From 3% lime treated sample after drying ((a)-before first cycle, (b) – before second cycle)

For the 5% lime treated sample, an increase in swell percentage was observed after the second cycle however this increase was negligible and caused by the fungi-shaped heave in the upper portion of sample formed in the drying period of cycles (Figure 6.2).



Figure 6.2. View from fungi-shaped heaves occurred in the upper portion of 5% lime treated sample

Axial swell percentages ($\Delta H_i/H_{id}$), volumetric swell percentages with respect to volume at dry state of each cycle ($\Delta V_i/V_{id}$) and volumetric swell percentages with respect to initial volume for the 5% fly ash samples without cure, 7 days cured and 28 days cured conditions are tabulated in Table 6.7

Table 6.7. Swell percentages for 5% fly ash samples with no cure, 7 days cured and 28 days cured

Samples	Swell Type	Swell Percentages (%)					
		First Condition	First Cycle	Second Cycle	Third Cycle	Fourth Cycle	Fifth Cycle
5% FA	$\Delta H_i/H_{id}$	27.5	14.0	12.8	13.0	13.6	12.8
	$\Delta V_i/V_{id}$	27.5	18.3	17.4	17.2	17.9	16.4
	$\Delta V/V_0$	27.5	29.5	28.2	28.6	29.6	28.7
5% FA 7 days cured	$\Delta H_i/H_{id}$	26.2	14.6	14.1	13.6	13.8	13.5
	$\Delta V_i/V_{id}$	26.2	18.2	17.5	17.3	17.8	17.1
	$\Delta V/V_0$	26.2	27.5	27.5	27.6	27.8	27.2
5% FA 28 days cured	$\Delta H_i/H_{id}$	25.7	13.5	13.5	12.8	13.0	12.6
	$\Delta V_i/V_{id}$	25.7	17.9	17.6	17.4	18.0	17.4
	$\Delta V/V_0$	25.7	26.3	26.6	26.7	27.2	27.4

As can be seen in Table 6.7, swell percentages of samples after swell-shrink cycles were nearly same for 5% fly ash samples without cure, 7 days cured and 28 days cured conditions. Temperature and water are the two important factors that affect the pozzolonic reactions. Therefore, swell-shrink cycles could be considered as a condition that accelerates the pozzolonic reactions with a higher water content and temperature (45°C). For samples, reason for reaching such equilibrium in the swell percentage could be explained by this. The effect of temperature in pozzolonic reactions could be clearly seen in the study conducted by Beeghly, (2003). In that study, unconfined compressive strength tests were performed on the soil that were improved by 4% lime and 8% fly ash and cured in different conditions. The curing conditions and results of the tests are tabulated in Table 6.8

Table 6.8. Curing conditions and unconfined compressive strength (q_u) values in Beeghly, (2003) study.

Sample	Curing Conditions		q_u (psi)
	Time	Temperature	
4% L + 8% FA	3 day	50°C	220
	7 day	40°C	180
	28 day	22°C	170
	56 day	22°C	200

6.13 Discussions on SEM-EDX Analysis

Plate like microstructure (Figure 5.35-after compaction) of Sample A showed that main clay mineral in that sample is kaolinite. This is an expected result since Sample A contains 85% kaolinite and 15% bentonite. Also from Figure 5.35, it could be observed that size of the minerals for Sample A decreased after swell-shrink cycles which could be reason of increase in swell percent (with respect to initial volume, V_0), since swelling is directly related to specific surface of the minerals (as the size of the minerals decrease specific surface area increases). Addition of chemical additives altered microstructure slightly, samples became more flocculated (Figures 5.34, 5.35, 5.36, 5.37, 5.40 and 5.41 (after compaction))

For the 5%FA sample, fly ash particles could not be observed in the sample after 5 cycles, this could be the result of the coating of hydration reaction products to the surface of soil and fly ash (Figure 5.36). Figures 5.37, 5.38 and 5.39 directly show the effect of cyclic swell-shrink cycles on 20% FA treated sample. Right after the compaction, ettringite and CSH crystals were not observed in the sample, however after 5 swell-shrink cycles, crystal formations could directly be seen. Formation of crystals was also observed, for the sample which was treated with 35% fly ash and cured for 28 days, in the study performed by Ismaiel (2006). SEM views for natural soil and 35% fly ash treated sample with 28 days curing are presented in Figure 6.3.

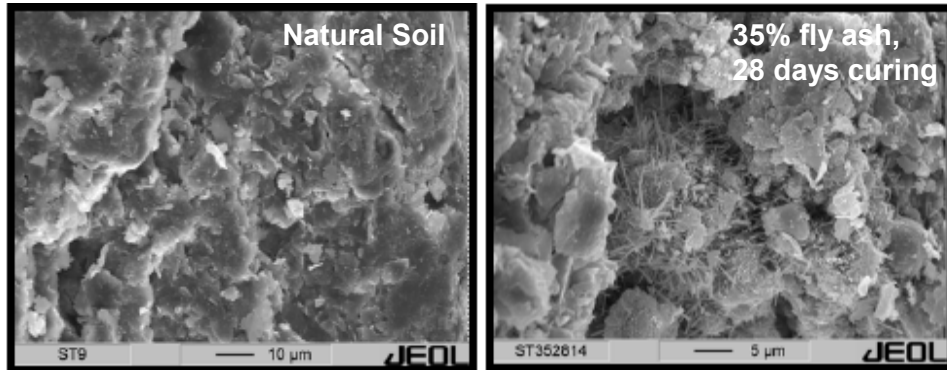


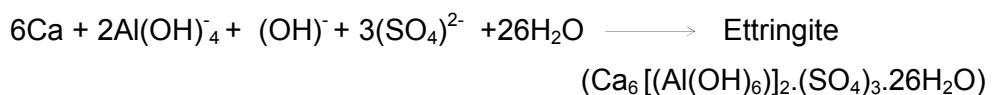
Figure 6.3. SEM views obtained in Ismaiel, (2006) study

Therefore, it may be stated that during swell-shrink cycles fly ash treated samples were cured.

For the 3%L sample (Figure 5.40), after first condition (dry state of first cycle), pores occurred which could be the result of increase in swell (by absorbing more water). For the 5%L sample (Figure 5.41), after cycles change in microstructure was observed which may be due to the pozzolonic reactions (cementation).

Gold (A_u) element observed in the EDX analyses of fly ash within 5% FA (Figure 5.42) sample (after compaction) was due to the covering of sample with gold and palladium before the test.

Sulfate that observed in EDX diagram of fly ash within the 20%FA treated sample (after cycles) (Figure 5.43) explains the formation of ettringite (Figures 5.38 and 5.39) in that sample as ettringite is formed by the modification of soil-fly ash reactions with the presence of sulfate. The reaction sequence of ettringite formation is presented below. (Ismaiel, 2006)



CHAPTER 7

CONCLUSIONS

The aim of this study is to investigate the effects of addition of Class C Fly Ash on atterberg limits, grain size distribution, swell percentage and then to investigate the effect of cyclic swell-shrink on swell percentage of an expansive soil stabilized by Class C Fly Ash. Also 1%, 3% and 5% lime and 5% sand was used for comparison. By considering the results of experiments, following conclusions could be reached;

1. Grain size distribution curves shifted to coarser side with the addition of fly ash and lime as a result of the addition of silt size particles and chemical reactions. However, grain size distribution curves of 1% and 3% lime treated samples were not altered much.
2. Specific gravity of Sample A increased with the addition of fly ash, and lime, except for 1% lime treated sample, due to the chemical reactions.
3. Liquid limit and plasticity index generally decreased with the addition of fly ash and lime as a result of the flocculation of particles. However, for 1% lime treated sample liquid limit and plasticity index nearly remained same.
4. Plastic limit and shrinkage limit increased with the addition of fly ash and lime.
5. Linear Shrinkage and Shrinkage Index decreased with the addition of fly ash and lime.

6. Activity values decreased with the addition of fly ash and lime except for the 1% lime treated sample.
7. Swell percentage of Sample A decreased with the addition of fly ash and lime. Reduction in swell percentage increased with the increase in amount of stabilizers. Therefore both lime and fly ash are effective stabilizers. Addition of 20% fly ash and 5% lime reduced the swell percentage of Sample A by 77.5% and 68% respectively. However, effect of addition of 15% or 20% fly ash not differed much by means of swell percentage.
8. Change in swell percent was ignorable for no cured, 7 days cured and 28 days cured 5% fly ash treated samples.
9. When the axial swell after each cycle considered; swell percentages decreased at the first cycle and nearly remained same or slightly increased or decreased in the successive cycles for all samples. Addition of 10, 15 and 20 % fly ash provided the maximum advantage and nearly same swell percentages were obtained for 15% and 20% fly ash treated samples.
10. When the volume at the dry state of each cycle considered, swell percentages decreased at the first cycle and nearly remained same or slightly increase or decrease in the successive cycles for the samples except for Sample A and 1% lime treated sample. However, any significant change in swell potential was not observed for Sample A, and 1% lime treated samples.
11. When the initial volume considered, volumetric swell percentage of Sample A increased after first cycle and increase in swell percentage continued for the successive cycles and rate of increase reached to equilibrium after third cycle. Swell percentage with respect to initial volume not differed much after wetting-drying cycles for fly ash treated samples. Volumetric swell percentages of 1% lime treated samples increased after the first cycle and reached to equilibrium after

fourth cycle. For the 3% lime treated sample, an increase in swell percentage was observed after the first cycle and swell percentage reached to equilibrium at the end of the third cycle. For the 5% lime treated sample, an increase in swell percentage was observed after the second cycle however this increase was negligible.

12. Swell percentages of samples after swell-shrink cycles were nearly same for 5% fly ash samples without cure, 7 days cured and 28 days cured conditions.

In this study, when the index properties and swell percentages before and after swell-shrink cycles considered, it was observed that 1% lime treatment was not effective in stabilizing Sample A.

When the swell percentages at the first condition are considered both 3% and 5% lime treatment nearly provided the same beneficiary effect. However, threshold value for lime was 5% for this study which also protected its' beneficiary effect after swell-shrink cycles. All fly ash treated samples saved their beneficiary effect after cyclic-swell shrink tests. However, considering the swell percentages before and after cycles, it could be stated that optimum fly ash is 15% for this study. This fly ash could be used to stabilize expansive soils near the thermal power plant considering the transportation cost.

Recommendations for Future Researches

It should be considered that this was a specific study for this fly ash, expansive soil and the applied conditions as the chemical reactions depend on calcium content of fly ash and chemical composition and index properties of expansive soils. Therefore, for better estimating the long-term behaviour of fly ash treated samples, different fly ashes should be used for different expansive soils having different mineralogical conditions and cycles should be applied under different surcharges, with different drying conditions (temperatures). It should also be taken into account before starting the tests that, applying

cycles takes considerable time. In this study, one cycle (wetting-drying), took nearly 7.5 days for untreated sample and 3 days for treated samples and occurrence of cracks makes it necessary to repeat the tests more than 2 times.

REFERENCES

Akcanca, F. and Aytekin M., Effect of Wetting-Drying Cycles on Swelling Behavior of Lime Stabilized Sand-Bentonite Mixture, *Environmental Earth Science*, 2011

Alkaya, D., Investigation of Using Fly Ash in Ground Improvement, *Electronic Journal of Construction Technologies*, Vol: 5, No: 1, pp. 61-72, 2009, in Turkish

Al-Homoud, A.S., Basma, A.A., ASCE, Hussein, A.I.M. and Al Bashabsheh, M.A., Cycling Swelling Behavior of Clays, *Journal of Geotechnical Engineering*, Vol. 121, No.7, p.562-565, 1995

Al-Mhaidib, A. I. and Al-Shamrani, M.A., Swelling Characteristics of Lime-Treated Expansive Soils, *Geotechnical Engineering, Journal of Southeast Asian Geotechnical Society*, Vol. 27, No. 2, pp. 37-53, 1996

Al-Rawas, A.A. and Goosen, M., *Expansive Soils Recent Advances and Characterization and Treatment*, Taylor and Francis, Balkema, 2006

ASTM, Standard Test Methods for One-Dimensional Swell or Settlement Potential of Cohesive Soils, *Annual Book of ASTM Standards*, D4546 – 08, Vol. 04 -08, pp. 733-738, 2008

ASTM, Standard Test Method for Chemical Analysis of Limestone, Quick Lime and Hydrated Lime, *Annual Book of ASTM Standards*, C25 – 11, 2011

ASTM, Standard Specification for Coal Fly Ash and Raw or Calcined Natural Pozzolan for Use in Concrete, *Annual Book of ASTM Standards*, C618 – 08a, 2008

American Coal Ash Association, ACAA, www.acaa-usa.org, (last visited on 28/06/2011)

Baba, A., Kaya, A., Leaching Characteristics of Fly Ash From Thermal Power Plants of Soma and Tunçbilek, Turkey, *Environmental Monitoring and Assessment*, Vol.91, pp. 171-181, 2004

Basma, A.A., Al-Homoud, A.S., Malkaw, A.I.H., and Al-Bashabsheh, M.A., Swelling – Shrinkage Behavior of Natural Expansive Clays, *Applied Clay Science*, Vol.2, pp.211-227, 1996

Beeghly, J.H., Recent Experiences with Lime-Fly Ash Stabilization of Pavement Subgrade Soils, Base and Recycles Asphalt, *Proceeding of International Ash Utilization Symposium, Lexington*, pp. 435-452, 2003

Chen, F. H., *Foundations on Expansive Soils*, Elsevier Scientific Pub. Co., Amsterdam, 1975

Chiottori, B.C.S., Clay Mineralogy Effects on long-term Performance of Chemically Treated Expansive Clays, *Ph. D. Thesis*, The University of Texas, USA, 302 pages, 2008.

Craig, R.F., *Soil Mechanics*, 7th edition, Spon Press, London, 2004

Çelik, Ö., The Effects of Fly Ash, Silica Fume and Sludge Additives on the Strength of Cement, *Concrete Congress 2004*, İstanbul, pp 657-663, 2004.

Çetiner, S.I., Stabilization of Expansive Soils by Çayırhan Fly Ash and Desulphogypsum, *M.S. Thesis*, METU, Turkey, 107 pages, 2004

Çokça, E., Use of Class C Fly Ashes for the Stabilization of Expansive Soil, *Journal of Geotechnical and Geoenvironmental Engineering*, Vol. 127, No.7, pp.568-573, 2001

Direskeneli, H., Soma Manisa Turkey-Thermal Power Plant: Brief Report for Future Investors, *The Journal of Turkish Weekly*, 2007

Doostmohammadi, R., Moosavi, M., Mutschler, Th. and Osan, C., Influence of Cycling Wetting and Drying on swelling behavior of Mudstone in South West of Iran, *Environmental Geology*, Vol. 58, p.999-1009, 2009.

Erol, M.M., Küçükbayrak, S. and Meriçboyu, A., The Recycling of the Coal Fly Ash in Glass Production, *Journal of Environmental Science and Health*, Vol.41, pp.1921-1929, 2006.

Fang, H., *Foundation Engineering Handbook*, 2nd edition, Van Nostrand Reinhold, America, 1991

Foster, M. D., The Relation between Composition and Swelling in Clays, *Clays and Clay Minerals*, Vol.3 No.1, pp. 205-220, 1954

Görhan, G., Kahraman, E., Başpınar, M. S. and Demir, İ., Fly Ash Part II: The Properties of Chemical, Mineralogy and Morphology, *Electronic Journal of Construction Technologies*, Vol.5, No.2, pp.33-42, 2009

Greenpeace, [http:// www.greenpeace.org](http://www.greenpeace.org), (last visited on 20.09.2011)

Guney, Y., Sari, D., Cetin M, and Tuncan, M., Impact of Cycling wetting-drying on swelling behavior of lime-stabilized soil, *Building and Environment*, Vol. 42, p.681-688, 2007

Hausman, M.R., *Engineering Principles of Ground Modification*, 2nd edition, Mc Graw-Hill, Newyork, 1990

Ismaiel, H. A. H., Treatment and Improvement of the Geotechnical Properties of Diffrent Soft Fine-Grained Soils Using Chemical Stabilization, *Ph. D. Thesis*, Martin Luther Hate- Wittenberg University, 121 pages, 2006

İpek. T., Stabilization of Expansive Soils Using Lime, Cement and Fly Ash, *M.S. Thesis*, METU, Turkey, 119 pages, 1998

Ji-Ru, Z. and Xing, J., Stabilization of Expansive Soils by Lime and Fly Ash, *Journal of Wuhan University of Technology-Material Science Ed.*, Vol. 17, No. 4, pp.73-78, 2002

Kalkan, E., Impact of Wetting-Drying Cycles on Swelling Behavior of Clayey Soils Modified by Silica Fume, *Applied Clay Science*, Vol.52, pp. 345-352, 2011

Koteswara, K.D., The Efficacy of Reinforcement Technique on the Fly Ash Stabilized Expansive Soil as a Subgrade Embankment for Highways, *Internatiaonal Journal of Engineering Science and Technology*, Vol. 3, No.2, pp.772-782, 2011.

Mackiewicz S.M., Ferguson, E.G., Stabilization of Soil with Self-Cementing Coal Ashes, *2005 World of Coal Ash (WOCA)*, Lexington, Kentucky, USA

Minerology Database, Illite Image, <http://webmineral.com/specimens/picshow.php?id=1284&target=Illite> (last visited on 11/06/2011)

Mitchell, J.K., Soga, K., *Fundamentals of Soil Behaviour*, 3rd edition, John Wiley & Sons Inc, New Jersey, 2005

Murray, H. H., *Applied Clay Mineralogy*, 1st edition, Elsevier, Amsterdam, 2007

Nalbantoğlu, Z., and Güçbilmez, E., Improvement of Calcareous Expansive Soils in Semi-Arid Environments, *Journal of Arid Environments*, Vol. 47, Issue 4, pp.453-463, 2001

Nalbantoğlu, Z., Effectiveness of Class C Fly Ash as an Expansive soil stabilizer, *Construction and Building Materials*, Vol. 18, p.377-381, 2004

Nelson, J.D. and Miller, D.J., *Expansive Soils, Problems and Practice in Foundation and Pavement Engineering*, 1st edition, John Wiley and Sons Inc., United States, 1992

Oweis, I. S., Khera, R. P., *Geotechnology of Waste Management*, 2nd Edition, PWS Publishing Company, Boston, 1998.

Phanikumar, B. R. and Sharma R.S., Volume Change Behavior of Fly-Ash Stabilized Clays, *Journal of Materials in Civil Engineering*, Vol. 19, No.1, pp.67-74, 2007

Rao, S.M., Reddy. B.V.V. and Muttharam, M., *The impact of cycling wetting and drying on the swelling behaviour of stabilized expansive soils*, *Engineering Geology*, Vol. 60, p.223-233, 2001

Rao, S.M., Reddy. B.V.V. and Muttharam, M., Effect of cycling wetting and drying on the index properties of a lime-stabilized expansive soil., *Ground Improvement*, Vol.5, No.3, p.107-110, 2001

Rao, A.S. and Rao, M.R., Swell-Shrink Behavior of Expansive Soils Under Stabilized Fly Ash Cushions, *The 12th International Conference of International Association for Computer Methods and Advance in Geomechanics*, India, pp.1539-1546, 2008.

Robinson. R. and Thagesen B., *Road Engineering for Development*, 1st edition, Spoon Press, London, 2004

Santos, F., Li, L., Li, Y. and Amini, F., Geotechnical Properties of Fly Ash and Soil Mixtures for use in Highway Embankments, *World of Coal Ash (WOCA) Conference*, Denver, CO, USA, 2011.

Sivapullaiah, P.V., Prashanth, J.P., Sridharan, A., Narayana, B.V., Technical Note Rective Silica and Strength of fly ashes, *Geotechnical and Geological Engineering*, Volume 16, No.3, pp.239-250, 1998

Şenol, A., Use of Class C Fly Ash for Stabilization of Soft Subgrade, *ARI, The Bulletin of the İstanbul Technical University*, Volume 53, No.1, pp.98-104, 2003

Tawfig, S. and Nalbantoğlu, Z., Swell-Shrink Behavior of Expansive Clays, *International Conference on New Developments in Soil Mechanics and Geotechnical Engineering*, Near East University, Nicosia, North Cyprus, 2009

Tripathy, S., and Subba Rao, S.K., Cycling Swell-Shrink Behavior of a compacted Expansive Soil , *Geotechnical Geological Engineering*, Vol. 27, p.89-103, 2009

Türker, P., Erdoğan B., Katnaş, F. and Yeğınobalı, A., *Classification and Properties of Fly Ashes in Turkey*, 4th edition, Türkiye Çimento Mühtahsilleri Birliđi, 2009

Türköz, M., Effect of Cyclic Swell-Shrink on Microstructural Changes of Compacted Swelling Clays, *Journal of Engineering and Architecture Faculty of Eskişehir Osmangazi University*, Vol 22. No.1, pp.77-91, 2009

USGS, <http://pubs.usgs.gov/of/2001/of01-041/html/docs/clay.htm>, (last visited on 11/06/2011)

Walker, D.D., *Innovations and Uses for Lime*, American Society for Testing Material, Baltimore, 1992.

Wan, Y., Kwong, J., Brandes, H.G., Jones, R.C., Influence of Amorphous Clay-Size Materials on Soil Plasticity and Shrink-Swell Behavior, *Journal of Geotechnical and Geoenvironmental Engineering*, Vol. 128, No. 12, pp. 10126-1031, 2002

Zha, F., Liu, S., Du, Y. and Cui, K., Behavior of Expansive Soils Stabilized with Fly Ash, *Natural Hazards*, Vol. 47, pp. 509-523, 2008

APPENDIX A

CHEMICAL ANALYSIS REPORT OF SOMA FLY ASH

Numune No	Numune İşareti	SiO ₂	Al ₂ O ₃	Fe ₂ O ₃	CaO	MgO	Na ₂ O	K ₂ O	TiO ₂	P ₂ O ₅	MnO	A.Za
11-H-3253	-	38.10	16.55	4.10	31.45	1.35	0.35	1.40	0.70	0.20	0.10	0.45

Analiz/Test Sonucu (%)
Analysis/Test Result

Müşterinin Adı/Adresi : Prof. Dr. Erdal ÇOKÇA
Customer Name/Address : ODTÜ Mühendislik Fakültesi İnşaat Mühendisliği Bölümü
06531 ANKARA

Proje Kodu : 20
Project Code

Numune Kayıt No/Tarih : 11-H-3253/ 12.07.2011
No. of receipt of sample/Date

Analiz/Testin Yapıldığı Tarih : 22/07/2011
Date of Analysis/Test

Numunenin Tanımı ve Cinsi : C Sınıfı Uçucu Kül
Identity and type of sample

Raporun Sayfa Sayısı : 1
Number of pages of the Report

Açıklamalar : Numune 105°C'de kurutulmuştur.
Remarks : Analizler, 2315 No.lu THERMO marka XRF Spektrometresinin UQ programında yapılmıştır.
Ateş Zaiyatı, yaş metot (gravimetrik yöntem) ile 1050 °C' de yapılmıştır.

Analiz/Test Sonucu (%)
Analysis/Test Result

Numune No	Numune İşareti	SiO ₂	Al ₂ O ₃	Fe ₂ O ₃	CaO	MgO	Na ₂ O	K ₂ O	TiO ₂	P ₂ O ₅	MnO	A.Za
11-H-3253	-	38.10	16.55	4.10	31.45	1.35	0.35	1.40	0.70	0.20	0.10	0.45

İrem PEKDEMİR
Kimyager
Analiz/Test Sorumlusu
Person in charge of analysis/test

Dilara ÖZŞUCA
Birim Yöneticisi
Supervisor of laboratory

Gülden DEMİRTAŞ
Koordinatör
Head of laboratory

Mühür
Seal

Tarih
Date

Sayfa 1/1
Page 1 of 1

MTA
Rapor No
2267
Rapor Tarihi
26/07/2011

T.C.
ENERJİ VE TABİİ KAYNAKLAR BAKANLIĞI
MADEN TETKİK VE ARAMA GENEL MÜDÜRLÜĞÜ
Maden Analizleri ve Teknolojisi Dalresi Başkanlığı
Universiteler Mahallesi Dumlupınar Bulvarı No : 139 06800 Çankaya/ANKARA

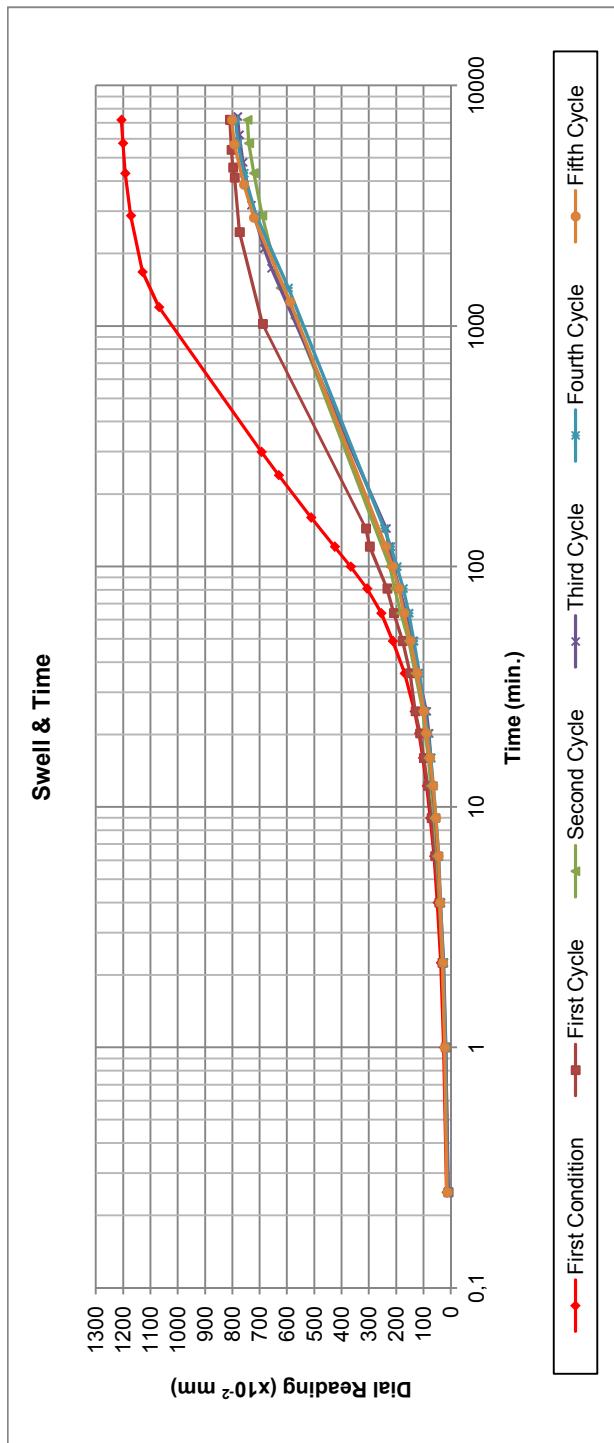
ANALİZ/TEST RAPORU
ANALYSIS/TEST REPORT

Figure A.1. Chemical Analysis Report of Soma Fly Ash

APPENDIX B

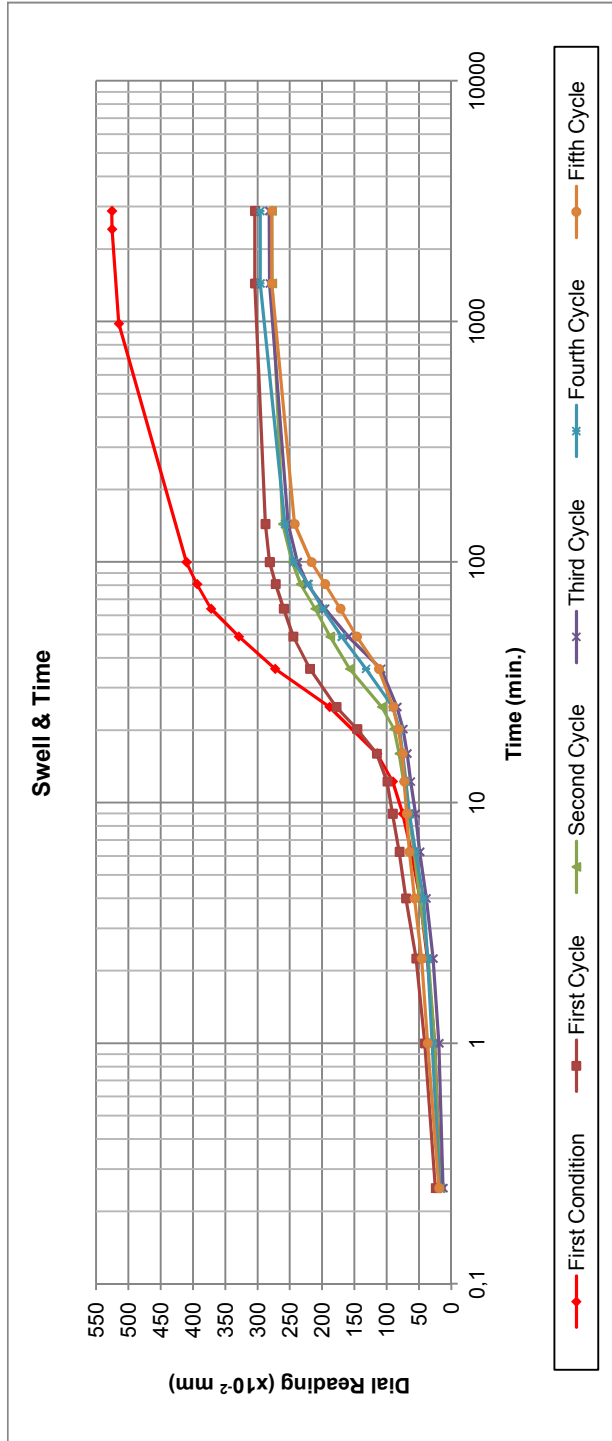
SWELL VERSUS TIME GRAPHS

Swell amount versus time graphs for Sample A, 5%FA treated sample with no curing, 7 days and 28 days curing, 10%FA, 15%FA, 20%FA, 1%L, 3%L, 5%L and 5%S treated samples, for the first condition and for each cycle are presented in Appendix B.



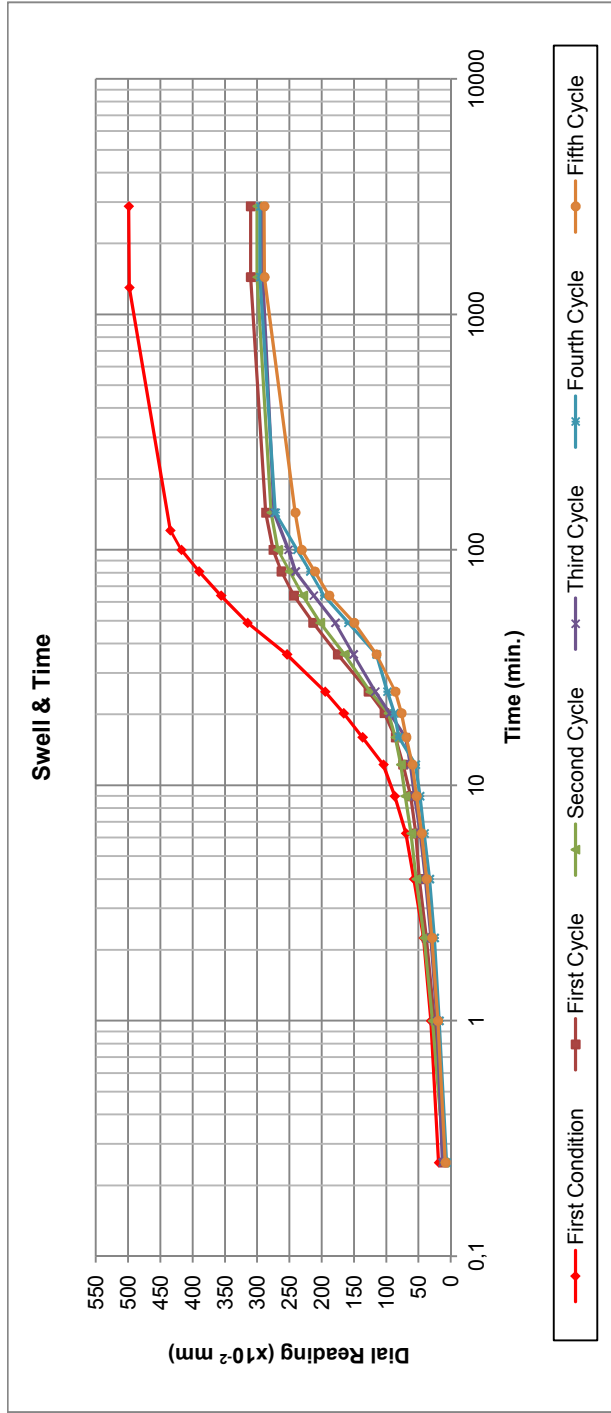
	First Condition	First Cycle	Second Cycle	Third Cycle	Fourth Cycle	Fifth Cycle
Initial Height (h _i), mm	19.10	24.50	25.75	25.80	26.00	26.15
Final Height (h _f), mm	31.17	32.59	33.20	33.61	33.89	34.17
Initial Volume (V _i), cm ³	61.12	65.75	67.45	67.90	67.50	67.50
Final Volume (V _f), cm ³	99.73	104.29	106.23	107.54	108.43	109.33

Figure B.1. Swell Amount versus Time Graph for Sample A



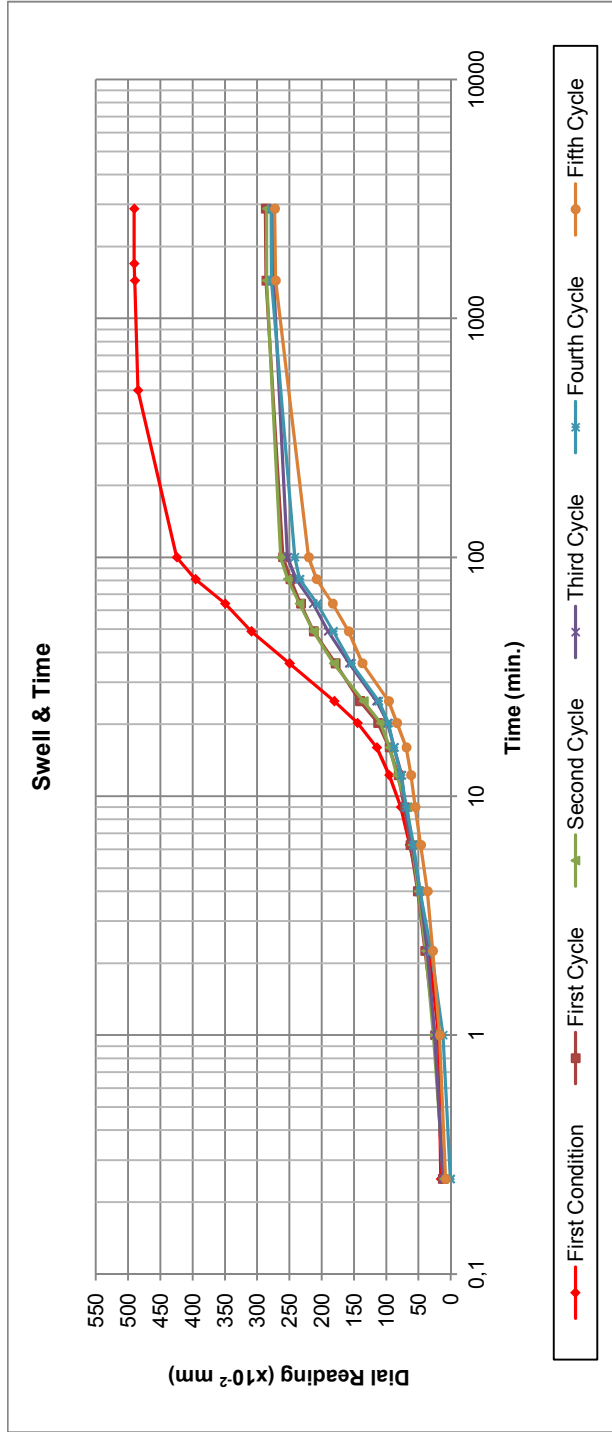
	First Condition	First Cycle	Second Cycle	Third Cycle	Fourth Cycle	Fifth Cycle
Initial Height (h_i), mm	19.10	21.70	21.70	21.75	21.80	21.80
Final Height (h_f), mm	24.36	24.74	24.48	24.57	24.76	24.58
Initial Volume (V_i), cm^3	61.12	66.92	66.70	67.10	67.20	67.60
Final Volume (V_f), cm^3	77.93	79.17	78.33	78.62	79.23	78.65

Figure B.2. Swell Amount versus Time Graph for 5%FA treated sample with no curing



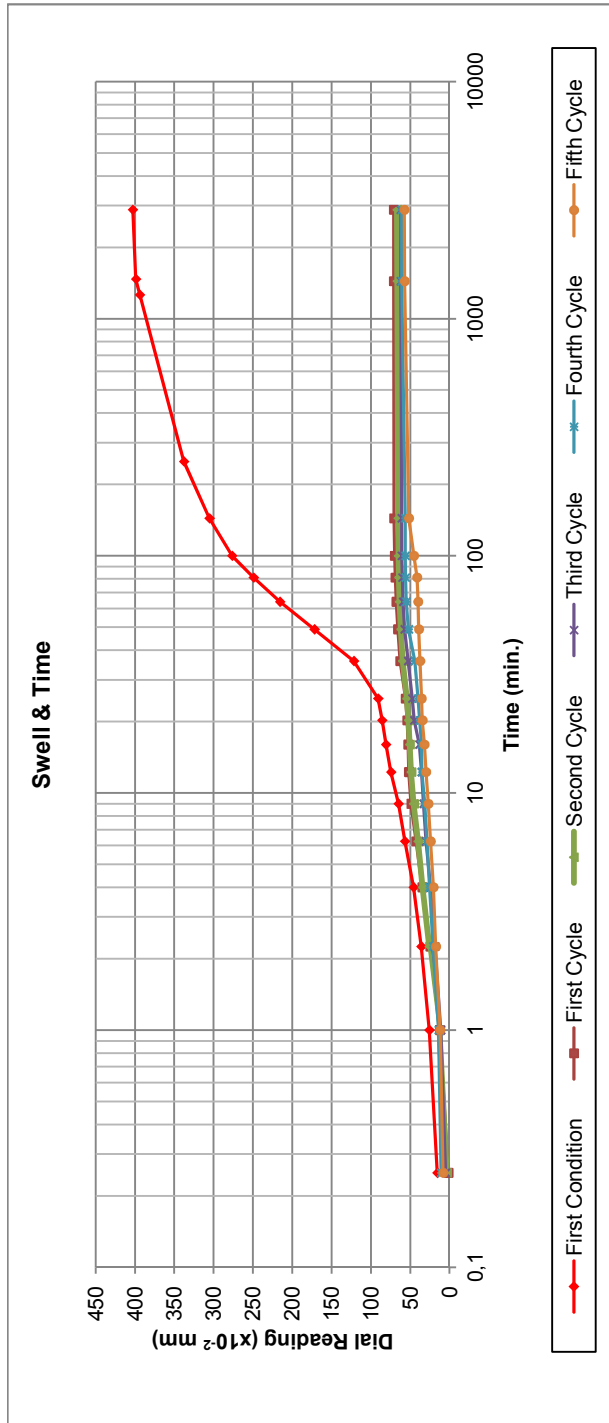
	First Condition	First Cycle	Second Cycle	Third Cycle	Fourth Cycle	Fifth Cycle
Initial Height (h_i), mm	19.10	21.25	21.35	21.45	21.45	21.40
Final Height (h_f), mm	24.09	24.35	24.35	24.37	24.41	24.29
Initial Volume (V_i), cm^3	61.12	65.90	66.30	66.45	66.30	66.40
Final Volume (V_f), cm^3	77.09	77.92	77.92	77.97	78.09	77.73

Figure B.3. Swell Amount versus Time Graph for 5%FA treated sample with 7 days curing



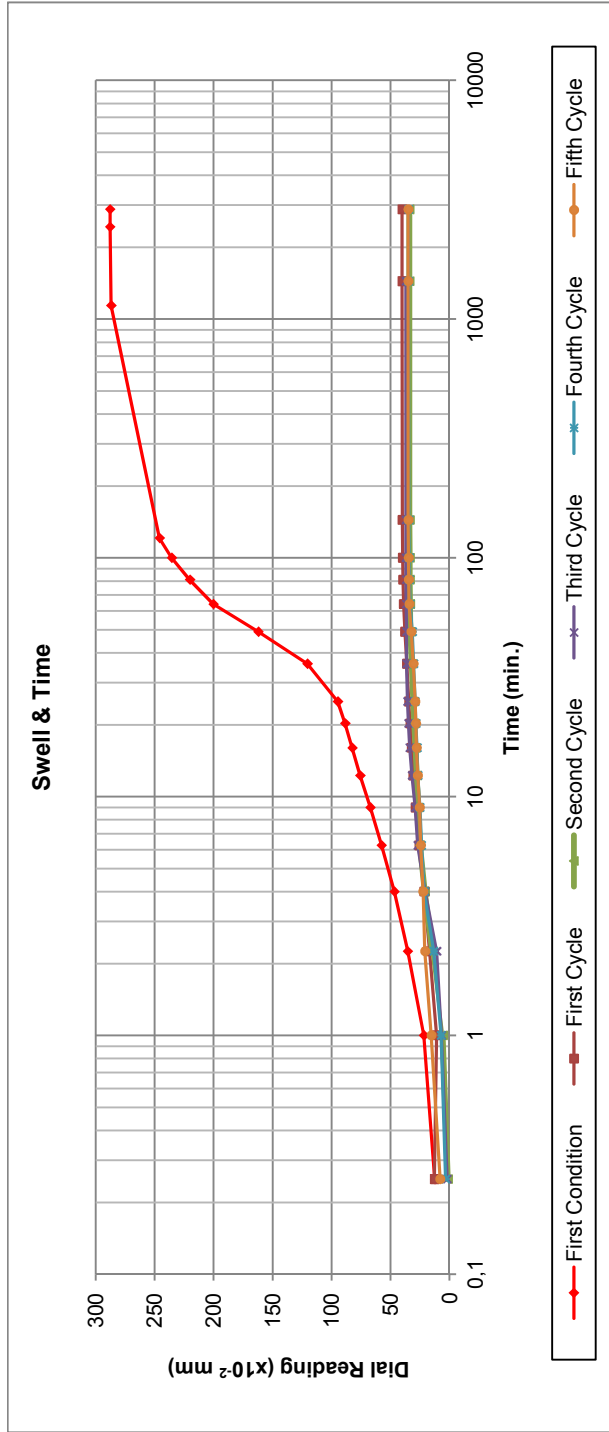
	First Condition	First Cycle	Second Cycle	Third Cycle	Fourth Cycle	Fifth Cycle
Initial Height (h_i), mm	19.10	21.25	21.30	21.45	21.50	21.60
Final Height (h_f), mm	24.01	24.12	24.18	24.19	24.29	24.33
Initial Volume (V_i), cm^3	61.12	65.50	65.80	65.95	65.85	66.30
Final Volume (V_f), cm^3	76.82	77.19	77.36	77.41	77.71	77.85

Figure B.4. Swell Amount versus Time Graph for 5%FA treated sample with 28 days curing



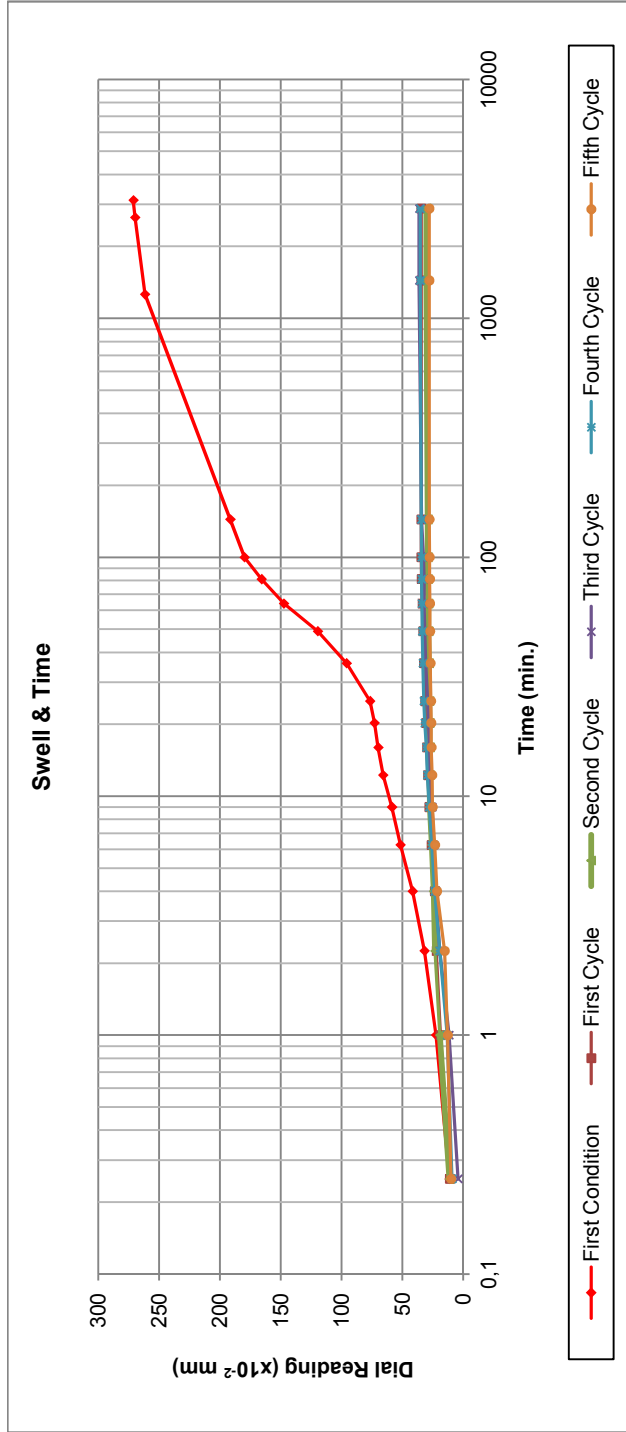
	First Condition	First Cycle	Second Cycle	Third Cycle	Fourth Cycle	Fifth Cycle
Initial Height (h_i), mm	19.10	22.30	22.40	22.40	22.30	22.30
Final Height (h_f), mm	23.13	23.01	23.07	23.02	22.91	22.88
Initial Volume (V_i), cm ³	60.55	69.00	69.50	69.60	69.80	69.50
Final Volume (V_f), cm ³	73.31	72.94	73.12	72.97	72.62	72.51

Figure B.5. Swell Amount versus Time Graph for 10%FA treated sample



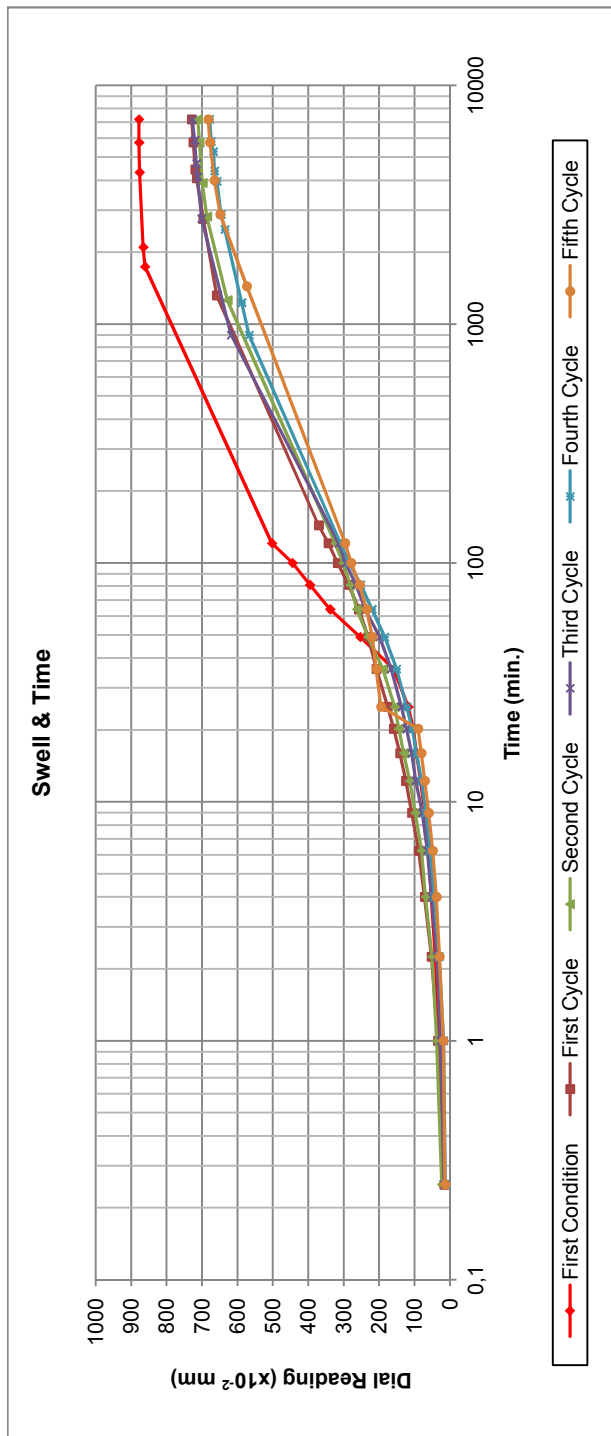
	First Condition	First Cycle	Second Cycle	Third Cycle	Fourth Cycle	Fifth Cycle
Initial Height (h_i), mm	19.10	21.64	21.65	21.70	21.70	21.70
Final Height (h_f), mm	21.98	22.04	21.99	22.07	22.05	22.05
Initial Volume (V_i), cm ³	61.12	67.81	68.00	68.10	68.20	68.00
Final Volume (V_f), cm ³	70.33	70.53	70.37	70.63	70.55	70.56

Figure B.6. Swell Amount versus Time Graph for 15%FA treated sample



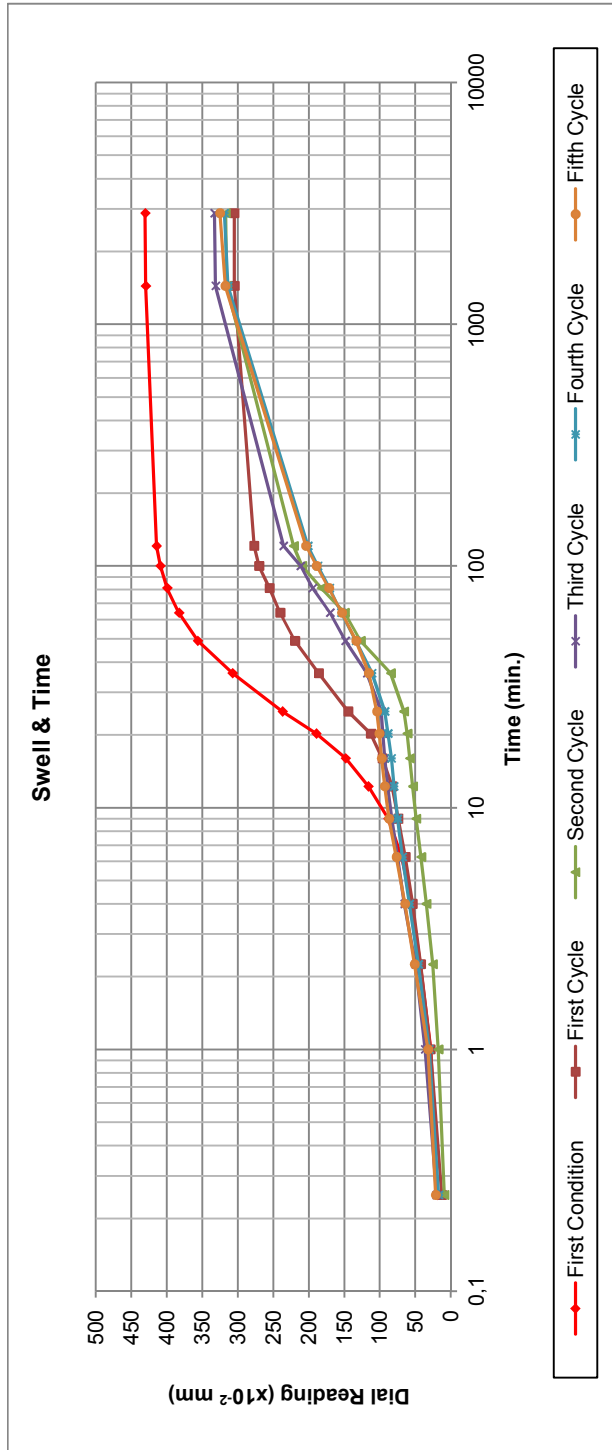
	First Condition	First Cycle	Second Cycle	Third Cycle	Fourth Cycle	Fifth Cycle
Initial Height (h_i), mm	19.10	21.70	21.75	21.73	21.75	21.75
Final Height (h_f), mm	21.81	22.05	22.04	22.09	22.10	22.03
Initial Volume (V_i), cm^3	60.55	68.00	68.00	68.05	68.10	68.00
Final Volume (V_f), cm^3	69.14	69.88	69.87	70.03	70.06	69.83

Figure B.7. Swell Amount versus Time Graph for 20%FA treated sample



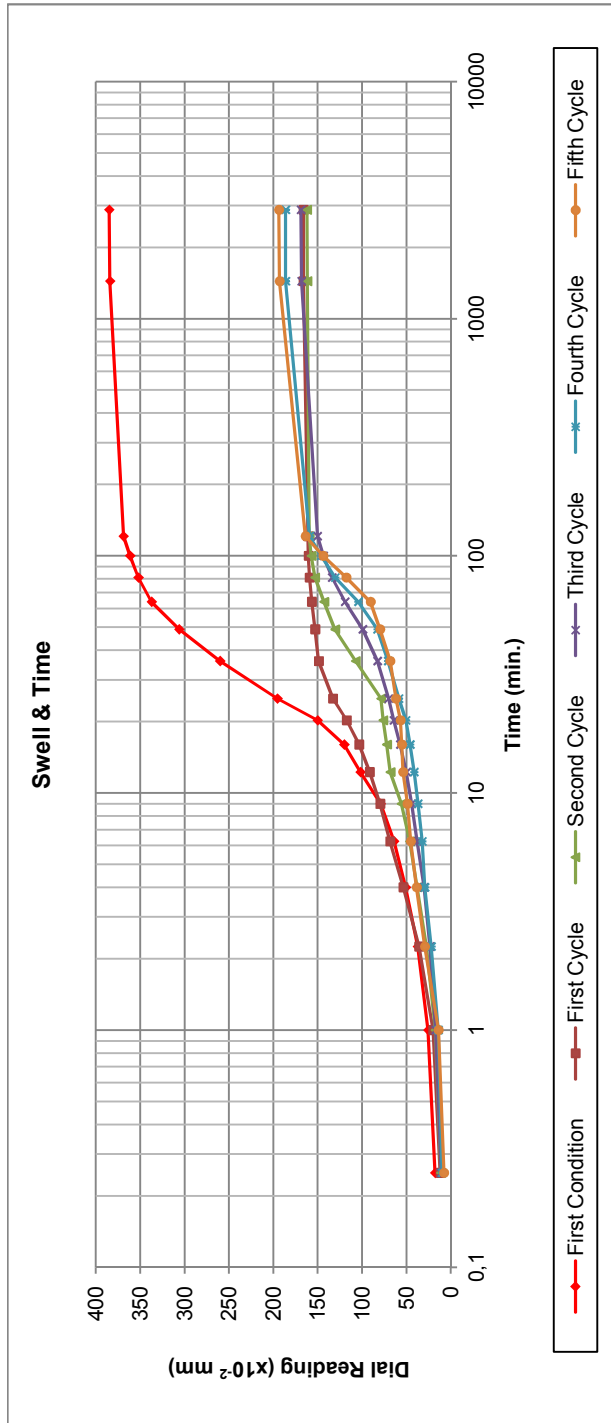
	First Condition	First Cycle	Second Cycle	Third Cycle	Fourth Cycle	Fifth Cycle
Initial Height (h_i), mm	19.10	22.65	23.75	24.35	25.15	25.25
Final Height (h_f), mm	27.88	29.94	30.87	31.62	31.94	32.07
Initial Volume (V_i), cm ³	60.55	65.95	67.00	67.10	67.95	67.75
Final Volume (V_f), cm ³	88.38	94.91	97.86	100.24	101.23	101.67

Figure B.8. Swell Amount versus Time Graph for 1%L treated sample



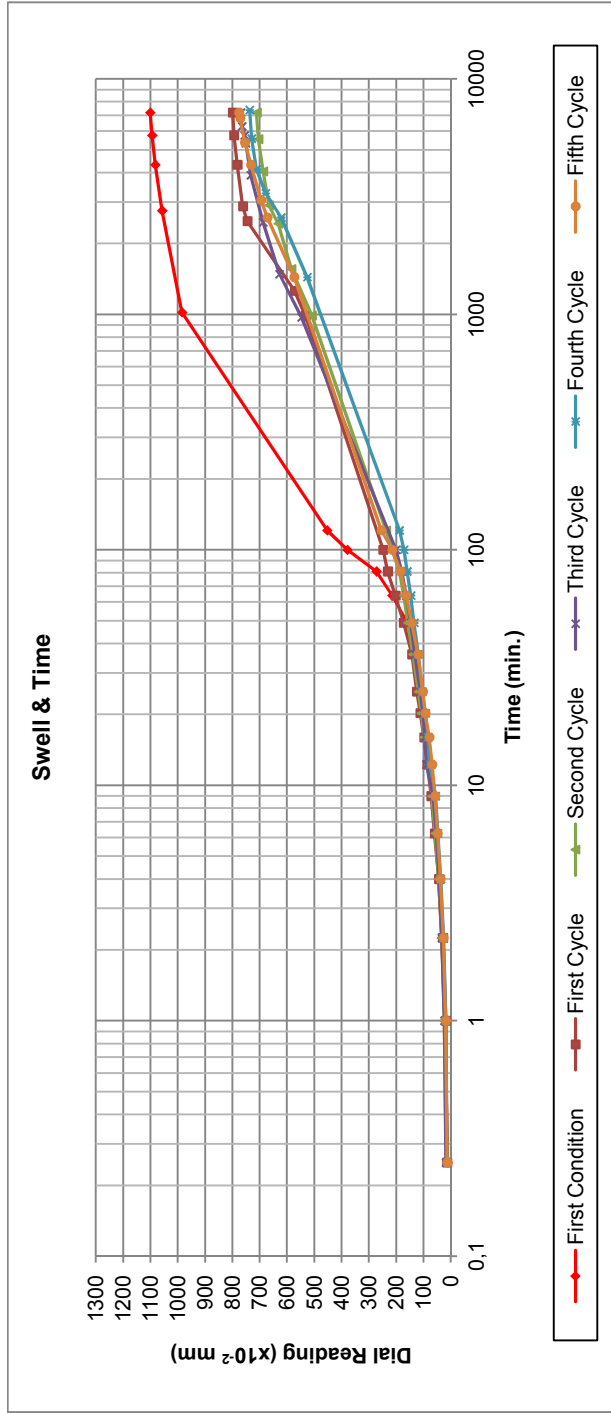
	First Condition	First Cycle	Second Cycle	Third Cycle	Fourth Cycle	Fifth Cycle
Initial Height (h_i), mm	19.10	21.50	21.90	22.20	22.35	22.35
Final Height (h_f), mm	23.41	24.57	25.07	25.53	25.54	25.60
Initial Volume (V_i), cm^3	60.55	67.15	68.26	69.20	69.65	69.65
Final Volume (V_f), cm^3	74.19	77.89	79.50	80.92	80.96	81.16

Figure B.9. Swell Amount versus Time Graph for 3%L treated sample



	First Condition	First Cycle	Second Cycle	Third Cycle	Fourth Cycle	Fifth Cycle
Initial Height (h_i), mm	19.10	21.35	21.45	21.60	21.60	21.60
Final Height (h_f), mm	22.95	23.01	23.07	23.29	23.46	23.54
Initial Volume (V_i), cm^3	60.55	66.70	67.06	67.56	67.75	67.75
Final Volume (V_f), cm^3	72.73	72.94	73.13	73.82	74.37	74.61

Figure B.10. Swell Amount versus Time Graph for 5%L treated sample



	First Condition	First Cycle	Second Cycle	Third Cycle	Fourth Cycle	Fifth Cycle
Initial Height (h_i),mm	19,10	24,30	25,75	25,90	26,50	26,00
Final Height (h_f),mm	30,11	32,29	32,86	33,59	33,87	33,80
Initial Volume (V_i),cm³	60,55	65,56	67,68	67,95	68,87	67,16
Final Volume(V_f),cm³	95,45	102,34	104,16	106,48	107,35	107,14

Figure B.11. Swell Amount versus Time Graph for 5%S treated sample